UNIVERSITA' DEGLI STUDI DI PADOVA

_____

SCUOLA DI DOTTORATO DI RICERCA IN

SCIENZE DELLE PRODUZIONI VEGETALI

INDIRIZZO AGRONOMIA AMBIENTALE - CICLO XXI

Dipartimento di Agronomia Ambientale e Produzioni Vegetali

Sampling and hydraulic properties of stony soils

Direttore della Scuola : Ch.mo Prof. Andrea Battisti

Supervisore : Ch.mo Prof. Francesco Morari

Dottoranda : Chiara Pagliarin

DATA CONSEGNA TESI

02 febbraio 2009

Declaration

I hereby declare that this submission is my own work and that, to the best of my knowledge and belief, it contains no material previously published or written by another person nor material which to a substantial extent has been accepted for the award of any other degree or diploma of the university or other institute of higher learning, except where due acknowledgment has been made in the text.

Chiara Pagliarin, Padova, 02/02/2009

A copy of the thesis will be available at *http://paduaresearch.cab.unipd.it/*

Dichiarazione

Con la presente affermo che questa tesi è frutto del mio lavoro e che, per quanto io ne sia a conoscenza, non contiene materiale precedentemente pubblicato o scritto da un'altra persona né materiale che è stato utilizzato per l'ottenimento di qualunque altro titolo o diploma dell'università o altro istituto di apprendimento, a eccezione del caso in cui ciò venga riconosciuto nel testo.

Chiara Pagliarin, Padova, 02/02/2009

Una copia della tesi sarà disponibile presso *http://paduaresearch.cab.unipd.it/*

A chi vuole
il mio bene

Index

Summary

Subjects of this thesis were sampling and hydraulic properties of stony soils.

Sampling is important to achieve knowledge of soil spatial variability. Soil surveys are generally time-consuming, labour-intensive and costly. This is especially true in stony soils where large numbers of samples are required to obtain a rappresentative sample size, and where sampling efforts are bigger than in non-stony soils. The potential use, of electro-magnetic induction scans (EMI) to measure bulk electrical conductivity (EC) and improve the estimate precision of sparsely sampled primary variables, was assessed in a 5-ha gravelly soil vineyard in Valpolicella, North-Eastern Italy. EMI measurements were taken using a Geonics EM38DD operating in both horizontal and vertical mode. Geoelectrical investigations were also done in 18 positions with the electrical resistivity tomography (ERT) method in order to obtain high-resolution images of soil profile. The spatial variability of soil properties and their relationships with EC, in horizontal and vertical mode, was estimated by multivariate geostatistical techniques. There was generally close relationship between EC and the measured physical properties. The results proved that EM38DD could be advantageously used to infer soil spatial variability in gravelly soils, even if ground-truth soil samples are necessary to understand and interpret EC measurements.

Hydraulic properties were studied by different approaches.

Reconstructed samples were manually constructed using sieved clay soil and synthetic sand, as fine earth fraction, and glass spheres or cylinders, as coarse fraction. The choice to use the glass was to have a material which did not have any porosity, so it could be possible to evaluate the steric role of coarse fragment on soil hydraulic properties. Saturated hydraulic conductivity (K_s) measurements and evaporation experiments were conducted to determine hydraulic conductivity function and soil water retention characteristic. K_s values were compared with the theoretical approaches as literature describes. These approaches decrease the soil water content and hydraulic conductivity as stone content increases.

Evaporation results were fitted by RETC to determine the van Genuchten-Mualem parameters. Nevertheless the observed high variability, results showed that coarse fragment effect on soil hydraulic properties has to be considered, both in terms of reduction of area for water flow and increase of the tortuosity, and as a factor which influences fine earth characteristics, determining a fine earth bulk density variation (bd_{fe}). Saturated hydraulic conductivity measurements, evaporation experiments and mercury intrusion porosimetry analyses were conducted on undisturbed samples. Evaporation results were inverted by Hydrus 1D to estimate the van Genuchten-Mualem parameters. Correlation matrix showed stone positive effect on saturated hydraulic conductivity, which might be explained by the negative relationship between fine earth bulk density and coarse fragment content and by the positive relationship between coarse fragments and macro-porosity classes.

Eighteen tension disc infiltration experiments were conducted in three soils of Regione Lombardia, Northern Italy. Soils were different for texture, stone content and organic matter content. Infitrometry experiments were used to determine the van-Genuchten Mualem parameters by mean of Hydrus 2D/3D, used in parameter estimation mode. Some pedotransfer functions (PTFs) were used as multiple regression tool to better understand the effects of the analysed factors. Results showed high variability and it was not possible to clearly define the coarse fragment effect on soil hydraulic properties. PTFs showed, by the way, the importance of using the fine earth bulk density, both measured and estimated, to improve the estimation of saturated hydraulic conductivity.

PEST-Hydrus 3D interface was used to determine the van Genuchten-Mualem parameters of the fine earth fraction (sieved clay), of some previously described reconstructed samples, on which evaporation experiments were conducted. Unsaturated hydraulic conductivity, as influenced by tortuosity, was determined by simulated infiltration events by Hydrus 3D, using different domains which contained different "empty spaces", comparable to the coarse fragment content. K_{soil}/K_{fe} ratio is normally used to determine hydraulic conductivity reduction in increasing coarse fragment content. K_{soil}/K_{fe} was used to observe the stone positive effect on fine earth characteristics: it showed a tendency of increase of the hydraulic conductivity as stone content increased. K_{soil}/K_{fe} ratio was also used to determine tortuosity effect: for the studied soils, there were not differences

2

between cylinder and sphere effect on hydraulic conductivity. Moreover, it was observed that tortuosity effect decreased as matric potential, in absolute value, increased.

Results proved that the theoretical approach used to determine the water content reduction in increasing coarse fragment content is a realistic estimation tool. Approaches used to determine hydraulic conductivity in increasing stone content should consider both the tortuosity effect and the fine earth bulk density variation as determined by the presence of coarse fragments.

Riassunto

In questo lavoro di tesi si sono approfondite tematiche legate al campionamento e alle proprietà idrauliche dei suoli scheletrici.

Il campionamento è un aspetto fondamentale per conoscere la variabilità presente in un suolo. La capacità di descrivere dettagliatamente la realtà in esame è influenzata, oltre che dai mezzi tecnici utilizzati per effettuare il campionamento, anche dalla disponibilità in termini economici e di tempo. Nei suoli scheletrici tali limiti sono aumentati dalla maggiore quantità di suolo necessaria per ottenere un campione significativo e dalla maggiore difficoltà di campionamento rispetto ai suolo non scheletrici. Sul suolo di un vigneto di 5 ha in Valpolicella (VR) è stata valutata la possibilità di utilizzare strumenti ad induzione elettromagnetica (EMI) per misurare la conducibilità elettrica (EC) e la possibilità di tali strumenti di migliorare la stima di variabili primarie del suolo. Lo strumento impiegato per determinare EC è stato Geonics EM38DD, utilizzato sia in modalità orizzontale che verticale. Si sono inoltre condotte 18 tomografie di resistenza elettrica (ERT) al fine di ottenere immagini ad alta risoluzione del profilo del suolo. La variabilità spaziale delle proprietà del suolo e i valori di EC, orizzontali e verticali, è stata stimata utilizzando tecniche geostatistiche multivariate. In generale si è trovata una buona relazione tra EC e le proprietà fisiche misurate, dimostrando che EM38DD potrebbe essere utilizzato in modo vantaggioso per inferire la variabilità spaziale in suoli scheletrici, anche se rimane necessario il campionamento in campo per capire ed interpretare le misure di EC.

Le proprietà idrauliche sono state analizzate utilizzando diversi approcci.

Si sono innanzitutto ricostruiti dei campioni, utilizzando come terra fine un terreno argilloso e della sabbia sintetica, e sfere e cilindri di vetro come materiale grossolano. Il vetro è stato scelto in quanto rappresenta un materiale non poroso e adatto a studiare l'influenze sterica di tali materiali sulle caratteristiche idrauliche del suolo. Al fine di determinare la ritenzione idrica e la conducibilità idraulica insatura sono state effettuate delle misure di conducibilità idraulica satura (K_s) ed esperimenti evaporimetrici. I valori di

K_s sono stati confrontati con gli approcci teorici presenti in letteratura. Questi prevedono una riduzione della ritenzione idrica e della conducibilità idraulica in funzione del contenuto di scheletro. I dati derivanti dagli esperimenti evaporimetrici sono stati interpolati utilizzando RETC per determinare i parametri dell'equazione di van Genuchten-Mualem. Da tali prove, nonostante l'alta variabilità presente, è emerso che l'influenza del materiale grossolano sulle proprietà idrauliche deve essere considerata sia in termini di riduzione dell'area disponibile per il flusso di acqua e di tortuosità, sia come fattore che influenza le caratteristiche della terra fine, determinando una variazione della massa volumica apparente della stessa (bd_{fe}). Misure di conducibilità satura, esperimenti evaporimetrici e analisi di porosimetria ad intrusione di mercurio sono stati condotti su campioni indisturbati. I dati evaporimetrici ottenuti sono stati analizzati utilizzando Hydrus 1D al fine di stimare i parametri dell'equazione di van Genuchten-Mualem. Da un'analisi di correlazione è emersa la positiva influenza dello scheletro sulla conducibilità satura, che è spiegabile dalla relazione negativa tra massa volumica apparente e lo scheletro stesso, e dalla relazione positiva tra scheletro e le classi più macroporose.

Diciotto analisi di infiltrazione, utilizzando un infiltrometro a tensione, sono state condotte in tre siti lombardi, differenti per tessitura, contenuto in scheletro e sostanza organica. Gli esperimenti infiltrometrici sono stati modelizzati con Hydrus 2D/3D, permettendo di stimare i parametri dell'equazione di van Genuchten-Mualem. Alcune funzioni di pedotrasferimento (PTFs) sono state inoltre utilizzate come strumento di regressione multipla per meglio capire l'influenza dei diversi fattori analizzati. La variabilità presente è risultata elevata, e non si è potuta determinare in modo chiaro l'influenza del solo scheletro sulle caratteristiche idrauliche. PTFs hanno, comunque, permesso di evidenziare l'importanza di utilizzare la densità apparente della terra fine, misurata o stimata, come fattore che migliora la capacità predittiva per la determinazione della conducibilità idraulica satura.

Utilizzando PEST-Hydrus 3D è stato possibile determinare i parametri dell'equazione di van Genuchten-Mualem della sola terra fine, di alcuni dei campioni ricostruiti descritti in precedenza, su cui si erano condotti esperimenti evaporimetrici. Effettuando simulazioni di infiltrazione in Hydrus 3D, utilizzando domini a differente contenuto di "spazi vuoti", assimilabili al contenuto di scheletro, si è inoltre determinato il comportamento della

conducibilità idraulica insatura in funzione della tortuosità. Utilizzando K_{soil}/K_{fe}, rapporto che è normalmente utilizzato per determinare la riduzione della conducibilità in funzione del contenuto di scheletro, si è potuto osservare la positiva influenza dello scheletro sulle caratteristiche della terra fine, evidenziando una tendenza all'aumento della conducibilità all'aumentare del contenuto di scheletro. Lo stesso approccio è stato utilizzato per determinare l'influenza della tortuosità: per i suoli studiati non sono emerse differenze tra l'influenza dei cilindri e delle sfere su questo parametro e si è osservato che l'incidenza della tortuosità decresce all'aumentare, in valore assoluto, del potenziale matriciale.

Dai risultati ottenuti è un approccio realistico ipotizzare che in un suolo, mantenendo costanti le caratteristiche della terra fine, diminusca la ritenzione idrica in funzione dell'aumento del contenuto di scheletro su base volumetrica. Gli approcci utilizzati per determinare della conducibilità idraulica all'aumentare dello scheletro dovrebbero considerare, oltre all'influenza delle tortuosità, anche la variazione di massa volumica apparente della terra fine determinata dalla presenza dello scheletro stesso.

1 Preface

"Soil science has always had strong ties with agriculture and soil science knowledge has made large contributions to the increase in agricultural production. A better understanding of soils has been essential for research questions on climate change, environmental regulation and ecosystem services" (Hartemink and McBratney, 2008).

In soil science, great attention has been paid to the study of the role played by the fine earth particle (≤ 2 mm) while the effects of the coarsest soil fraction (> 2 mm) have been almost neglected (Poesen and Lavee, 1994). These coarse fractions might be defined in several ways , depending on the classification used (fig. 1), but in this work, for simplicity, when referring to them, we will use in the same way terms as "stone", "skeletal", "gravel" and "rock fragments". Stony soils are widespread; they occupy more than 60% of the land in the Mediterranean area (Poesen, 1990). Stony soils are found on depositional as well as on erosional landforms (Poesen and Levee, 1994); moreover robust knowledge on their behaviour is especially needed because of their potential limitations or benefits for landuse (Nichols et al., 1984; Morari et al., 2004).

"Effective soil management requires an understanding of soil distribution patterns within the landscape. Conventionally, soil survey can be considered as inventories of soil, including field description and laboratory analysis and subsequent classification and mapping. However, with increasing concern on environmental issues related to our planet, soil survey has moved from its traditional subjective conjecture to more quantitative modelling with accompanying accuracy and uncertainty issues" (Mc Bratney et al., 2000). Soil survey is generally considered labour-intensive, time-consuming and costly, especially in stony soils where, indeed, the soil sample has to be larger that the stone-free sample and it depends on the gravel size and percentage (Buchter et al., 1994).

Illogically, while stony soils are recognised and mapped as such, in reality within the gravelly soils only the fine earth is analysed. Therefore, when the measured parameters in the fine earth are expressed on an area basis, stony soils appear not to be stony at all. Instead, they appear as "fine textured soils", thus taking into account the skeleton as an inert diluent of the fine earth or considering the entire mass of the soil only made of fine earth

determines a wrong estimation of the properties of the stony soil itself (Ugolini et al., 1998).

Characterization of the hydrophysical properties of stony soils is both theorically and experimentally difficult. Rock fragments in soil profiles cause heterogeneity and anisotropy of the system, while most models are dealing with homogeneous and isotrope systems. Problems are related to the installation of experimental devices in the field and to the ability of collect representative sampling without altering the soil structure (Ingelmo et al, 1994).

The amount and type of rock fragments in surface soil layers can affect infiltration and water storage, which in turn influence land use and site productivity (Sauer and Logsdon, 2002). Hydrophysical properties of stony soils are influenced in complex and contrasting ways by the presence of the coarse fractions, i.e. bulk density of the fine earth fraction decreases (Torri et a., 1994); porosity of the fine earth fraction increases (Fiès et al., 2002); available area for the flow path decreases and tortuosity increases (Mehuys et al., 1975), water retention and saturated hydraulic conductivity decrease (Rawls et al., 1993), unsaturated hydraulic conductivity-matric potential relationship may not change in presence of rock fragments, while it may happen in the unsaturated hydraulic conductivity-water content relationship (Mehuys et al., 1975).

The general aim of this work is to better understand the hydraulic properties of stony soils, particularly to understand:

- the feasibility to use a new soil survey approach;
- the main influences of coarse fragments on the soil water retention and hydraulic conductivity, using both reconstructed and undisturbed samples, both at laboratory and field level;
- to characterize fine earth properties and tortuosity effect caused by steric influence of stones, as simulated by 3D modelling using PEST-Hydrus 3D interface.

References

Buchter B., Hinz C. and Fltihler H., 1994. Sample size for determination of coarse fragment content in a stony soil. Geoderma, 63: 265-275;

Casenave A. and Valentin C., 1989. Les Etats de Surface de la Zone Sahélienne. Influence sur l'Infiltration. ORSTOM, Paris, 227 pp;

F.A.O. (Food and Agriculture Organization of the United Nations), 1979. A provisional methodology for soil degradation assessment. F.A.O., Rome, 84 pp;

Fiès J.C., De Louvigny N., and Chanzy A., 2002. The role of stones in soil water retention. European Journal of Soil Science 53:95-104;

Hartemink A. E. and McBratney A., 2008. A soil science renaissance. Geoderma, 148: 123-129;

Hodgson J.M., 1978. Soil Sampling and Soil Description. Clarendon Press, Oxford, 241 pp;

Ingelmo F., Cuadrado S., Ibanez A. and Hernandez J., 1994. Hydric properties of some spanish soils in relation to their rock fragment content - implications for runoff and vegetation. Catena 23:73-85;

Miller F.T. and Guthrie R.L., 1984. Classification and distribution of soils containing rock fragments in the United States. In: Nichols J.D., Brown P.L. and Grant W.J. (Editors), Erosion and Productivity of Soils Containing Rock Fragments. Soil Sci. Soc. Am. Spec. Publ., 13: 1-6.

Ministerio de Agricultura, Pesca y Alimentacion, 1983. Sinedares. Sistema de Informacion Edafologia y Agronomica de Espana, Madrid, 92 pp;

McBratney A.B., Odeh I.O.A., Bishop T.F.A., Dunbar M.S. and Shatar T.M., 2000. An overview of pedometric techniques for use in soil survey. Geoderma, 97:293–327;

Mehuys G.R., Stolzy L.H., Letey J. and Weeks L.V., 1975. Effect of stones on the hydraulic conductivity of relatively dry desert soils. Soil Sci. Soc. Amer. Proc, 39: 37-42;

Morari F., Lugato E. and Borin M., 2004. An integrated non-point source model-GIS system for selecting criteria of best management practices in the Po Valley, North Italy. Agriculture Ecosystems & Environment 102:247-262;

Nichols J.D., Brown P.L. and Grant W.J., 1984. Preface. In: Nichols J.D., Brown P.L. and Grant W.J. (Editors). Erosion and Productivity of Soils Containing Rock Fragments. Soil Science Society Special Publication 13;

Poesen, J., 1990. Erosion process research in relation to soil erodibility and some implications for improving soil quality. In: Albaladejo J., Stocking M.A and Diaz E. (Editors), Soil Degradation and Rehabilitation in Mediterranean Environmental Conditions. C.S.I.C., Murcia, pp. 159 170;

Poesen J. and Lavee H., 1994. Rock fragments in top soils - significance and processes. catena 23:1-28;

Rawls W.J., Brakensiek D.L. and. Logsdon S.D., 1993. Predicting saturated hydraulic conductivity utilizing fractal principles. Soil Science Society of America Journal 57:1193-1197.

Sanesi G., 1977. Guida alla descrizione del suolo. C.N.R., Firenze, pp. 37-38.

Sauer T.J. and Logsdon S.D., 2002. Hydraulic and physical properties of stony soils in a small watershed. Soil Science Society of America Journal 66:1947-1956;

Schachtschabel P., Blume H.-P., Brüimmer G., Hartge, K.-H. and Schwertmann, U., 1989. Lehrbuch der Bodenkunde. Ferdinand Enke Verlag, Stuttgart, pp. 21 23;

Torri D., Poesen J., Monaci F. and Busoni E., 1994. Rock fragment content and fine soil bulk-density. Catena 23:65-71;

Ugolini F. C., Corti G., Agnelli A. and Certini G., 1998. Under- and overestimation of soil properties in stony soils. 16th World Congress of Soil Science, Montpellier, France.

ROCK FRAGMENT SIZE

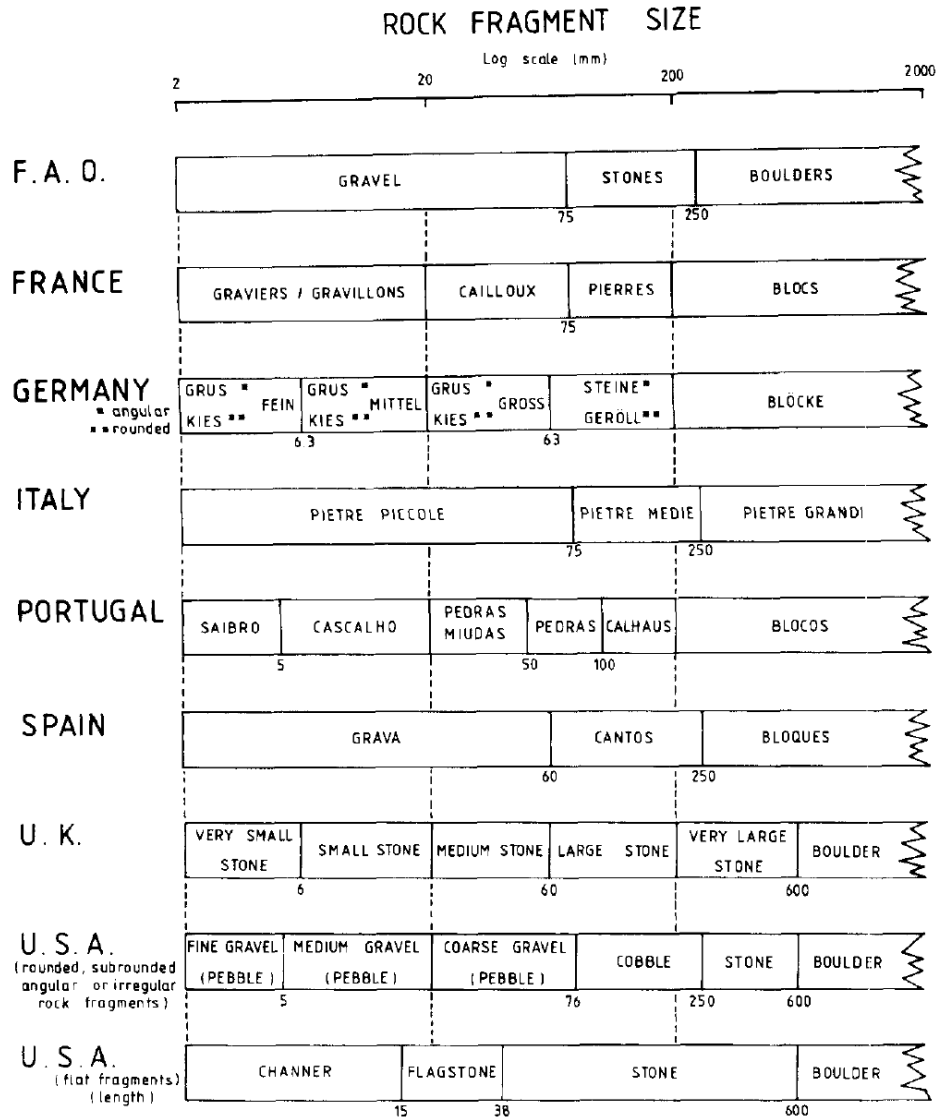**Figura 1: Some classification system of coarse soil fragments (>2 mm) in soils by size and shape used by F.A.O. (F.A.O., 1977) and used in France (Casenave and Valentin, 1989), Germany (Schachtschabel et al., 1989), Italy (Sanesi, 1977), Portugal (Hodgson, 1978), Spain (Ministerio de Agricultura, Pesca y Alimentaction, 1983), UK (Hodgson, 1978) and USA (Miller and Guthrie, 1984). (from Poesen and Levee, 1994)**

2 Sampling of stony soils: "Delineating soil variability within a gravelly vineyard using geo-electrical sensors"

F. Morari[1], Castrignanò A. [2], C. Pagliarin [1]

1) Dipartimento di Agronomia Ambientale e Produzioni Vegetali, University of Padova , Viale dell'Università, 16, Legnaro (PD), Italy

2) CRA –I.S.A., Via Celso Ulpiani, Bari, Italy,

Corresponding Author: Francesco Morari

phone +39-049-8272857; fax +39-049-8272839; e-mail: francesco.morari@unipd.it

Abstract

In gravelly soils, surveys are generally time-consuming, labour-intensive and costly. This limits the possibility of adopting an appropriate sampling to determine within-field spatial variability. The potential use of electro-magnetic induction scans (EMI) to measure bulk electrical conductivity (EC) and improve the estimate precision of sparsely sampled primary variables was assessed in a 5-ha gravelly soil vineyard in Valpolicella, north-eastern Italy. EMI measurements were taken using a Geonics EM38DD operating in both horizontal and vertical mode. Geoelectrical investigations were also done in 18 positions with the electrical resistivity tomography (ERT) method to obtain high-resolution images of the soil profile. The spatial variability of soil properties and their relationships with EC in horizontal and vertical mode was estimated using multivariate geostatistical techniques. Spatial dependence between EC and soil properties was also explored with Factorial

Kriging Analysis (FKA), which was integrated with fuzzy c-means classification for zoning the vineyard.

There was a generally close relationship between EC and the measured physical properties. EMI measurements were also consistent with ERT profiles, evidencing the presence of gravelly parent material, with low electrical conductivity, variably distributed in the 3 dimensions and affecting vine rooting depth. FKA isolated two significant regionalized factors which, with an acceptable loss of information, give a concise description of the soil physical variability at the different selected spatial scales and allowed the delineation of zones to be managed separately. The results prove that EM38DD could be advantageously used to infer soil spatial variability in gravelly soils, even if ground-truth soil samples are obligatory to understand and interpret the EC measurements.

Introduction

Efficient methods for accurately measuring within-field variations in soil properties are crucial for Precision Viticulture (Bramley, 2005). Sampling at discrete places has been the traditional means of obtaining information about the soil, but soil surveys are generally time-consuming, labour-intensive and costly, especially in the gravelly soils characterising some of the most important terroirs in the world. The large numbers of samples required in gravelly areas in order to attain a good representation of the soil properties (Buchter et al., 1994) limit the possibility of adopting an appropriate sampling intensity to determine the spatial variability within vineyards.

The potential use of ancillary data that can be intensively recorded, such as soil bulk electrical conductivity (EC) measured by electro-magnetic induction (EMI) surveys, has been well examined over the last decade. This is because data are relatively easy and inexpensive to collect (Blackmer et al., 1995; Mulla, 1997). If the sparse and more intensive data are spatially correlated, then the additional information from the ancillary

16

data can be used to improve the estimate precision of the sparsely sampled primary variable. Several scientists have used EMI surveys to characterise soil salinity (Rhoades et al., 1999a) and nutrients (Kaffka et al., 2005), texture (Triantafilis and Lesch; 2005), bulk density related (Rhoades et al., 1999b) and many other properties (Corwin and Lesch, 2005). EMI investigations were also applied to identify morphological features such as depth to boulder clay (Brus et al., 1992) or clay pan (Sudduth et al., 1995). Although EMI is useful for looking at lateral spatial variation, it gives limited information on how conductivity varies with depth because the relationship between a specific earth domain and a particular EC reading is poorly quantified (Pellerin and Wannamaker, 2005). To improve the characterisation of the soil profile EMI can be coupled with electrical resistivity methods. They have largely been applied in near-surface geophysical investigations, improving soil survey with 2D or 3D high-resolution electrical images of the subsurface (Electrical Resistivity Tomography-ERT) (Rizzo et al., 2004). Here are no many papers that use different geo-electrical techniques in an integrated way (De Benedetto et al., 2008).

Modelling the relationships between primary soil variables and EC is essential to assess and describe the spatial variability within a vineyard with sufficient precision and then identify management zones. The task is not generally easy, because EC depends on many soil properties over different spatial scales, in a very complex and non-linear way. Moreover, difficulties increase when sampling intensity is reduced by unfavourable soil conditions such those in gravelly soils. Several methods have been proposed to incorporate secondary information. A number of "hybrid" interpolation techniques, combining geostatistical technique of (co)kriging with exhaustive secondary information, have been developed and tested to improve primary variable precision (Goovaerts, 2000; McBratney et al., 2000; Frogbrook and Oliver, 2001). Kriging with external drift (Royle and Berliner, 1999; Wackernagel, 2003) is a non-stationary geostatistical technique, based on a model assumed for the conditional distribution of the primary variable and taking into account the linear relationship between primary and auxiliary data. Hierarchical spatial regression models (Triantafilis and Lesch, 2005) and regression kriging (Hengl et al., 2004) have been used as an alternative to cokriging. Another technique is an approximation of multivariate extension of kriging, known as collocated cokriging, which has proved to be well-suited to merging types of information with different resolution (Castrignanò et al., 2008). A

geostatistical method of multivariate continuous clustering, known as factor cokriging (Castrignanò et al., 2000; Bocchi et al., 2000; Casa and Castrignanò, 2008), is also available to evaluate the spatial relationship between soil properties and EMI variables, in order to identify characteristically different zones within a field.

Little has been done to define mapping protocols in gravelly soils. This work proposes a procedure for conducting EC surveys in a vineyard with a gravelly soil, gives guidelines for interpreting the EC measurements and lastly applies a geostatistical approach to build maps and classify vineyards in zones to be managed differently.

Materials and Methods

Study site

The study site is a 5-ha vineyard at San Pietro in Cariano, Valpolicella (north-eastern Italy; 45°31' N 10°53' E, 145 m a.s.l.), located in a DOC (controlled specifications of origin) area producing Valpolicella and Amarone wines. The climate is sub-humid, with mean annual rainfall of about 850 mm distributed fairly uniformly throughout the year. From December to February the temperature rarely falls below zero, while maximum temperatures in summer vary from 25 to 30° C during the day and 18 to 20° C at night. The soil is a calcari-epileptic cambisol (FAO, 1998), clay-loam, with 400 g kg^{-1} gravel in the surface layer and more than 600 g kg^{-1} in the sub-surface. The vineyard is cropped with cv. *Corvinone* trained to a Guyot system at a density of 4000 plants/ha (1 x 2.5 m).

Mobile EC – measuring equipment

Measurements of electromagnetic induction (EMI) were taken in November 2005, when soil was close to field capacity (average water content of fine components was 0.18 g g^{-1}). A detailed description of the theory, operation and construction of EMI instrumentation is provided by Rhoades et al. (1999b) and Hendrickx et al. (2002). The

mobile EC measuring equipment used in this trial consisted of four components (Figure 1): 1) the EMI sensor; 2) global positioning system (GPS); 3) hardware interfacing and 4) transport platform. The commercial EMI sensor used was a Geonics EM38DD, with a distance of 1 m between the transmitting coil at one end of the instrument and the receiver coil at the other. It was operated in both horizontal and vertical mode. The sensor provided a weighted depth reading to approximately 0.5 m in horizontal mode and about 1.5 m in vertical mode. The instrument response to soil conductivity varies as a nonlinear function of depth (Mc Neill, 1990). Sensitivity in the vertical mode is highest at about 0.4 m (0.3 - 0.5 m) beneath the instrument (Dalgaad et al., 2001).

The GPS system was a stand-alone receiver that required external data logging. Hardware (Allegro Field PC, Juniper System) and software (TrackMaker38, Geomar software) interfacing was needed to link the EC measurements sensor data with associated GPS coordinate data, upgraded by using EGMOS correction, and to control the timing of data acquisition and recording. The transport platform consisted of a simple non-metallic platform towed behind a tractor. Observations were made along parallel transects approximately 5 m apart, and both types of data (EMI data in both modes and positional data) were simultaneously recorded every 1 second, resulting in 5782 values (Figure 2).

Electrical Resistivity Tomography (ERT)

Geoelectrical investigations were done in July 2006 with Electrical Resistivity Tomography (ERT) to obtain high-resolution images of the soil profile. Average moisture of soil fine components was 0.13 g g^{-1}. Eighteen profiles 5.75 m long, N-S oriented along the vine rows (Figure 2) were performed using an Iris-Syscal Pro resistivity meter. Each profile was done by means of dipole-dipole electrode arrays using 24 electrodes with 0.25 m spacing: the electrical current (I) is delivered into the ground via two contiguous electrodes x meters apart, and the potential drop (ΔV) is measured between two other electrodes x meters apart in line with the current electrodes. The spacing between the nearest current and potential probes is an integer n times the basic distance x and the maximum number of measurements depend on the signal-to-noise ratio of the voltage

recordings (Rizzo et al., 2004). The values of apparent resistivity for each transverse are assigned, along a horizontal axis, at the intersections of two converging lines at 45 degrees from the centre of the current dipole and centre of the measuring dipole. All the values of apparent resistivity form a first tomographic image of the electrical subsurface structure, called "pseudo-section" (Rizzo et al., 2004). The apparent resistivity values of the "pseudo-section" were then inverted by the ERTLab software (Multi-Phase Technologies and Geostudi Astier), which uses a Finite Elements (FEM) forward modelling algorithm to incorporate topography (Zhou and Greenhalgh, 2001). The inversion procedure is based on a least squares smoothness constrained approach (LaBrecque et al., 1995). Noise is appropriately managed using a data weighting algorithm (Morelli and LaBrecque, 1996).

Soil sampling

Soil sampling was done in two phases. In July 2005 the top layer (0-20 cm) was sampled in 39 points: thirty samples (Figure 2) were collected at the nodes of a 40 x 40 m grid mesh, with 3 additional clusters each composed of 3 samples located 1 m apart from 3 randomly selected grid points. Soil samples had an average weight of 4.5 kg and volume of 2800 cm^3 which, according to the study of Buchter et al. (1994) in stony soils, is sufficient to average out the discontinuities caused by the spatial arrangement of pores and particles (representative elementary volumes –REV). Although a higher density of sampling points could have improved the estimation of the experimental variograms (Webster and Oliver, 2001), the time-consuming and labour-intensive sampling operations limited the number of possible samples. Samples were analysed for particle-size distribution by gravitational sedimentation for the fine components (<2 mm) and dry sieving for the gravel components in the following ranges 2-20 mm, 20-100 mm and >100 mm (Gee and Or, 2002). Bulk density inclusive of gravel was calculated with the sand-cone method (Grossman and Reinsch, 2002), while bulk density of the fine component was calculated indirectly from the overall bulk density and gravel specific density (Grossman and Reinsch, 2002). Specific density of the gravel was measured by the pycnometer method (Flint and Flint, 2002). The fine component was also analysed for pH and electrical conductivity (ECe) measured in a 1:2 (soil:water) suspension, soil organic carbon (SOC) determined by dichromate oxidation

(Walkley and Black, 1934) and Total Nitrogen (TKN) determined by the Kjeldahl method (Kjeldahl, 1883).

The second sampling phase was conducted after the geoelectrical investigations to confirm the ERT signal evidence and profile texture discontinuities. Twelve profiles with contrasting ERTs were selected. In the middle position of each electrode array, a 1-m deep pit was dug using a backhoe, collecting 10-kg samples from each of the five 20-cm thick layers. The soil samples were analysed for particle-size distribution: fine components and gravel components in the three ranges: 2-20 mm, 20-100 mm and >100 mm.

Geostatistical procedures

Before applying multivariate analysis, the variables which were transformed and standardised using a very flexible approach based on Hermite polynomials for transforming a variable with a skewed distribution into a standard Gaussian variable (Wackernagel, 2003).

Modelling the coregionalization of the set of selected variables was performed using the Linear Model of Coregionalization (LMC), developed by Journel and Huijbregts (1978), which assumes that all the n studied variables are the result of the same independent processes, acting at different spatial scales u. The $n(n+1)/2$ simple and cross semivariograms of the n variables are modelled by a linear combination of N_S standardized semivariograms to unit sill $g^u(\mathbf{h})$. Using the matrix notation, the LMC can be written as:

$$\boldsymbol{\Gamma}(\mathbf{h}) = \sum_{u=1}^{N_S} \mathbf{B}^u g^u(\mathbf{h}) \qquad (1)$$

where $\boldsymbol{\Gamma}(\boldsymbol{h}) = [\gamma_{ij}(\mathbf{h})]$ is a symmetric matrix of the order $n \times n$, the diagonal and non-diagonal elements of which represent simple and cross semivariograms, respectively, for lag $\mathbf{h}$; $\boldsymbol{B}^u = [b^u_{ij}]$ is called coregionalization matrix and is a symmetric positive semi-definite matrix of the order $n \times n$ with real elements b^u_{ij}, which represent the sills of the (cross-) variograms ij at a specific spatial scale u. The model is authorized if the mathematical functions $g^u(\boldsymbol{h})$ are authorized semivariogram models.

21

The choice of number, type and parameters (sill, range) of the functions $g^u(\boldsymbol{h})$ is quite critical, but is made easier by good experience of the studied phenomena (Chiles and Guillen, 1984). Fitting of the LMC is performed by weighted least-squares approximation under the constraint of positive semi-definiteness of the $\boldsymbol{B}^u$, using the iterative procedures developed by Goulard and Voltz (1992). The best model is chosen by comparing the goodness of fit for several combinations of functions of $g^u(\boldsymbol{h})$ with different ranges on the basis of different types of cross-validation results.

Collocated cokriging

Collocated cokriging is a way of integrating exhaustive secondary information into primary variable modelling, where the contribution of the secondary variable to the cokriging estimate relies only on the cross-correlation with the primary variable. The approach is quite similar to ordinary cokriging (Wackernagel, 2003), with the only difference being in the neighbourhood search: the initial solution of collocated cokriging was to use the single secondary value located at the target grid node location. However, in ordinary cokriging the weights attached to the secondary variable must add up to zero, so if only one data value is used, its single weight is zero. The original technique is then extended so that the secondary variable is used at the target location and also at all the locations where the primary variable is defined within the neighbourhood. This solution has generally produced more reliable and stable results (Rivoirard, 2001). The modified version, also referred to as "Multi-Collocated Cokriging" in the literature, is less precise than full cokriging, as it does not use all the auxiliary information contained within the neighbourhood. However, because the co-located secondary datum tends to screen the influence of more distant secondary data, there is actually little loss of information. In this modified approach the influence of the secondary variable on the primary variable is explicitly taken into account through the estimation of both direct secondary variable variogram and cross-variogram.

FKA Analysis

Multivariate spatial datasets can also be analysed through FKA, a geostatistical method developed by Matheron (1982). The theory underlying FKA has been described in several publications (Goovaerts and Webster, 1994; Castrignanò et al., 2000; Wackernagel, 2003; Bourennane et al., 2004), so only the more salient points are reported here.

The three basic steps of FKA are as follows:

1) modelling the coregionalization of a set of variables, using Linear Model of Coregionalization (LMC) (Eq. 1);

2) analysing the correlation structure between the variables, at the different spatial scales, by

applying Principal Component Analysis (PCA);

3) cokriging regionalised factors at the characteristic scales and mapping them.

LMC was described above. Regionalized PCA consists of decomposing each coregionalization matrix $\boldsymbol{B}^u$ into two other diagonal matrices: the matrix of eigenvectors and the diagonal matrix of eigenvalues for each spatial scale u through the matrix $\boldsymbol{A}^u$ of the order n x n of the transformation coefficients a_{iv}^u (Wackernagel, 2003). The transformation coefficients a_{iv}^u in the matrix $\boldsymbol{A}^u$ correspond to the covariances between the original variables $Z_i(x)$ and a set of reciprocally orthogonal regionalized factors $Y_v^u(\mathbf{x})$:

$$Z_i(\mathbf{x}) = \sum_{u=1}^{N_S} \sum_{v=1}^{n} a_{iv}^u Y_v^u(\mathbf{x}) \tag{2}$$

The behaviour and relationships among variables at different spatial scales can be displayed by interpolating the regionalized factors $Y_v^u(\mathbf{x})$ using cokriging and mapping them (Castrignanò et al., 2000). The cokriging system in FKA has been thoroughly described by Wackernagel (2003).

Identification of potential management zones

To identify potential management zones, fuzzy c-means classification procedure was applied to cokriged maps of regionalised factors. Only factors with eigenvalues greater than 1 were used for the classification, since the soil variability represented by them was assumed significantly different from residual variation (Li et al., 2007). Fuzzy c-means classification produces a continuous grouping of objects by assigning partial class membership values, which is to be preferred for grouping properties in the soil continuum (Odeh et al., 1992).

There are three primary matrices involved in the clustering process (Fridgen et al., 2004): first there are the data to classify, the data matrix **Y**, consisting of n observations with p classification variables each (regionalised factors). Second is the cluster centroid matrix **V**, consisting of c cluster centroids located in the feature space defined by the p classification variables. Lastly, there is the fuzzy membership matrix **U**, consisting of membership values (uik) to every cluster in **V** for each observation in **Y**, bounded by the constraints that for all $i = 1$ to c and all $k = 1$ to n:

$$u_{ik} \in [0-1], \quad 1 \leq i \leq c, \quad 1 \leq k \leq n \quad \text{and} \quad \sum_{i=1}^{c} u_{ik} = 1, \quad 1 \leq k \leq n \tag{3}$$

To locate minimal solutions, the weighted within-groups sum of squared errors objective function, J_m, was applied :

$$\mathbf{J}_m(\mathbf{U}, v) = \sum_{k=1}^{n} \sum_{i=1}^{c} (u_{ik})^m (d_{ik})^2 \tag{4}$$

where m is the fuzziness weighting exponent ($1 \leq m < \infty$) and $(d_{ik})^2$ is the squared distance in feature space between the observation x_k and the centroid v_i of the cluster i. Fuzzy k-means classification was performed using the Management Zone Analysis (MZA) software (Fridgen et al., 2004). The fuzziness exponent was set at the conventional value of 1.35 (Odeh et al., 1992). The classification was repeated for a range of classes (c) between 2

and 6. The optimum *c*-value was identified on the basis of minimizing two indices: the fuzziness performance index (FPI) and the normalized classification entropy (NCE) (Odeh et al., 1992). FPI ($0 \leq FPI \leq 1$) is a measure of the degree of membership sharing among classes, where a value close to 1 indicates a strong sharing of membership and 0 represents distinct classes with no membership sharing. The NCE ($0 \leq NCE \leq 1$) estimates the degree of disorganization in the classification: a value close to 1 indicates strong disorganization and 0 reflects high organization.

Results and discussion

Gravel in the top layer ranged from 190 g kg^{-1} to 750 g kg^{-1}, with an average of 470 g kg^{-1} (Tab. 1). Gravel of 20-100 mm diameter was the most representative fraction (67% of the total gravel), while stones >100 mm in diameter were not found in the majority of samples. Gravel content sharply increased with depth, with values higher than 600 g kg^{-1} in layers deeper than 40 cm (Tab. 2). Gravel fraction >100 mm also increased with depth, reaching a content of 117 g kg^{-1} in the 80-100 cm layer. This fraction showed the highest CV, with a maximum of 225% observed in the 20-40cm layer (Tab. 2).

Fine components were equally distributed in the top layer (Tab. 1), with 33.7 % sand, 34% silt and 32.3% clay, whereas the sandy fraction prevailed in the deeper layers, up to 74% in the 80-100 cm layer (Table 2). Bulk density ranged from 1.0 to 2.3 g cm^{-3} in proportion to the gravel content (Table 1). EC (1:2) averaged 0.31 mS cm^{-1} and did not show a high variability (CV 22%), ranging from 0.2 to 0.49 mS cm^{-1}. Comparable CVs were observed for soil organic matter (15.3%) and TKN (18.1%), which had mean values of 6.67 and 2.1 g kg^{-1}. A slight increase in apparent EC was observed in depth: EC_h averaged 208 mSm^{-1}, ranging from 132 to 306 mSm^{-1}, while EC_v averaged 237 mSm^{-1}, with a minimum of 193 mSm^{-1} and a maximum of 557 mSm^{-1}.

The Pearson's correlation coefficient matrix of the measured variables in the top soil layer (Table 3) shows that significant correlations were only found between variables in a few cases. As regards the electromagnetic variables, EC_h shows higher correlations than EC_v and is negatively correlated with the coarser texture components (gravel, r = -0.5, sand, r = -0.56) and positively with the finer ones (silt, r= 0.69, clay, r = 0.67) and SOC (r =

0.43). A number of studies (e.g. Corwin and Lesch, 2005; Vitharana et al., 2008) reported similar relationships between EC_a and soil texture fractions. The significant correlation between EC_h and SOC appears to be more an indirect consequence of the texture effect on SOC than a direct effect of SOC on electrical conductivity. Generally, greater C input conversion efficiency and higher adsorption capacity are observed in clay soils, which allow stabilization of the organic carbon limit and prevent mineralisation (Morari et al., 2006). In the vineyard, positive correlations were observed between clay and SOC (r = 0.56), and silt and SOC (r = 0.54), while there was a negative correlation between sand and SOC (r = -0.48). No significant correlation was found between the electrical conductivity measured in a 1:2 suspension and EC_h or EC_v, most likely due to the relatively low variation of the salinity content in the 0-20 cm layer.

Significant correlations between EC and particle-size distribution were also estimated comparing data in the 1-m profiles (Tab. 4). ECh showed higher correlations with the fine texture components in the surface layers (0-20 and 20-40 cm), while no significant relationships were found in the deeper layers. On the contrary, ECv was negatively correlated with gravel content to 100 cm in depth, with the highest sensitivity in the 20-40 (r=-0.87) and 40-60 cm (r= -0.82) layers.

ERTs confirmed the relationships obtained by EMI analysis even if investigations were conducted in drier soil conditions. On average, ER increased from the surface layer (126 Ωm at 0-20 cm) to 45-70 cm (285 Ωm) and then gradually decreased in depth, reaching a value of 168 Ωm at 130-145 cm. Positive correlations were estimated between ER and the coarser components (sand, r = 0.45; gravel, r = 0.70), whereas negative correlations were estimated between ER and clay (r = -0.48).

Geostatistical elaborations

In order to save computing time and facilitate geostatistical elaborations, five variables showing the highest correlation coefficients in the top layer were selected: clay, sand, gravel, EC_h and EC_v (Table 3). However, correlation analysis, factor analysis and the calculations of probability levels are based on the assumption of a normal data distribution.

Because the selected variables did not show a Gaussian distribution at a χ^2 test with

26

p<0.05, they were submitted to Gaussian modelling before tackling the multivariate analysis. Each original variable was transformed using the first thirty Hermite polynomials, because this was sufficient to accurately reproduce the value of the variance for all variables. The variograms of the Gaussian variables (both direct and cross-variograms) were jointly fitted by a nested function with a nugget effect, a cubic model with a range of 70 m (short-range component) and a spherical model with a range of 120 m (long-range component). The spatial correlations between the EMI measurements and soil variables were evaluated from the cross-variograms of the corresponding Gaussian variables (Figure 3). The degree of coregionalization was assessed by the closeness of the cross-variogram to the "hull of perfect correlation" (Wackernagel, 2003), which comprises the lines of perfect positive and negative correlation between two variables. So, the spatial correlation resulted as higher and positive between EC_h and clay content, whereas it was higher and negative between EC_h and gravel and sand contents, which confirms what was observed in the correlation matrix (Tables 3 and 4). In the light of these results, EC_h was preferred to EC_v as auxiliary variable in multicollocated-cokriging. The Gaussian variables were estimated at the nodes of a 1-m grid and then back-transformed to the original variables.

The cokriged maps (Figure 4) show a prevalence of the finest soil fractions (clay) in the north-east of the vineyard, with a wide central area characterised by coarser material (high sand and gravel contents). The map of EC_h mode shows similar spatial features to those identified with clay, giving consistently high readings in the areas with finer texture. It is worth underlining that, despite the different sampling scale, both EC and soil properties share approximately the same basic structures of spatial dependence even if, of course, the electromagnetic measurements focus better on short-range variation, due to their much finer resolution. However, the absolute values of conductivity may not necessarily be diagnostic, so only the variations in conductivity should be used to identify anomalies (Benson et al., 1988).

ERT analysis confirmed the EC spatial pattern measured by EMI. Figure 5 shows the series of ERTs performed along the eastern side of the vineyard: in the NE corner, the 2D image reveals the presence of a homogeneous profile with relatively low resistivity (40-100 Ωm); resistivity increased moving southwards, where heterogeneous profiles were found characterised by a high resistivity layer (> 400 Ωm). The resistivity layer thickness

increased from 0.4 m to a maximum of 1.2 m in the central zone and then decreased and almost disappeared in the SE corner. This pattern was also observed in the central series of ERTs, while in the western one the resistivity layer was also almost continuous in the SW and NW corners (data not presented). The results confirm the presence of a lens formed by gravelly parent material, with low conductivity, variably distributed in the 3 dimensions, with an upper limit at 0.3-0.4 m depth (Tab. 2). The consistency between ERT and EMI demonstrates the capacity of the latter to indirectly represent the 3D variability in the gravel content. This has important implications for the adoption of Precision Viticulture as the gravelly lens could limit the rooting depth, affecting the quantity-quality performances of the vineyard. The use of EMI to estimate soil depth in a vineyard was experimented by Bramley at al. (2000). They applied a moving window regression technique using data from 190 georeferenced pits to infer soil depth from EMI measurements in a terra rossa soil. However, the relationship was valid only for that particular type of weathered soil, involving a sharp boundary with the limestone parent material, and could not be extended to other types of soils.

The spatial dependence between the two EMI variables and soil properties was also explored with FKA to provide a basis for zoning the vineyard. Table 5 reports the structure of the regionalised factors at the given spatial scales. From the addition of the eigenvalues corresponding to the different scales, 1.38 at nugget effect, 1.45 for short-range and 3.22 for long-range, it results that the total spatial variation is mostly dominated by spatially correlated variation at long scale. After the decomposition into regionalised factors, the first factor (F1) at short-range explains 85.3% of the variance at this spatial scale and is mainly and positively correlated with clay, but negatively with sand and gravel contents and, to a lesser extent, with EC_v. Another 15% of spatial variation at this scale is mainly explained by EC_h, which weighs positively on the second factor. The first regionalised factor at long-range explains 93% the total spatial variance at this scale and is positively correlated with clay and EC_h, but negatively with sand and gravel contents.

Ignoring the nugget effect, because it is most affected by measurement error, FKA has isolated two regionalised factors, which, with an acceptable loss of information, give a concise description of the studied process at the selected spatial scales. The spatial distributions of the two components are reported in the maps of figure 6, which were

obtained using an equal number of estimates in each of the four classification intervals. They show completely different patterns of spatial structure: at short-range the patterns run parallel to the longitudinal axis of the field, with a wide central strip characterized by coarser material, whereas at long-range the zonal distribution looks more erratic.

The fuzzy c-means classification procedure was applied to the two regionalised factors, which had an eigenvalue > 1. As the variables are orthogonal and with the same variance, the simpler Euclidean distance was calculated in the classification procedure. Results of clustering analysis (Fig. 7) clearly indicate that grouping data in three classes allowed both FPI and NCE indexes to be minimized. The concordance of the two indexes is an indication of the goodness of the classification and no further analyses were conducted to verify the results (Fridgen et al., 2004). Moreover, the use of significant regionalized variables, which integrated the information of the primary variables, avoided applying time-consuming clustering analysis to different input combinations to verify the most important variables for creating management zones (Fridgen et al., 2004).

The map of the potential management classes (Fig. 8) was obtained by a generalization of the fuzzy k-means class membership map by removing a few small spot clusters which were insignificant for practical site-specific management purposes. A clear link exists between these management classes and soil maps. Class 1 coincides with zones characterized by high clay and low gravel contents, class 2 occupied the central zones with high coarse material contents but intermediate values of EC_h and class 3 the zones with the lowest EC_h. The agronomic significance of this classification will be tested in the future by comparing the management zone map with grape quality and quantity maps.

Conclusions

In this work, multivariate geostatistical analysis has allowed the relationship between EMI observations and some soil physical properties to be described and, coupled with fuzzy k-means classification, to delineate potential management zones. Soil EC has no direct effect on crop growth or yield, so the utility of EMI mapping comes from the relationships that often exist between EC and a variety of soil properties. Spatial variation

of soil properties could therefore be advantageously inferred, using ancillary data, which are less expensive to obtain. In gravelly soils, this means that a good representation of the variability can be obtained with much less effort than that required for a traditional survey, e.g. in our study, sampling and sieving the 39 points required the work of 2 men for 3 weeks. However, it should not be forgotten that apparent soil EC is a quite complex measurement that requires knowledge and experience to be interpreted. Ground-truth soil samples are thus obligatory to understand and interpret EMI mapping. Furthermore, integration of EMI with other geophysical methods can improve the description of the soil profile, as we observed integrating EMI surveys with ERT.

Acknowledgements

References

Benson, R., Glaccum, R.A., Noel, M.R., 1988. Geophysical techniques for sensing buried wastes and waste migration. National Water Well Association, Dublin, OH, USA.

Blackmer, T.M., Schepers, J.S., Meyer, G.E., 1995. Remote sensing to detect nitrogen deficiency in corn. In: Robert, P.C., Rust, R.H., Larson, W.E. (Eds.), Proceedings of Site-specific Management for Agricultural Systems. Second International Conference, March 1994, Minneapolis, MN, USA, pp. 505-512.

Bocchi, S., Castrignanò, A., Fornaio, F., Maggiore, T., 2000. Application of factorial kriging for mapping soil variation at field scale. Eur. J. Agronomy 13, 295-308.

Bourennane, H., Nicoullaud, B., Couturier, A., King, D. 2004. Exploring the spatial relationships between some soil properties and wheat yields in two soil types. Prec. Agric. 5, 521-536.

Bramley, R.G.V., Proffitt, A.P.B., Corner, R.J., Evans, T.D., 2000. Variation in grape yield and soil depth in two contrasting Australian vineyards. In: Adams, J.A., Metherell, A.K. (Eds.), Soil 2000: New Horizons for a New Century, Australian & New Zealand 2nd Joint Soils Conference, No. 2: Oral Papers, New Zealand Society of Soil Science, Lincoln University, NZ, pp. 29-30.

Bramley, R.G.V., 2005. Understanding variability in winegrape production systems 2. Within vineyard variation in quality over several vintages. Aust. J. Grape Wine Res. 11, 33-42.

Brus, D.J., Knotters, M., van Dooremolen, P., van Kernebeek, P., van Seeters, R.J.M., 1992. The use of electromagnetic measurements of apparent soil electrical conductivity to predict the boulder clay depth. Geoderma 84, 79–84.

Buchter, B., Hinz. C., Flühler, H., 1994. Sample size determination of coarse fragment content in a stony soil. Geoderma 63, 265-275.

Casa, R., Castrignanò, A., 2008. Analysis of spatial relationships between soil and crop variables in a durum wheat field using a multivariate geostatistical approach. Eur. J. Agron. 28, 331-342.

Castrignanò, A., Giugliarini, L., Risaliti, R., Martinelli, N., 2000. Study of spatial relationships among some soil physico-chemical properties of a field in central Italy using multivariate geostatistics. Geoderma, 97, 39-60

Castrignanò, A., Buttafuoco, G., Giasi, R.C., 2008. Assessment of the Risk of Groundwater Salinisation Using Multivariate Geostatistics. GeoEnv VI – Geostatistics for Environmental Applications. Quantitative Geology and Geostatistics, Vol. 15, Springer, Berlin, Germany, pp. 191-202.

Chiles, J.P., Guillen, A., 1984. Variogrammes et krigeages pour la gravimétrie et le magnétisme. [Variograms and kriging for gravimetry and magnetism]. Sciences de la Terre, Série Informatique, 20, 455-468.

Corwin, D.L., Lesch, S.M., 2005. Apparent soil electrical conductivity measurements in agriculture. Comp. Electron. Agric. 46, 11-43.

Dalgaad, M., Have, H., Nehmdahl, H., 2001. Soil clay mapping by measurements of electromagnetic conductivity. In: Grenier, G., Blackmore, S. (Eds.), Proceedings of the 3rd

European Conference on Precision Agriculture, Agro, Vol. 1, Montepellier, France, pp. 367-372.

De Benedetto, D., Castrignanò, A., Sollitto, D., Campi, P., Modugno, F., 2008. Non-intrusive mapping of subsoil properties in agricultural fields with GPR and EMI. 1st Global Workshop on High Resolution Digital Soil Sensing & Mapping, 5-8 February 2008, Sydney, Australia, CD-ROM.

FAO, 1998. World reference base for soil resources. World Soil Resources, Report No. 84, FAO, Rome, Italy.

Flint, L.E., Flint, A.L., 2002. Porosity. In: Dane, J.H., Topp, G.C. (Eds.), Methods of Soil Analysis, Part 4-Physical Methods, SSSA Book Series 5, Soil Science Society of America, Inc., Madison, WI, USA, pp. 241-254.

Fridgen, J.J., Kitchen, N.R., Sudduth, K.A., Drummond, S.T., Wiebold, W.J., Fraisse, C.W., 2004. Management zone analyst (MZA): software for subfield management zone delineation. Agron. J. 96, 100-108.

Frogbrook, Z.L., Oliver, M.A., 2001. Comparing the spatial prediction of soil organic matter by two laboratory methods. Soil Use Manag. 17, 235-244.

Gee, G.W., Or, D., 2002. Particle-size analysis. In: Dane, J.H., Topp, G.C. (Eds.), Methods of Soil Analysis, Part 4-Physical Methods, SSSA Book Series 5, Soil Science Society of America, Inc., Madison, WI, USA, pp. 255-293.

Goovaerts, P., Webster, R., 1994. Scale dependent correlation between topsoil copper and cobalt concentrations in Scotland. Eur. J. Soil Sci. 45, 79-95.

Goovaerts, P., 2000. Geostatistical approaches for incorporating elevation into the spatial interpolation of rainfall. J. Hydr. 228, 113-129.

Goulard, M., Voltz, M., 1992. Linear coregionalization model: tools for estimation and choice of cross-variogram matrix. Math. Geo. 24, 269-286

Grossman, R.B., Reinsch, T.G., 2002. Bulk density and linear extensibility. In: Dane, J.H., Topp, G.C. (Eds.), Methods of Soil Analysis, Part 4-Physical Methods. SSSA Book Series 5, Soil Science Society of America, Inc., Madison, WI, USA, pp. 201-227.

Hendrickx, J.M.H., Das, B., Corwin, D.L., Wraith, J.M., Kachanoski, R.G., 2002. Indirect measurement of solute concentrations. In: Dane, J.H., Topp, G.C. (Eds.), Methods

of Soil Analysis, Part 4-Physical Methods. Book Series 5, Soil Science Society of America, Inc., Madison, WI, USA, pp. 1274-1306.

Hengl, T., Heuvelink, G.B.M., Stein, A., 2004. A generic framework for spatial prediction of soil variables based on regression-kriging. Geoderma 120, 75-93.

Journel, A.G., Huijbregts, C.J., 1978. Mining Geostatistics. Academic Press, London, UK.

Kaffka, S.R., Lesch, S.M., Bali, K.M., Corwin, D., 2005. Site-specific management in salt-affected sugar beet fields using electromagnetic induction. Comp. Electron. Agric. 46, 329-350.

Kjeldahl, J., 1883. Neue Methode zur Bestimmung des Stickstoffs in organischen Körpern. [New method for the determination of nitrogen in organic bodies]. Zeitschreft fur Analytische Chemie 22, 366-382.

LaBrecque, D.J., Morelli, G., Daily, B., Ramirez, A., Lundegard, P., 1995. Occam's inversion of 3-D ERT data. In: Spies, B. (Ed.), Three-Dimensional Electromagnetics, SEG, Tulsa, 575-590.

Li, Y., Shi, Z., Li, F., Li, H., 2007. Delineation of site-specific management zones using fuzzy clustering analysis in a coastal saline land. Comp. Electron. Agric. 56, 174–186.

Matheron, G., 1982. Pour une analyse krigeante des données regionalisées [For a kriging analysis of regionalized data]. Report No. 732, Centre de Geostatistique, Fontainebleau, France.

McBratney, A.B., Odeh, I.O.A., Bishop, T.F.A., Dunbar, M.S., Shatar, T.M., 2000. An overview of pedometric techniques for use in soil survey. Geoderma 97, 293-327.

McNeil, J.D., 1990. Geonics EM38 Ground Conductivity Meter: EM38 Operating Manual. Geonics Limited, Ontario, Canada.

Morari, F., Lugato, E., Berti, A., Giardini, L., 2006. Long-term effects of recommended management practices (RMPs) on soil carbon evolution and sequestration in north-eastern Italy. Soil Use Manag. 22, 71–81

Morelli, G., LaBrecque, D.J., 1996. Advances in ERT inverse modelling. Eur. J. Environ. Eng. Geophys. 1, 171-186.

Mulla, D.J., 1997. Geostatistics, remote sensing and precision farming. In: Lake, J.V., Bock, G.R., Goode, J.A. (Eds.), Precision Agriculture: Spatial and Temporal Variability of Environmental Quality, John Wiley and Sons Ltd, Chichester, United Kingdom, pp. 1-18.

Odeh, I.O.A., McBratney, A.B., Chittleborough, D.J., 1992. Soil pattern recognition with fuzzy-c-means: application to classification and soil–landform interrelationships. Soil Sci. Soc. Am. J. 56, 505–516.

Pellerin, L., Wannamaker, P.E., 2005. Multi-dimensional electromagnetic modeling and inversion with application to near-surface earth investigations. Comp. Electron. Agric. 46, 71–102.

Rhoades, J.D., Corwin, D.L., Lesch, S., 1999 a. Geospatial measurements of soil electrical conductivity to assess soil salinity and diffuse salt loading from irrigation. In: Corwin, D.L., Loague, K., Ellsworth, T.R. (Eds.), Assessment of Non-point Source Pollution in the Vadose Zone, Geophysical Monograph., 108, AGU, Washington, DC, USA, pp. 197-215.

Rhoades, J.D., Chanduvi, F., Lesch, S., 1999 b. Soil salinity assessment: methods and interpretation of electrical conductivity measurements. FAO Irrigation and Drainage. Paper No. 57, FAO, Rome, Italy.

Rivoirard, J., 2001. Which models for collocated cokriging? Math. Geo. 33, 117-131.

Rizzo, E., Colella, A., La penna, V., Piscitelli, S. 2004. High-resolution images of the fault-controlled High Agri Valley basin (Southern Italy) with deep and shallow electrical resistivity tomographies. Phys. Chem. Earth 29, 321-327.

Royle, J.A., Berliner, L.M., 1999. A hierarchical approach to multivariate spatial modelling and prediction. J. Agric. Biol. Environ. Stat. 4, 29-56.

Sudduth, K.A., Kitchen, N.R., Hughes, D.F., Drummond, S.T., 1995. Electromagnetic induction sensing as an indicator of productivity on claypan soils. In: Probert, P.G., Rust, R.I.H., Larson, W.E., (Eds.), Proceedings of the Second International Conference on Site Specific Management for Agricultural Systems. Minneapolis, MN, USA, pp. 671–68.

Triantafilis, J., Lesch, S.M., 2005. Mapping clay content variation using electromagnetic induction techniques. Comp. Electron. Agric. 46, 203-237.

Vitharana, U.W.A., Van Meirvenne, M., Simpson, D., Cockx, L., De Baerdemaeker, J., 2008. Key soil and topographic properties to delineate potential management classes for precision agriculture in the European loess area. Geoderma 143, 206-215.

Wackernagel, H., 2003. Multivariate Geostatistics. An Introduction with Applications. Third Edition Springer Verlag, Berlin, Germany.

Walkley, A., Black, I.A., 1934. An examination of the Degtjareff method for determining soil organic matter and a proposed modification of the chromic acid titration method. Soil Sci. 37, 29-38.

Webster, R., Oliver, M.A., 2001. Geostatistics for Environmental Scientists. J. Wiley and Sons, Chichester, United Kingdom.

Zhou, B., Greenhalgh, S., 2001. Finite element three-dimensional direct current resistivity modelling: accuracy and efficiency considerations. Geophys. J. Int. 145, 679-688.

Figure 1 Mobile EC equipment: a) EMI sensor; b) GPS; c) hardware interfacing (hidden inside tractor cabin); d) transport platform.
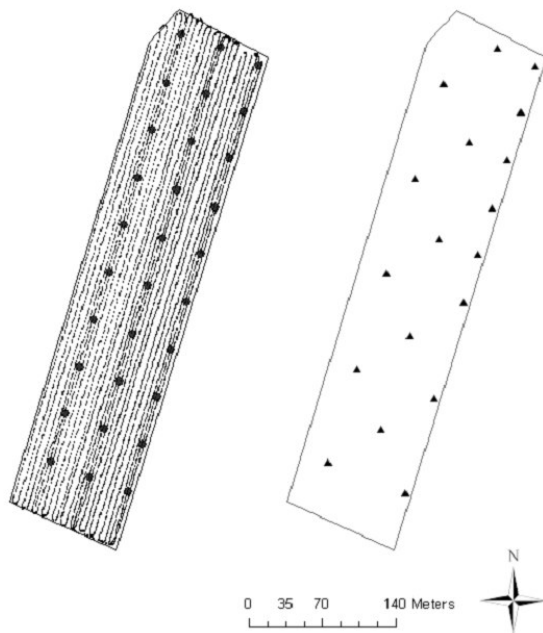
Figure 2 Left: main sampling grid (bigger dots) and EMI measurement transects (smaller dots). Right: positions of the Electrical Resistivity Tomographies.
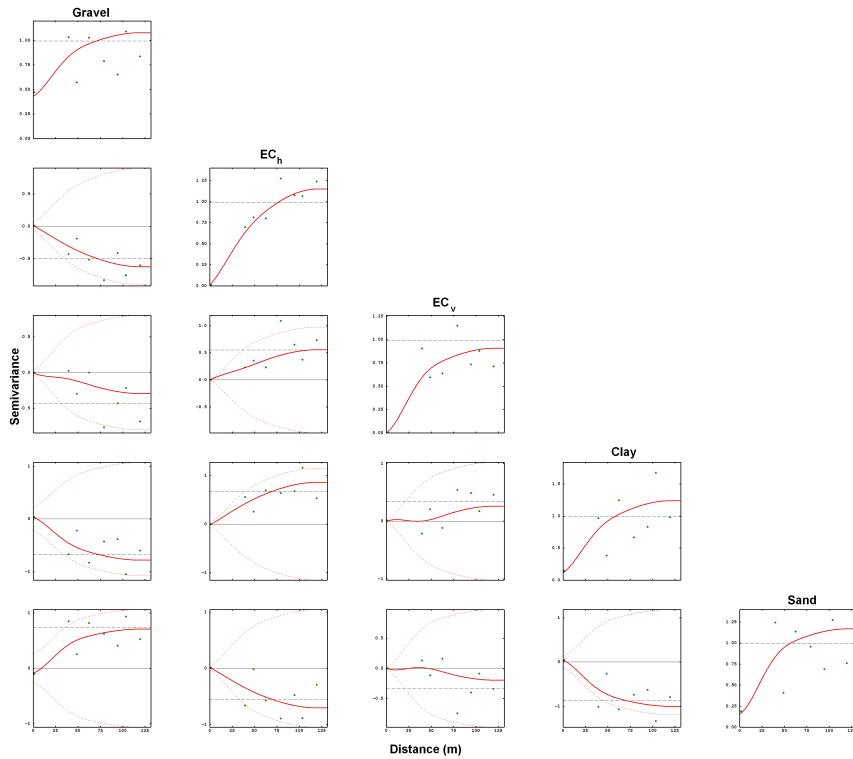
Figure 3 Direct variograms and cross-variograms between electrical conductivity in horizontal (ECh) and vertical modes (ECv) and selected soil variables.
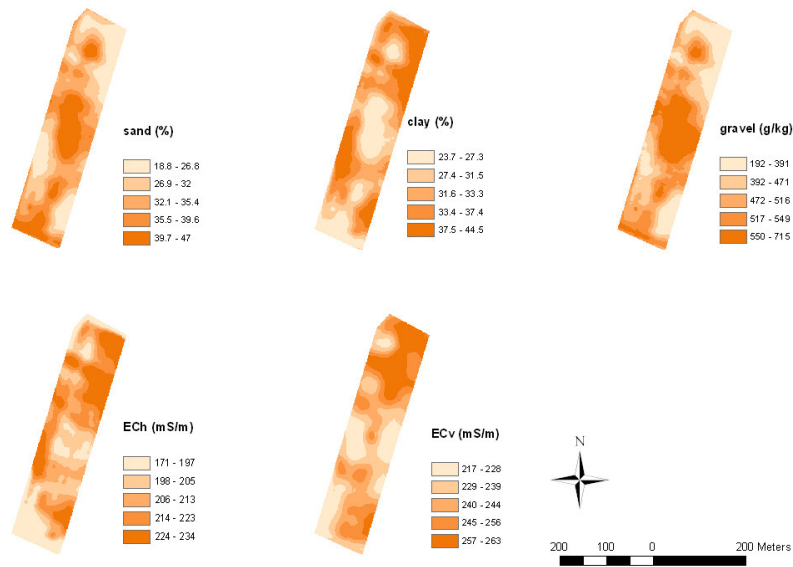
Figure 4 Maps of clay, silt, sand, gravel and electrical conductivity in horizontal (ECh) and vertical modes (ECv).
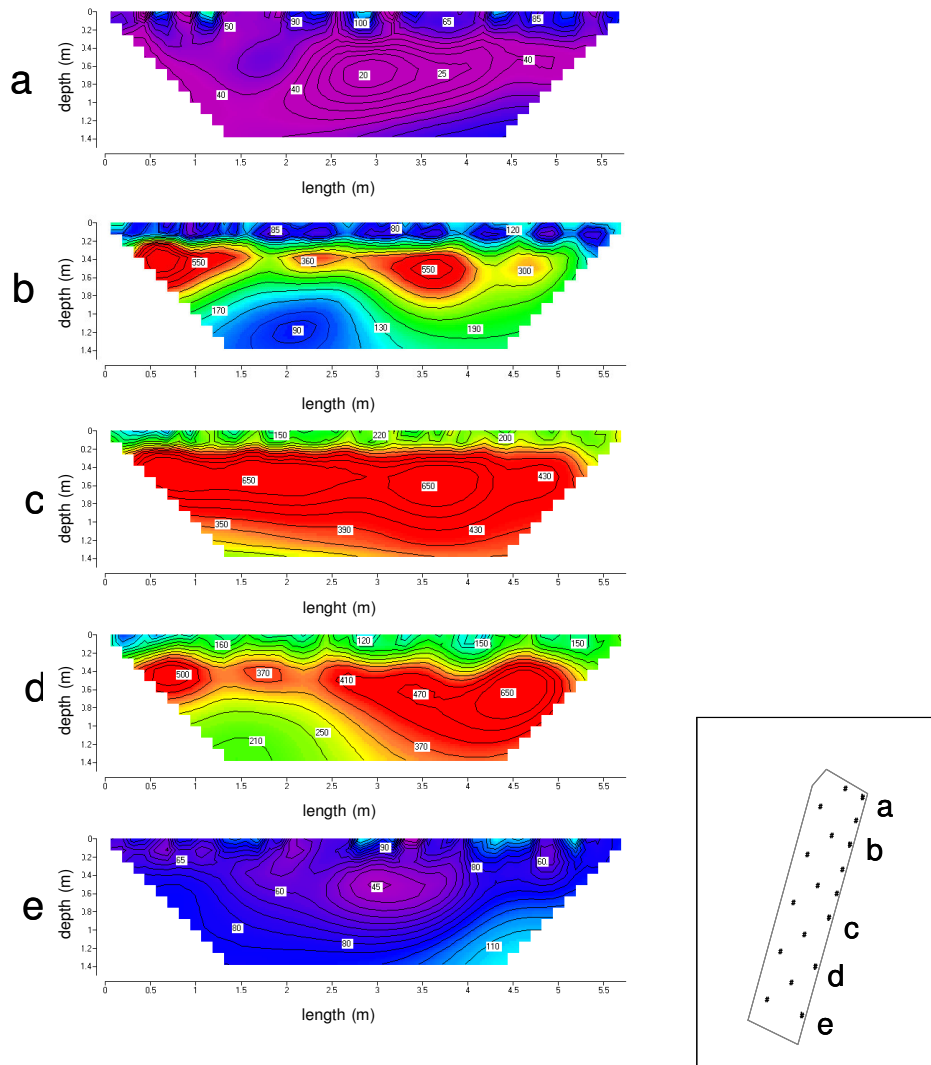
Figure 5 Electrical Resistivity Tomography profiles (Ω*m) of eastern side.
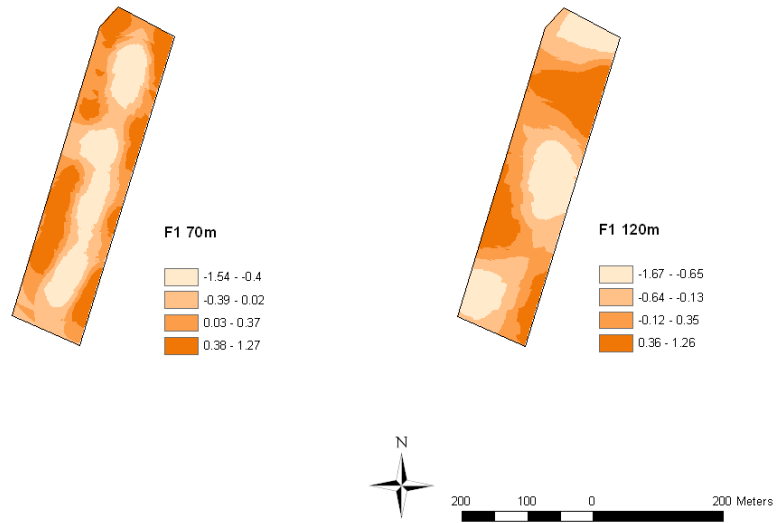
Figure 6 Maps of the short- (1-70 m) and long-range (1-120m) components of the first factor.
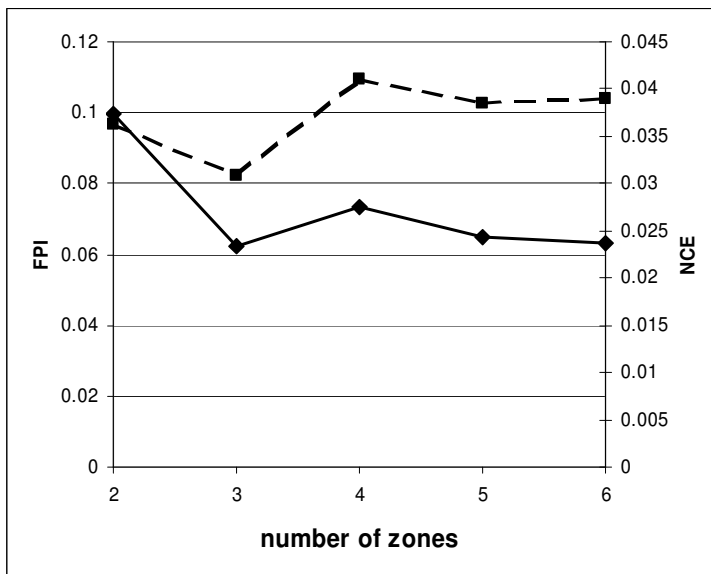
Figure 7 Fuzziness performance index (FPI) and the normalized classification entropy (NCE) as calculated for the study area.
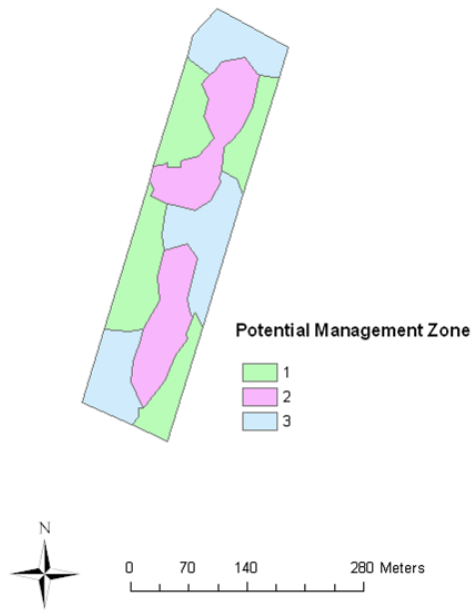
Figure 8 Management zones map (three clusters).

Tables

	Mean	S.E.	Min	Max	CV, %
gravel (> 2 mm), g kg^{-1}	474	23.7	191.9	750.6	31.2
gravel (2-20 mm), g kg^{-1}	143	9.5	31.4	242.6	15.3
gravel (20-100 mm), g kg^{-1}	325	19.7	117.8	642.1	31.6
gravel (> 100 mm), g kg^{-1}	7	6.5	0.00	25.40	10.4
fine component (<2 mm), g kg^{-1}	526	23.7	249.4	808.1	38.0
sand (0.05-2 mm), %	33.7	1.26	18.83	47.76	23.4
silt (0.002-0.05 mm), %	34.0	0.57	27.64	41.61	10.4
clay (< 0.002 mm), %	32.3	0.96	20.18	44.45	18.5
bulk density, g cm^{-3}	1.64	0.04	1.00	2.27	14.4
bulk density (< 2mm), g cm^{-3}	1.23	0.04	0.80	1.71	18.9
particle density (>2mm), g cm^{-3}	2.55	0.03	2.19	2.71	1.2
pH	7.04	0.02	6.69	7.36	2.2
EC (1:2), mS cm^{-1}	0.31	0.01	0.20	0.49	21.5
SOC, g kg^{-1}	6.67	0.17	5.00	8.60	15.3
TKN, g kg^{-1}	2.10	0.10	1.40	3.17	18.1

Table 1 Mean physical-chemical characteristics of the top layer (0-20 cm; 39 samples)

	SOIL LAYER														
	0-20cm			20-40cm			40-60cm			60-80cm			80-100cm		
	Mean	S.E.	CV	Mean	S.E.	CV	Mean	S.E.	CV	Mean	S.E.	CV	Mean	S.E.	CV
gravel (> 2 mm), g kg^{-1}	332	51.5	51.5	440	77.8	58.7	613	61.7	33.4	683	68.2	33.1	723	59.5	27.3
Gravel (2-20 mm), g kg^{-1}	172	26.8	51.7	15.2	28.5	62	218	18.0	27.5	254	30.6	40.1	265	30.5	38.2
Gravel (20-100 mm), g kg^{-1}	160	30.8	63.8	23.9	47.7	66.1	323	42.7	43.8	381	52.2	45.4	341	27.2	26.4
Gravel (> 100 mm), g kg^{-1}	0	0	0	48	32.8	225.1	72	37.8	173.9	48	22.5	155.5	117	44.1	125.6
fine component (<2 mm) g kg^{-1}	668	51.5	25.6	560	77.8	46.1	387	61.7	52.9	317	68.2	71.3	277	59.5	71.2
sand (0.05-2 mm), %	36.6	3.12	28.3	40.1	5.08	42	55.5	4.22	25.2	66.6	5.36	26.7	73.6	5.21	23.5
silt (0.002-0.05 mm), %	28.7	1.23	14.3	27.3	2.29	27.8	22.5	2.24	33	17.8	2.71	50.5	13.7	2.29	55.4
clay (< 0.002 mm), %	34.8	2.21	21.1	32.6	3.01	30.7	21.9	2.56	38.8	15.6	3.06	64.9	12.7	3.05	79.7

Table 2 Particle size distribution (fine components and gravel) in the 1-m profile (12 profiles)

	Gravel	Sand	Silt	Clay	BD	BD (< 2mm)	pH	Ec (1:2)	TKN	SOC	EC_h	EC_v
Gravel	**1.00**											
Sand	**0.78**	**1.00**										
Silt	**-0.70**	**-0.92**	**1.00**									
Clay	**-0.73**	**-0.90**	0.39	**1.00**								
BD	**0.54**	**0.47**	-0.28	-0.37	**1.00**							
BD (< 2mm)	-0.16	-0.05	0.22	0.14	**0.73**	**1.00**						
pH	0.02	0.11	-0.14	0.01	0.08	0.07	**1.00**					
EC (1:2)	0.19	0.16	-0.38	-0.26	0.03	-0.10	-0.29	**1.00**				
TKN	0.36	0.38	**-0.43**	**-0.43**	0.03	-0.22	-0.07	0.32	**1.00**			
SOC	-0.22	**-0.48**	**0.54**	**0.56**	-0.15	-0.03	-0.01	-0.29	-0.37	**1.00**		
EC_h	**-0.50**	**-0.56**	**0.69**	**0.67**	-0.33	-0.02	0.02	-0.14	-0.20	**0.43**	**1.00**	
EC_v	**-0.40**	-0.30	0.36	0.30	-0.26	0.00	-0.08	0.32	-0.04	0.27	**0.53**	**1.00**

Table 3 Matrix correlation between parameters in top soil layer. Bold coefficients indicate p<0.05 [BD = bulk density]

	sand 1	clay 1	gravel 1	sand 2	clay 2	gravel 2	sand 3	clay 3	gravel 3	sand 4	clay 4	gravel 4	sand 5	clay 5	gravel 5	Ech	Ecv
sand 1	1.00																
clay 1	**-0.95**	1.00															
gravel 1	**0.70**	**-0.65**	1.00														
sand 2	**0.74**	**-0.67**	**0.77**	1.00													
clay 2	**-0.82**	**0.81**	**-0.74**	**-0.97**	1.00												
gravel 2	0.59	-0.53	**0.81**	**0.69**	**-0.67**	1.00											
sand 3	0.33	-0.21	**0.73**	0.58	-0.46	**0.67**	1.00										
clay 3	-0.45	0.40	**-0.76**	-0.55	0.50	**-0.85**	**-0.90**	1.00									
gravel 3	0.50	-0.50	**0.82**	**0.64**	**-0.63**	**0.92**	**0.73**	**-0.88**	1.00								
sand 4	0.12	0.00	0.38	0.31	-0.18	0.33	**0.64**	-0.46	0.16	1.00							
clay 4	-0.24	0.14	**-0.63**	-0.49	0.36	-0.52	**-0.79**	0.64	-0.40	**-0.94**	1.00						
gravel 4	0.32	-0.13	**0.71**	0.56	-0.42	**0.77**	**0.74**	**-0.66**	**0.68**	0.57	**-0.68**	1.00					
sand 5	-0.10	0.19	0.27	0.32	-0.19	0.43	0.61	-0.49	0.34	**0.78**	**-0.77**	**0.65**	1.00				
clay 5	0.13	-0.20	-0.31	-0.29	0.17	-0.42	**-0.65**	0.54	-0.39	**-0.73**	0.77	-0.65	**-0.98**	1.00			
gravel 5	0.22	-0.04	**0.64**	0.47	-0.33	**0.78**	**0.77**	**-0.71**	**0.69**	0.62	**-0.70**	**0.96**	0.70	-0.67	1.00		
Ech	**-0.89**	**0.93**	**-0.61**	**-0.64**	**0.78**	-0.42	-0.22	0.36	-0.42	0.02	0.08	-0.01	0.15	-0.17	0.03	1.00	
Ecv	**-0.72**	**0.70**	**-0.76**	-0.58	**0.63**	**-0.87**	-0.58	**0.77**	**-0.82**	-0.34	0.45	**-0.61**	-0.30	0.27	**-0.63**	0.64	1.00

Table 4 Matrix correlation between parameters in the 1-m soil profile. Bold coefficients indicate p<0.05 [1= layer 0-20cm ; 2= layer 20-40 cm ; 3= layer 40-60cm ; 4= layer 60-80cm ; 5= layer 80-100cm]

	Clay	Sand	Gravel	EC_H	EC_V	Eigen. Val.	Var. Perc.
Nugget effect							
Factor 1	0.077	-0.189	-0.037	-0.010	0.978	0.78	54.01
Factor 2	-0.082	0.253	-0.964	-0.014	0.019	0.46	31.50
Factor 3	-0.717	-0.682	-0.120	0.002	-0.080	0.16	11.04
Factor 4	-0.607	0.583	0.202	0.470	0.172	0.05	3.45
Factor 5	-0.324	0.308	0.122	-0.883	0.080	0.00	0.00
Cubic Range = 70.00m							
Factor 1	0.477	-0.650	-0.501	0.067	-0.308	1.08	85.27
Factor 2	0.132	-0.107	0.029	-0.970	0.173	0.19	14.73
Factor 3	0.322	-0.387	0.385	0.229	0.739	0.00	0.00
Factor 4	0.384	-0.024	0.736	-0.023	-0.557	0.00	0.00
Factor 5	0.710	0.645	-0.242	0.043	0.141	0.00	0.00
Spherical Range = 120							
Factor 1	0.562	-0.438	-0.358	0.554	-0.242	2.99	92.92
Factor 2	0.182	-0.104	0.102	-0.551	-0.801	0.23	7.08
Factor 3	-0.662	-0.545	0.303	0.322	-0.263	0.00	0.00
Factor 4	0.250	0.456	0.689	0.452	-0.226	0.00	0.00
Factor 5	0.388	-0.541	0.543	-0.285	0.424	0.00	0.00

Table 5 Structure of the regionalised factors

3 Hydraulic properties of stony soils: laboratory applications

Abstract

Hydraulic properties were studied comparing reconstructed and undisturbed soil sample behavior by saturated hydraulic conductivity (K_s) measurements and evaporation experiments. Reconstructed samples were manually constructed using sieved clay soil and synthetic sand, as fine earth fraction, and glass spheres or cylinders, as coarse fraction. Glass was chosen because it has not any porosity, so it could be possible to evaluate the steric role of coarse fragment on soil hydraulic properties. Volume coarse fractions used were: no fragments, 5%, 10%, 20%, 30%. The van Genuchten-Mualem (VGM) parameters of reconstructed and undisturbed samples were estimated by RETC and Hydrus 1D, respectively. Regarding the reconstructed samples, correlations among R_v, fine earth bulk density (bd_{fe}) and VGM parameters were useful to understand stone effects on water retention curve and on unsaturated hydraulic conductivity function (K_u). The undisturbed samples results underlined the importance of the R_v-bd_{fe} relationship. Moreover, K_s showed a positive relationship with R_v, which is in contrast with the theoretical approaches. The effect of R_v on the retention curve was well explained by the theoretical approach, in all the observed results, thus the nowadays applied correction is accurate. K_s and K_u, probably due also to their intrinsically high variability, could not always be explained by any normally used equations, nevertheless do consider the bd_{fe} might help to better describe the influence of the rock fragment content on the hydraulic conductivity.

Keywords: coarse fragments, soil hydraulic properties, bulk density, van Genuchten-Mualem parameters.

Introduction

Stony soils are widespread: they occupy more than 60% of the land in the Mediterranean area (Poesen, 1990). The relative amount of coarse fragment in the topsoil may be expressed as: rock fragment coverage of the soil surface (R_c), rock fragment content by weight (R_w) and rock fragment content by volume (R_v). R_c can be assessed by visual estimates (by comparing with area charts), by the point-count method or by transecting (Poesen and Levee, 1994) or by image processing (Graham et al., 2005). The amount of coarse fragments has to be known to quantify its role, and if direct measurements are not available then the amount of stones must be estimated (tab 1). When converting data on R_w to R_v and vice versa, caution is required. Particle density value between 2.65 and 2.75 g cm^{-3} for the stones might be used only if the rock fragments have no porosity (Poesen and Levee, 1994).

Stones play a role in soil by modifying the pore space (Fiès et al.,2002). In natural soils, increasing rock fragment content is correlated with increasing total bulk density of the soil (bd_t - stones plus fine earth) and decreasing bulk density of the fine earth (bd_{fe}) (Torri et al., 1994). There are a number of possible reasons for the occurrence of the latter negative relationship (Poesen and Levee, 1994):

- at high stone contents there may happen a situation where fine earth is insufficient to fill the voids in between the rock fragments determining lower bd_{fe} values;
- in a mixture of different particle size grades, the smaller particles cannot pack as closely to the larger particles as they can within each other;
- fine earth and stones react in a different way when expanding and contracting (e.g. during the process of wetting and drying or of freezing and thawing), thus causing void formation;
- nature of the fine earth fraction is changed by the presence of stones, indeed in a decreasing mass of fine earth several biogeochemical processes are concentrated, i.e. decay of organic matter, fertilizer inputs, etc., thus affecting other soil properties such as soil structure.

Ingelmo et al. (1994) reported that the formation of macroporosity might be a consequence of physical processes (swelling-shrinking; freezing-thawing), chemical processes (aerobic-anaerobic conditions), and ecological changes (soil fauna may dig deeper to find favorable conditions in the contact areas between soil and rock fragments).

The effect of stones on the hydraulic properties of the soil is associated with the (re)-arrangement of fine soil particles. Fiès et al. (2002) in a study of the behaviour of two soil (clay and silt-clay) in mixture with different percentage of glass fragments showed that when a solid material such as glass are incorporated into soils, this always causes a reduction in total water storage. Available water content of soils containing rock fragments depends on several parameters (Cousin et al., 2003) :

- − the origin of the rock fragments;
- − the volumetric percentage of the rock fragments;
- − the size and the porosity of the rock fragments;
- − the position of the rock fragments.

Peck and Watson (1979) (*P&W*) determined, based on the heat transfer theory, a formula for a homogeneous medium containing non-porous spherical inclusions to calculate the hydraulic conductivity of a stony soil from the hydraulic conductivity of the fine earth and the volumetric percentage of rock fragments:

$$K_{soil}/K_{fe} = (2*(1-R_v))/(2+R_v) \qquad (1)$$

where K_{soil} represents the hydraulic conductivity of the soil and K_{fe} of the fine earth and R_v is the volumetric fraction of the rock fragments.

Bouwer and Rice (1984) (*B&R*) evidenced that the previous equation overestimated the hydraulic conductivity for high water content, thus they proposed :

$$K_{soil}/K_{fe} = e_{soil}/e_{fe} \qquad (2)$$

where e_{soil} and e_{fe} are respectively the void ratio of the gravelly soil and of the fine earth fraction alone.

Brakensiek et al. (1986) (*B*) underlined that the stone volume fraction is not as available as the weight one, thus referring to Flint and Childs (1984), they define the following conversion equation:

$$R_v = \alpha(R_w)/[1 - R_w(1-\alpha)] \tag{3}$$

where R_w is the weight coarse fraction and α is the ratio between the bulk density of the fine earth and the bulk density of the stones (2.65 g cm^{-3}). Substituting (3) into (1), defines:

$$K_{soil}/K_{fe} = (1 - R_w)/((1 - R_w * (1 - 3\alpha/2))) \tag{4}$$

According to Flint and Childs (1984), α approximate 0.5, thus Brakensiek et al. (1986) could further reduce the previous equation to (*B-s*):

$$K_{soil}/K_{fe} = 1 - R_w \tag{5}$$

Bagarello and Iovino (2007) showed that, considering a unique particle density for both the fine-earth fraction and the rock fragments, equation (2) is equal to equation (5).

Finally, Morgan et al. (1998) (*M*), in a soil erosion model used the following equation proposed by Woolhiser et al. (1990):

$$K_{soil}/K_{fe} = 1 - R_v \tag{6}$$

where R_v is the volume based coarse fraction content. This equation considers a smaller influence of the stones than equation (5): indeed R_w is bigger that R_v.

Using reconstructed samples Mehuys et al. (1975) studied the unsaturated hydraulic conductivity (K_u) of stony and non-stony dry soils and they find that the relationship between K_u and matric potential of stony soils can be described by that one of the non-stony soil. On the contrary, the relationship K_u -water content of the non-stony soil may not be used in the same way because they found an higher K_u in the stony soil in respect with the non-stony one. Moreover, they underlined that if the bulk density of the reconstructed column is the same of the bulk density of the field, it is possible to use the hydraulic properties of the fine earth particle without any correction.

Bouwer and Rice (1984) studied the behaviour of saturated (K_s) and unsaturated hydraulic conductivity (K_u) in reconstructed stony columns and they concluded that:

1. K_s of the stony soil (stones plus fine particles - K_{soil}) can be calculated multiplying the K_s of the fine earth particle (K_{fe}) with the void ratio of stony – non-stony soils. (eq. 2);

50

2. K_u of the stony soil can be determined from K_u of the fine earth fraction, by moving down the K_u curve of the soil alone until its K_s coincides with the bulk K_s of the stony soil calculated as previously mentioned, thus the air entry value remains the same for the stony and non-stony soils;

3. the volumetric water content of the stony soil (θ_{soil}) can be reduced multiplying the volumetric water content of the fine particle (θ_{fe}) with the stone volume fraction (R_v):

$$\theta_{soil} = \theta_{fe} * (1 - R_v) \tag{7}$$

On the other hand, Ravina and Magier (1984) studied the behaviour of compacted clayey stony soil and they affirmed that "the effect of rock fragments on hydraulic conductivity and moisture retention of aggregated clay soils cannot be adequately accounted for by simple corrections for the reduced area available for flow and reduced total pore volume, at least not in the high moisture (low suction) range".

The main objectives of this work are:

    a. to describe the steric influences of "artificial" coarse fragment content, such as spherical and cylindrical glass, on the soil hydraulic properties of reconstructed clay and sand soil (250 cm^3);

    b. to describe the influence of stoniness on undisturbed soil samples (250 cm^3);

    c. to analyse how theoretical approaches can describe the above data.

To achieve them, evaporation experiments and saturated hydraulic conductivity analysis were conducted on those samples.

Material and methods

Reconstructed samples

The steric influence of the "coarse" fragments was studied by mean of reconstructed samples. They were manually constructed using 2 mm sieved clay (25% sand, 23 % silt and 52% clay –USDA, pH 6.5 , SOC 1.2%) or "sand" (synthetic material, constant diameter of 70 μm, without SOC) as fine earth fraction and glass spheres (average diameter 1.59 cm) or glass cylinders (2 cm x 1 cm) as coarse fraction. Arrangements of spheres and cylinders were as symmetrical as possible within the samples. The choice to use the glass was to have a material which did not have any porosity, so it could be possible to evaluate the steric role of coarse fragment on soil hydraulic properties. Volume coarse fractions used were: no fragments, 5%, 10%, 20%, 30%, with five replicates for the K_s measurements and three replicates for the evaporation experiments. (tab 2). As the samples were prepared, they were saturated by freely bottom infiltration at atmospheric pressure, laying the sample in a water bath for at least a couple of days. Samples were then set in the sandbox apparatus and subjected to -50 cm of matric suction, which was applied for at least a couple of days to consolidate the samples (Dane and Hopmans, 2002). The former procedure was the same for the K_s determination and the evaporation experiment replicates.

Undisturbed samples

Undisturbed soil samples (n. 37) (250 cm^3) were collected, using the core method (Grossman and Reinsch, 2002) at an average sampling depth of 30 cm, in Valpolicella (north eastern Italy) in 12 fields, different for texture and coarse fragment contents (fig 1 and tab 3). Those samples were firstly subjected to K_s measurements and subsequently to evaporation experiments. Moreover, disturbed samples were collected, thus it was possible to determine the texture by the hydrometer method (ASTM, 2000) and the water content at -15,000 cm by the

pressure plate extractor apparatus (Dane and Hopmans, 2002). Mercury intrusion porosimetry analysis were conducted on aggregates of about 8 g, which were air-dried prior to analysis. Pores within the range 10 μm-600 μm were analysed with Pascal 140 (Thermo Electron, 2004) using wide and ultra dilatometers; pores within the range 0.007 μm-10 μm were analysed with Pascal 240 (Thermo Electron, 2004) using wide dilatometer. Pore size distribution was classified according to the six classes proposed by Brewer (1964): 1) Ultramacropores: 100-5,000 μm; 2) Macropores: 75-100 µm; 3) Mesopores: 30-75 µm; 4) Micropores: 5-30 µm; 5) Ultramicropores: 0.1-5-µm; 6) Criptopores: < 0.1 µm. For the Ultramacropores class, as previously mention, the range was 100-600 µm.

Hydraulic Analyses

Both reconstructed and undisturbed samples were subjected at saturated hydraulic conductivity measurements and evaporation experiments. For reconstructed samples, the two analysis were conducted on different samples, while the same samples had been undergone both analysis.

Saturated hydraulic conductivity

Saturated hydraulic conductivity (K_s) measurements were conducted using the laboratory permeameter, with ascendant water flow (Eijkelkamp, 2003). Assuming uniformity of flow domain, K_s is determined using the Darcy equation:

$$q = -K_s \, \Delta H / \Delta z \qquad (8)$$

where q (cm d^{-1}) water flux, $\Delta H/\Delta z$ (cm cm^{-1}) hydraulic gradient, H (cm) total hydraulic head, h (cm) pressure head, z (cm) gravitational head (Jury and Horton, 2004)

Ks measurements was determined both with constant and variable head method, according to the hydraulic properties of the medium. As rule of thumb, K_s value greater than 50 cm d^{-1} are easily determined by the former method, while the latter is

normally conducted at smaller K_s values. Before conducting the analysis, samples were: a) freely upward saturated at atmospheric pressure, using de-aerated water with 5‰ of boric acid. Water bath reached ¾ of sample height; b) subjected at 0.6 atm. pressure, to completely de-aerated them; c) subsequently saturated again as previously described.

Unsaturated hydraulic conductivity and retention curve

Unsaturated hydraulic conductivity and retention curve were determined by evaporation experiments which were conducted using the ku-pF Apparatus DT 04-01 (UGT, 2005). Before starting the analysis, samples were saturated as previously explained for the K_s measurement. Two electronic tensionmeters, after calibration, were inserted inside the sample, at 1.5 cm and 4.5 cm height. Matric potential and water loss values were stored every 10 minutes using a datalogger. Samples were let to freely evaporate at the surface, while no flux was allowed at the bottom, since it was sealed. Experiments were stopped when the top tensionmeter reached a value of about -800÷-900 cm (UGT, 2005) or when the tensionmeters value were not reliable anymore (e.g. bottom value smaller than top one). At the end of the analysis, the samples were destroy, and after removal of the coarse fragments, the gravimetric water content of the fine earth fraction was determined after 12 h in oven at 105° C. For undisturbed samples coarse fragments were divided in two size classes: a) from 2 mm to 2 cm; b) from 2 cm to 10 cm (Glendon e Dani, 2002). Stored data were used to directly calculated the retention curve and the hydraulic conductivity. Assuming quasi-stationary flow, the Darcy- Buckingham equation was used to calculate the hydraulic conductivity of the soil samples:

$$q = -K(\theta)(\partial H/\partial z) = -K(h)(\partial H/\partial z); H = h + z \qquad (9)$$

where q (cm d^{-1}) water flux, $\partial H/\partial z$ (cm cm^{-1}) hydraulic gradient, $K(\theta)$ (cm d^{-1}) unsaturated hydraulic conductivity expressed in water content basis, $K(h)$ (cm d^{-1}) unsaturated hydraulic conductivity expressed in matric potential basis, H (cm) total hydraulic head, h (cm) pressure head, z (cm) gravitational head (Reynolds e al., 2002)

Constant hydraulic gradient was always considered throughout the sample height. The pressure (tensiometer measurement) and gravitation head formed the (total) gradient. Due to the experiment set up (freely evaporation at the top and sealed bottom), it was possible to consider a mean flow rate between tensionmeters, allowing to calculate a sample-halfway hydraulic conductivity, at least since the difference of the matric potential between the tensionmeters was less than about -50 cm. The retention curve was calculated as the relationship between the actual water content of the sample and the taken mean of the two tensiometer measurements.

<u>Parameter estimation</u>

To describe the hydraulic behaviour of reconstructed and undisturbed samples, the van Genuchten (VG) (1980) model for the retention curve and the Mualem (1976) model for the hydraulic conductivity function were chosen. VG equation is:

$$S_e = \frac{1}{\left[1 + (\alpha h)^n\right]^m} \tag{10}$$

where

$$S_e = \frac{\theta - \theta_r}{\theta_s - \theta_r} \tag{11}$$

with S_e ($0 \leq S_e \leq 1$) effective degree of saturation, θ_s and θ_r respectively saturated and residual water content, α, n e m (m set equal to 1-1/n) are empirical parameters which influence the shape of the curve. 1/α is normally considered as the air entry pressure, while n determines the slope of the curve.

Mualem (1976) model can be described:

$$K(S_e) = K_s S_e^l \left[\frac{f(S_e)}{f(1)}\right]^2 \tag{12}$$

where

$$f(S_e) = \int_0^{S_e} \frac{1}{h(x)} dx \tag{13}$$

S_e is the effective saturation degree (10), K_s is the saturated hydraulic conductivity, l is the pore connectivity and tortuosity parameter, estimated by Mualem (1976) equal to 0.5.

VGM parameters were estimated using two different methods: a) fitting process using RETC (van Genuchten et al., 1991) for the reconstructed samples; b) numerical simulation using HYDRUS 1D (Šimůnek et al., 2008) for the undisturbed samples.

RETC – Fitting process

Water content and hydraulic conductivity data of the reconstructed samples were subjected to the fitting process using RETC. RETC is a software which allows to describe hydraulic properties of soil. RETC is able to fit water retention curve and unsaturated hydraulic conductivity with, among others, van Genuchten (VG) model (1980) for the retention curve and the Mualem model (1976) for the hydraulic conductivity.

To find an equation that maximizes the sum of squares associated with the model is the aim of the curve fitting process. This is done by minimizing the residual sum of squares, SSQ (van Genuchten et al., 1991). RETC uses a nonlinear least-squares optimization approach to estimate the unknown model parameters from observed data, either water retention and hydraulic conductivity data. SSQ will be referred to as the objective function $O(b)$ in which b represents the unknown parameter vector.

$$O(b) = \sum^{N} i = 1 \left\{ w_i \left[\theta_i - \hat{\theta}_i(b) \right] \right\}^2 + \sum_{i=N+1}^{M} \left\{ w_i W_1 W_2 \left[Y_i - \hat{Y}_i(b) \right] \right\}^2 \qquad (14)$$

where $\hat{\theta}$ and θ, Y and $\hat{Y}$ are respectively observed and fitted retention and hydraulic conductivity data, N number of retention data, M number of conductivity data, w_i weighting coefficients, which may be used to assign more or less weight to a single data point depending upon a priori information. W_1 and W_2 are weights needed to correct difference in type and number of data between retention and hydraulic conductivity data.

RETC minimizes $O(b)$ iteratively by means of a weighted least-squares approach based on Marquardt's maximum neighbourhood method (Marquardt, 1963). During each iteration step, the elements bj of the parameter vector b are updated sequentially, and the model results are compared with those obtained for the current and previous iteration levels.

The fitting process was conducted using the replicates for each "theoretical R_v". The parameters fitted were θ_r, θ_s, α, n, K_s : nevertheless, sometime it was not possible to fit all these parameters together, thus some parameters were held fixed and the fitting was conducted in sub-steps, determining less parameters.

HYDRUS 1D – Numerical Simulation

Water content and hydraulic conductivity data of the undisturbed samples were analysed using HYDRUS 1D, in the parameter estimation mode. HYDRUS 1D solved numerically (Šimůnek et al 1998) the following modified Richards equation:

$$\frac{\partial \theta}{\partial t} = \frac{\partial}{\partial z}\left(K\frac{\partial h}{\partial z} + K\right) \tag{15}$$

where θ is the volumetric water content (cm^3 cm^{-3}), h is the soil-water pressure head (cm), K is the hydraulic conductivity (cm d^{-1}), z is a vertical coordinate (cm) positive upward, and t is time (d). Initial and boundary conditions used were:

$$h(z,0) = h_i(z) \tag{16}$$

$$-K\left(\frac{\partial h}{\partial z} + 1\right) = q_{evap}(L,t)) \tag{17}$$

$$q(0,t) = -K\left(\frac{\partial h}{\partial z} + 1\right) = 0 \tag{18}$$

where h_i is the initial soil-water pressure head (cm), $q_{evap}(t)$ is the time-variable evaporation rate imposed at the soil surface (cm d^{-1}) and L is a coordinate of the soil surface. Matric potential and volumetric water content value at the end of the evaporation experiment were the observation measurements which were to estimate to minimize the objective function Φ, which is defined as:

$$\Phi(b, p) = \sum_{j=1}^{m} v_j \sum_{i=1}^{nj} w_{i,j} \left[p_j * (t_i) - p(t_i, b) \right]^2 \qquad (19)$$

where m represents the different sets of measurements (pressure heads and volumetric water content), n_j is the number of measurements in each meaurement set, $p_j*(t_i)$ are specific measurements at time t_i for the j_{th} measurement set, $p_j(t_i,b)$ are the corresponding model predictions for the vector of optimized parameters b (e.g., θ_r, θ_s, α, n, and K_s), and v_j and $w_{i,j}$ are weights associated with a particular measurement set or point, respectively. The parameter optimisation method used was the non-linear Levenberg-Marquardt method (Marquardt, 1963). The fitted VGM parameters were θ_r, θ_s, α, n, K_s, l.

Results e discussion

K_{soil} (henceforth however called K_s for simplicity) results of the reconstructed samples were different for clay and sand samples. K_s in clay decreased as the coarse fragment content (R_v) increased: they were not statistically different between them. (p=0.0019) (tab. 4). K_s of the clay alone had an average value of about 21 cm d^{-1}, while at 30 % R_v, K_s value was of about 8 cm d^{-1} and 10 cm d^{-1} for spheres and cylinders respectively. At 20% R_v of spheres, K_s value behaved almost like an outlier. Mean K_s values in the sand (tab. 4) were higher than the clay, but with overall higher variability. Within the cylinders, it was not possible to distinguish a correlation (p=0.97). In the spheres, K_s decreased with increasing R_v (p=0.0083) with a minimum at 30 % R_v with a value of about 40 cm d^{-1}. Ks of clay and sand-spheres were compared with the theoretical values (tab. 5) Clay behavior (tab. 5 and fig. 2) was well explained by *B&R*, *B* and *B-s*, while the volume based theoretical approaches (*P&W* and *M*) were statistically different. *B&R*, *B* and *M* could well explained the sand spheres (tab. 5 and fig. 3), while *P&W* and *B-s* were statistically different. *B&R* ability of estimating both soils could be explain by the fact that this equation considered the ratio of void ratio (*e*), between "stony" and "non-stony" samples: indeed, even though the procedure to construct the samples was standardized, different fine earth bulk density were obtained (tab. 2), which could be

indirectly counted by the different *e* ratio. The evaporation experiments results are shown from table 6 to 10. Shown data are ratios, both for retention curve and hydraulic conductivity points, at -100, -200 and -330 cm, between each R_v data and the 0% data. Last considered point was -330 cm of matric potential because, especially for the sandy samples, it was not possible to have available data below this limit. Water retention decreased in both soils with increasing R_v. Spheres and cylinders did not behave differently, both in clay and sand. In clay, the *Rv-θ(h)* relationship showed an average *r* value of about -0.86 in all the considered matric potential (tab. 6), while in sand *r* value was about -0.95 at -100 and -200 cm and worsted at -330 cm of matric potential, with a *r* value of -0.67 (tab. 7).Theoretical approach could well estimate both clay (cylinders and spheres) and sand (cylinders and spheres) (tab. 8). Unsaturated hydraulic conductivity ratios were more variable than water content ratios. In clay, the unsaturated hydraulic conductivity at -100 cm was not correlated with the R_v, while at -200 and -330 cm, there was a positive relationship with *r* value of 0.62 and 0.53 respectively (tab 9). In sand too, hydraulic conductivity was not correlated with R_v at -100 cm. At decreasing matric potential, -200 and -330 cm, the relationship was negative, with a *r* value of -0.78 and -0.9, respectively (tab 10)

According to the fitting process conducted by RETC, the van Genuchten-Mualem parameters are shown in table 11. Even if θ_r was a fitting parameters, when RETC, during its iteration process, finds a θ_r lower than 0.001 cm^3 cm^{-3}, it sets θ_r to 0 cm^3 cm^{-3}. This is the reason of most of 0 cm^3 cm^{-3} θ_r value. In clay, considering both cylinders and spheres, θ_s values ranged from 0.54 cm^3 cm^{-3} at 5% spheres to 0.35 cm^3 cm^{-3} at 30% spheres, 0% R_v had a value of 0.53 cm^3 cm^{-3}. α values ranged from 0.018 cm^{-1} at 5% and 10% spheres to 0.004 at 20% and 30 % cylinders, 0% value was 0.015 cm^{-1}. *n* ranged from 1.278 at 10% cylinders to 1.764 at 20% cylinders, while 0% had a value of about 1.55. K_s at 0% was about 34 cm d^{-1}, 2.82 cm d^{-1} was the lowest value, at 30% cylinders. In sand, considering both cylinders and spheres, θ_s ranged from a value of about 0.48 cm^3 cm^{-3} at 0% R_v to 0.33 cm^3 cm^{-3} at 30 % cylinders. α had a quite narrow range, in comparison with variability observed in clay: smaller value (0.0067 cm^{-1}) was found at 10% cylinders, higher (0.0084 cm^{-1}) at 10% spheres and 30% cylinders. This behavior could be explained

by the kind of utilized "synthetic" sand, which is normally used in sandbox apparatus, where it is important to have an almost constant air entry value. n ranged from about 3.17 at 10% spheres to 5.41 at 5% cylinders. K_s ranged from 59 cm d^{-1} at 20% cylinders to about 5 cm d^{-1} at 10% cylinders.

Analyzing the relationship between coarse fragment and the VGM parameters (tab. 12 and 13), it is possible to affirm that increasing R_v determined:

- ♦ a decrease of θ_s, both in clay and sand (r=-0.96 and -0.97, respectively), as described by the theoretical approach;

- ♦ a decrease of α (r=-0.68) in clay, while α tended to increase (r=0.63) in sand as R_v increased;

- ♦ a slightly positive trend with n in clay, while n decreased in sand with increasing coarse fragments content ;

- ♦ a negative trend of K_s in clay, while in sand K_s tended to increase as R_v increased.

Analysis of the relationship between the parameters and the bd_{fe} might be useful to better understand the influence of the coarse fragments on the hydraulic properties, indeed as bd_{fe} increased:

- ✓ α decreased both in clay (r=-0.86) and sand (r=-0.69);

- ✓ n tended to increase (r=0.64) in clay and increased in sand (r=0.67);

- ✓ K_s increased (r=-0.76) in clay, while there was no relationship in sand.

Moreover, the bd_{fe} increased with increasing R_v in clay (r=0.73), while it tended to decreased (r=-0.61) in sand. The former might be explained by a coarse fragment effect in reducing the relative-macroporosity while increasing the relative-microporosity. This can be supported by the inverse relationship between coarse fraction content and α and thus a reduction of the air entry potential. On the contrary, R_v-bd_{fe} relationship in sand might be explained by a slightly increase of relative-macroporosity, as supported by the trend between coarse fraction and α and thus a decrease, in absolute value, of air entry potential.

Main charactericstics of undisturbed samples were summarized in table 14. Analysing the behaviour of the undisturbed samples, it is possible to find some trends that were described for the reconstructed samples, even though there were differences in sample kind (i.e. reconstructed vs. undisturbed samples) and analysis

conducted to estimate the van Genuchten-Mualem parameters. Increasing R_v, indeed, determined (table 15):

- a decrease of bd_{fe}, thus positively influencing the porosity;
- an increase of the measured (*log*) K_s: this is in contrast with the theoretical relationships, but the foregoing relationship might explain it;
- a decrease of θ_s, as described by the theoretical approaches;
- an increase of α, and thus a decrease, in absolute value, of the air entry potential, which might be determined by increasing of the macroporosity;
- an increase in macroporosity and mesoporosity: it is important to underline that these values came from a mercury intrusion analysis, made with soil aggregates of about 8 g. Nonetheless this relationship supports the foregoing found relationship.

None clear relation there was between K_s estimated by the inversion process, n and l and the coarse fragment content.

Conclusions

K_s of the reconstructed samples was negatively related with R_v in clay (cylinders and spheres) and in sand spheres. K_s was explained by both *B&R* and *B* theoretical approaches, both in clay (cylinders+spheres) and sand spheres. Moreover clay could be explained by *B-s*, while sand spheres by *M*.

From the evaporation experiment results, it is possible to affirm that the volumetric water content decreased with increasing coarse fragments content and it can be clearly described by the theoretical approach. Unsaturated hydraulic conductivity showed, at -200 and -330 cm matric head, opposite behaviors between clay and sand: as R_v increased, K_u increased in the former, while decreased in the latter. Correlations among R_v, bd_{fe} and VGM parameters showed that θ_s decreased in increasing R_v, both in clay and sand; while the other VGM parameters (α, n and K_s) could be partly explained by their relationship with bd_{fe} and by the bd_{fe}-R_v relationship. The undisturbed samples results underlined the importance of the R_v-bd_{fe} relationship, with an increase of the macroporosity, which was sustained both by

inversion process and by mercury intrusion analysis. Moreover α, and thus indirectly the air-entry value, was related with R_v: this may indirectly strength the importance of the bd_{fe} in determining the fine earth porosity. Moreover, K_s showed a positive relationship with R_v, which is in contrast with the theoretical approaches.

At conclusion, the effect of R_v on the retention curve was well explained by the theoretical approach, in all the observed results, thus the nowadays applied correction is accurate. K_s and K_u, probably due also to their intrinsically high variability, could not always be explained by any normally used equations, nevertheless do consider the bd_{fe} might help to better describe the influence of the rock fragment content on the hydraulic conductivity.

References

ASTM, 2000. Standard test method for particle-size analysis of soils. D 422-63 (1998). 2000 Annual book of ASTM Standards 04.08:10-17. ASTM, Philadelphia, PA, USA;

Bagarello V. and Iovino M., 2007. Comments on "Predicting the Effect of Rock Fragments on Saturated Soil Hydraulic Conductivity". Soil Science Society of American Journal, 71:1584;

Brakensiek D.L. Rawls W.J. and Stephenson G.R., 1986. Determining the saturated hydraulic conductivity of a soil containing rock fragments. Soil Sci. Soc.Am.J., 50(3):838-835;

Brewer R., 1964. Fabric and Mineral Analysis of Soils. Wiley, New York;

Bouwer H. and Rice R.C., 1984. Hydraulic properties of stony vadose zones. Ground Water 6: 696-705;

Cousin I., Nicoullaud B. and Coutadeur C., 2003. Influence of rock fragments on the water retention and water percolation in a calcareous soil. Catena 53:97-114.

Dane J.H. and Hopmans J.W., 2002. In: SSSA Book Series: 5 - Methods of Soil Analysis Part 4 Physical Methods: cap. 3.3. Eds: Dane J.H. e Topp G.C., Soil Science Society of America, Inc;

Dani O. and Glendon W.,2002. S.S.S.A. book series 5: Particle-Size Analysis cap 2.4. Ed: S.S.S.A;

Eijkelkamp, 2003. Laboratoty permeameter: operating instruction. Giesbeelk, NL;

Fiès J.C., De Louvigny N., and Chanzy A., 2002. The role of stones in soil water retention. European Journal of Soil Science 53:95-104;

Flint A.L. and Childs S., 1984. Physical properties of rock fragments and their effects on available water in skeletal soils. In: Erosion and productivity of soils containing rock fragments. Soil Science Society America, Madison, WI, Chap. 10, pp. 91-101;

Graham D.J., Reid I. and Rice S.P., 2005. Automated sizing of coarse grained sediments: Image-processing procedures. Mathematical Geology, 37(1): 1-28.

Grossman R.B. and Reinsch T.G., 2002. In: SSSA Book Series: 5 - Methods of Soil Analysis Part 4 Physical Methods: cap. 2.1. Eds: Dane J.H. e Topp G.C., Soil Science Society of America, Inc.;

Ingelmo F., Cuadrado S., Ibanez A. and Hernandez J., 1994. Hydric properties of some spanish soils in relation to their rock fragment content - implications for runoff and vegetation. Catena 23:73-85;

Jury W.A. and Horton R., 2004. Soil Physics. Sixth Edition. John Wiley & Sons, Inc.;

Marquardt D.W., 1963. An algorithm for least-squares estimation of non linear parameters. J.soc. Ind. Appl. Math.: 11, 431-441;

Mehuys G.R., Stolzy L.H., Letey J. and Weeks L.V., 1975. Effect of stones on the hydraulic conductivity of relatively dry desert soils. Soil Sci. Soc. Amer. Proc, 39: 37-42;

Morgan R.P.C., Quinton J.N., Smith R.E., Govers G., Poesen J.W.A., Auerswald K., Chisci G., Torri D. and Styczen M. E., 1998. The European Soil Erosion Model (EUROSEM): a dynamic approach for predicting sediment transport from fields and small catchments. Earth Surface Processes and Landforms 23: 527–544;

Mualem Y., 1976. A new model for predicting the hydraulic conductivity of unsaturated porous media. Water Resour. Res.: 12, 513-522

Peck A.J. and Watson J.D., 1979. Hydraulic conductivity of flow in non-uniform soil. Workshop on Soil Physics and Field heterogeneity;Camberra, Australia. Unpublished.

Poesen J., 1990. Erosion process research in relation to soil erodibility and some implications for improving soil quality. In: Albaladejo J., Stocking M.A and Diaz E. (Editors), Soil Degradation and Rehabilitation in Mediterranean Environmental Conditions. C.S.I.C., Murcia, pp. 159 170;

Poesen J. and Lavee H., 1994. Rock fragments in top soils - significance and processes. catena 23:1-28;

Ravina I. and Magier J., 1984. Hydraulic conductivity and water retention of clay soils containing coarse fragments Soil Sci. Soc. Am. J., Vol. 48:736-740;

Reynolds W.D., Elrick D.E., Youngs E.G., Amoozegar A., Booltink H.W.G., Bouma J., 2002. In: SSSA Book Series: 5 - Methods of Soil Analysis Part 4 Physical Methods: cap. 3.4. Eds: Dane J.H. e Topp G.C., Soil Science Society of America, Inc;

Russo D., 1983. Leaching characteristics of a stony desert soil. Soil Sci. Soc. Amer. J. 47:431-438;

Šimůnek J., Wendroth O. and van Genuchten M. Th., 1998. Parameter estimation analysis of the evaporation method for determining soil hydraulic properties. Soil Sci. Soc. Am. J. 62:894–905;

Šimůnek J., van Genuchten M. Th. and Šejna M., 2008. Development and applications of the HYDRUS and STANMOD software packages, and related codes, Vadose Zone Journal, Special Issue "Vadose Zone Modeling", 7(2):587-600;

Thermo Electron, 2004. Pascal 140 and 240: technical manual and related software. Milan, Italy;

Torri D., Poesen J., Monaci F. and Busoni E., 1994. Rock fragment content and fine soil bulk-density. Catena 23:65-71;

UGT, 2005. Operating instruction for ku-pF Apparatus DT 04-01. Müncheberg, Germany;

van Genuchten M. Th., 1980. A closed form equation for predicting the hydraulic conductivity of unsaturated soils. Soil Science Society of American Journal.:44, 892-898

van Genuchten M. Th., Leij F.J. and Yates S.R., 1991. The RETC Code for Quantifying the Hydraulic Functions of Unsaturated Soils. EPA/600/2-91/065;

Woolhiser D.A. and Liggett J.A., 1967. Unsteady one-dimensional flow over a plane – the rising hydrograph. Water Resources Research, 3, 753–771.
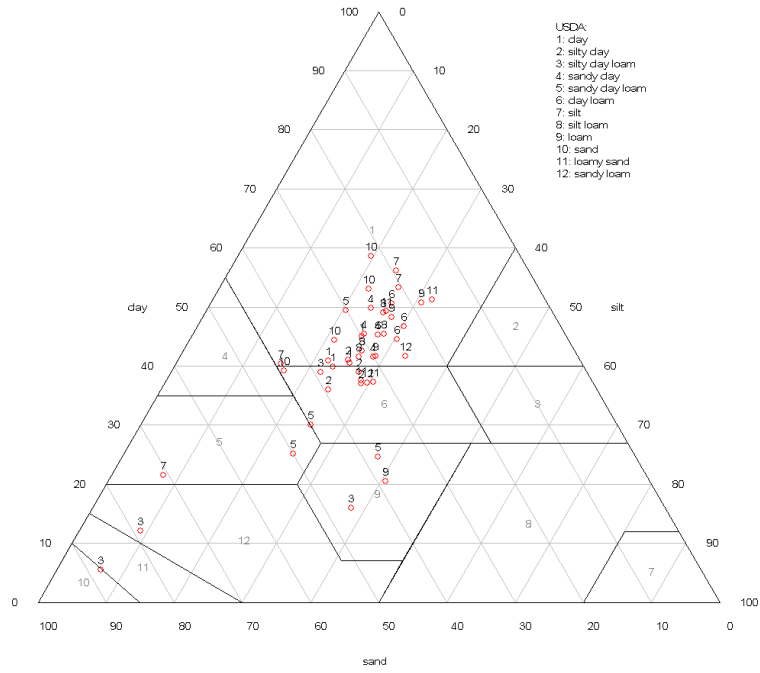
Figure 1: texture classification according the USDA of the undisturbed samples.
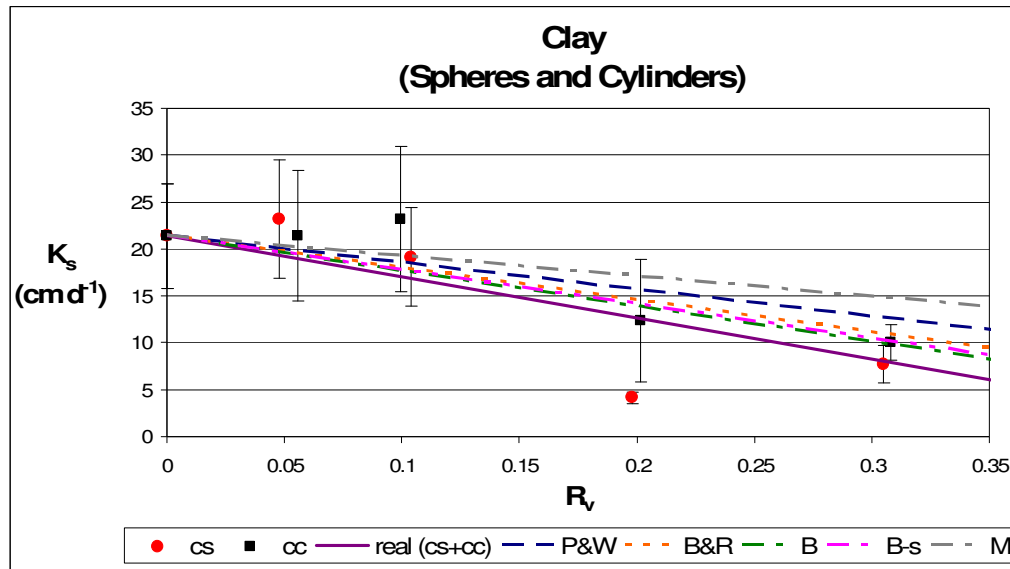
Figure 2: comparison of real and estimated Ks values using the theoretical approaches, in clay, spheres and cylinders
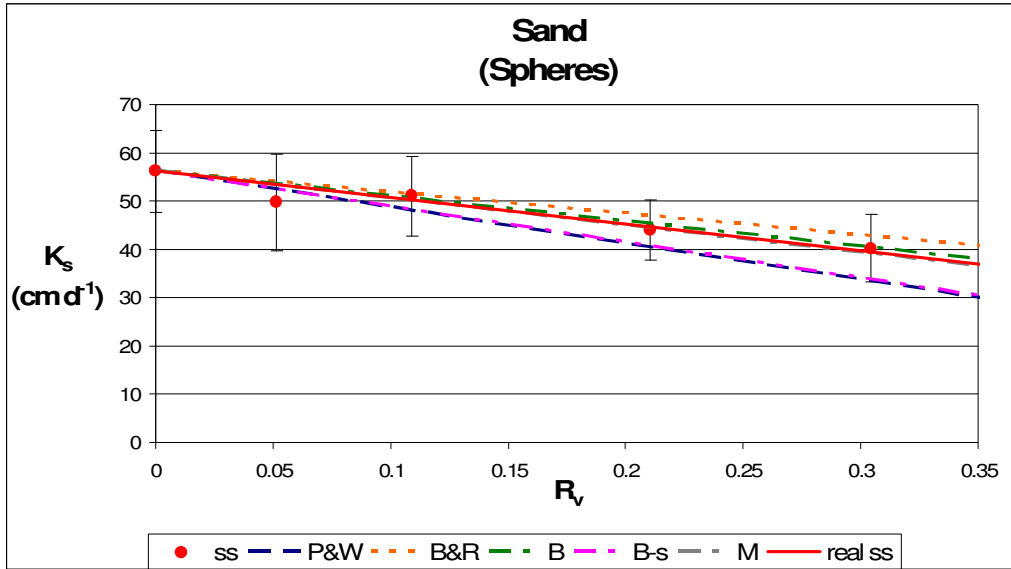
Figure 3: comparison of real and estimated Ks values using the theoretical approaches, in sand spheres

Tables

Soil property	Expression	Reference
Coarse Fraction	$$R_v = \left(\frac{bd_t}{bd_s}\right) * R_w$$	Flint and Childs (1984)
	$$R_w = \frac{1 - bd_{fe}/bd_t}{1 - bd_{fe}/bd_s}$$	Derived
	$$R_w = \frac{bd_t - bd_{fe}}{bd_{fe} - bd_s}$$	Flint and Childs (1984)
Bulk Density	$$bd_{fe} = bd_t \frac{(1 - R_w)}{(1 - R_v)}$$	Flint and Childs (1984)
	$$bd_t = \left[\frac{R_w}{bd_s} + \frac{(1 - R_w)}{bd_{fe}}\right]^{-1}$$	Russo (1983)
	$$bd_t = \left[\frac{R_w}{bd_s} * \frac{1}{bd_{fe}}\right]^{-1}$$	Mehuys et al. (1975)
	$$bd_t = (1 - R_v) * bd_{fe} + (R_v) * bd_s$$	Russo (1983)
	$$bd_t = bd_{fe} + R_v(bd_s - bd_{fe})$$	Flint and Childs (1984)
	$$bd_s = (1 - P_s) * pd_s$$	Flint and Childs (1984)

R_v= coarse fraction (>2mm) by volume; R_w = coarse fraction (>2mm) by weight; bd_t= bulk density of bulk soil; bd_s= bulk density of coarse fraction (>2mm);

bd_{fe}= bulk density of fine fraction; P_s= total porosity of coarse fraction (>2mm); pd_s= particle density of coarse fraction (>2mm).

Table 1 Equations used to describe coarse fraction and bulk density (modified from Brakensiek et al., 1986)

	Theoretical R_v	Actual R_v	S.E.	bd_{fe} (g cm^{-3})	S.E.	actual R_v -K_s	S.E.	bd_{fe} (g cm^{-3}) - K_s	S.E.
Clay Cylinders (cc)	0	0	0	1.031	0.006	0	0	1.083	0.014
	5	0.052	0.000	1.033	0.016	0.056	0.003	1.075	0.024
	10	0.101	0.002	1.034	0.008	0.1	0.001	1.057	0.017
	20	0.204	0.001	1.073	0.030	0.202	0.001	1.081	0.026
	30	0.306	0.003	1.113	0.092	0.308	0.002	1.092	0.023
Clay Spheres (cs)	0	0	0	1.031	0.006	0	0	1.083	0.014
	5	0.053	0.002	1.010	0.017	0.048	0	1.083	0.016
	10	0.102	0.000	1.000	0.023	0.104	0.003	1.081	0.019
	20	0.202	0.003	1.030	0.031	0.198	0.001	1.133	0.01
	30	0.311	0.003	1.057	0.044	0.305	0.002	1.073	0.011
Sand Cylinders (sc)	0	0	0	1.866	0.041	0	0	1.869	0.03
	5	0.053	0.000	1.827	0.055	0.052	0	1.814	0.033
	10	0.103	0.001	1.855	0.052	0.104	0	1.767	0.021
	20	0.206	0.000	1.852	0.065	0.201	0.001	1.74	0.023
	30	0.304	0.006	1.775	0.132	0.303	0.002	1.702	0.022
Sand Spheres (ss)	0	0	0	1.866	0.041	0	0	1.869	0.03
	5	0.051	0.000	1.787	0.060	0.051	0.002	1.834	0.024
	10	0.102	0.000	1.771	0.035	0.109	0.004	1.826	0.019
	20	0.204	0.003	1.798	0.044	0.21	0.009	1.816	0.018
	30	0.311	0.003	1.716	0.065	0.304	0.002	1.74	0.017

Table 2: volume coarse fragments (R_v) and fine earth bulk density (bd_{fe}) for the samples used for the evaporation experiments and the Ks measurements. 0% data, both for Clay and Sand samples, are shown twice, even tough they have to be considered as one bunch of replicates for Clay and Sand, for evaporation and Ks experiments, respectively.

	R_v	R_w	% R_w (2-10 mm)	% R_w (>10 mm)
mean	0.08 (0.1)	0.14 (0.17)	43.33 (27.25)	45.86 (27.76)
median	0.04	0.07	45.61	52.08
min	0	0	0	0
max	0.43	0.66	100	91.09

Table 3: mean, median, minimum and maximum value of the disturbed samples, expressed in volume (Rv) and weight (Rw) basis. Percentage on Rw, of coarse fragments smaller and bigger that 10 mm.

Theoretical R_v	K_s (cm d^{-1})	Regression	Theoretical R_v	K_s (cm d^{-1})	Regression
0c	21.37 (5.57)		0s	56.17 (8.43)	
5cc	21.38 (6.95)		5sc	50.58 (13.75)	
10cc	23.19 (7.77)		10sc	46.3 (8.96)	p=0.97
20cc	12.34 (6.52)		20sc	50.6 (5.75)	
30cc	10.03 (1.86)	p=0.0019 K_s=23.305-53.46*R_v	30sc	54.5 (8.03)	
0c	21.37 (5.57)	r=-0.8497	0s	56.17 (8.43)	
5cs	23.16 (6.3)		5ss	49.75 (10)	
10cs	19.14 (5.25)		10ss	51.04 (8.31)	p=0.0083 K_s=54.846-48.94*R_v r=-0.9636
20cs	4.17 (0.59)		20ss	44.01 (6.2)	
30cs	7.69 (1.98)		30ss	40.21 (7.02)	

Table 4: K_s values in clay (cc=clay cylinders, cs= clay spheres) and sand (sc= sand cylinders, ss= sand spheres) and regression with R_v

	P&W	B&R	B	B-s	M
cc + cs	p<0.05	n.s.	n.s.	n.s.	p<0.05
ss	p<0.05	n.s.	n.s.	p<0.05	n.s.

Table 5: Determination of statistical difference between K_s and theoretical values(cc=clay cylinders, cs= clay spheres, ss= sand spheres)

θ (h)	Th. Rv	real ratio	Regression	θ (h)	Th. Rv	real ratio	Regression	θ (h)	Th. Rv	real ratio	Regression
	0c	1 (0)			0c	1 (0)			0c	1 (0)	
	5cc	1 (0.02)			5cc	0.99 (0.02)			5cc	0.99 (0.02)	
	10cc	0.95 (0.01)			10cc	0.94 (0.01)			10cc	0.93 (0.01)	
	20cc	0.9 (0.02)			20cc	0.89 (0.01)			20cc	0.89 (0.02)	
θ (-100)	30cc	0.81 (0.04)	p=0.0012 $\theta(100)=0.99-0.77*R_v$ r= -0.8635	θ (-200)	30cc	0.83 (0.05)	p=0.0019 $\theta(200)=0.98-0.74*R_v$ r= -0.8557	θ (330)	30cc	0.83 (0.06)	p=0.001 $\theta(-330)=0.98-0.74*R_v$ r= -0.8771
	0c	1 (0)			0c	1 (0)			0c	1 (0)	
	5cs	0.89 (0.03)			5cs	0.88 (0.02)			5cs	0.88 (0.02)	
	10cs	0.83 (0.03)			10cs	0.83 (0.03)			10cs	0.86 (0.03)	
	20cs	0.79 (0.03)			20cs	0.79 (0.03)			20cs	0.79 (0.03)	
	30cs	0.7 (0.04)			30cs	0.7 (0.04)			30cs	0.7 (0.03)	

Table 6. Volumetric water content ratios in clay (cc=clay cylinders, cs= clay spheres) and regression with R_v

θ (h)	Th. Rv	real ratio	Regression	θ (h)	Th. Rv	real ratio	Regression	θ (h)	Th. Rv	real ratio	Regression
θ (-100)	0s	1 (0)	p=0.0000 $\theta(-100)=0.98-0.99*R_v$ r= -0.9757	θ (-200)	0s	1 (0)	p=0.0000 $\theta(-200)=0.97-0.85*R_v$ r= -0.9405	θ (-330)	0s	1 (0)	p=0.0346 $\theta(-330)=0.95-0.59*R_v$ r= -0.6727
	5sc	0.92 (0.06)			5sc	0.88 (0.01)			5sc	0.82 (0.02)	
	10sc	0.88 (0.05)			10sc	0.85 (0.02)			10sc	0.81 (0.04)	
	20sc	0.79 (0.04)			20sc	0.81 (0.02)			20sc	0.82 (0.06)	
	30sc	0.64 (0.06)			30sc	0.66 (0)			30sc	0.67 (0.01)	
	0s	1 (0)			0s	1 (0)			0s	1 (0)	
	5ss	0.89 (0.07)			5ss	0.89 (0.03)			5ss	0.92 (0.09)	
	10ss	0.87 (0.04)			10ss	0.89 (0.03)			10ss	0.96 (0.06)	
	20ss	0.81 (0.02)			20ss	0.82 (0.02)			20ss	0.85 (0.08)	
	30ss	0.69 (0.01)			30ss	0.74 (0.04)			30ss	0.89 (0.13)	

Table 7: Volumetric water content ratios in sand(sc=sand cylinders, ss= sand spheres) and regression with R_v

	θ (-100)	θ (-200)	θ (-330)
1-Rv (cc + cs)	n.s.	n.s.	n.s.
1-Rv (sc + ss)	n.s.	n.s.	n.s.

Table 8: Determination of statistical different between volumetric water content and theoretical values(cc=clay cylinders, cs= clay spheres, sc=sand cylinders and ss= sand spheres)

K (h)	Th. Rv	real ratio	Regression	K (h)	Th. Rv	real ratio	Regression	K (h)	Th. Rv	real ratio	Regression
K (-100)	0c	1 (0)	p=0.32	*K (-200)*	0c	1 (0)	p=0.0565 $K(-200)=1.185+2.96*Rv$ r= 0.62	*K (-330)*	0c	1 (0)	p=0.001 $K(-330)=1.17+2.13*Rv$ r= 0.53
	5cc	0.92 (0.03)			5cc	1.15 (0.27)			5cc	1.05 (0.23)	
	10cc	1.23 (0.3)			10cc	1.94 (0.53)			10cc	2.32 (0.55)	
	20cc	13.15 (7.36)			20cc	3.53 (1.27)			20cc	4.61 (1.84)	
	30cc	1.55 (0.66)			30cc	2 (0.57)			30cc	1.69 (0.27)	
	0c	1 (0)			0c	1 (0)			0c	1 (0)	
	5cs	0.78 (0.14)			5cs	2.14 (1.02)			5cs	1.21 (0.53)	
	10cs	0.97 (0.4)			10cs	1.2 (0.53)			10cs	1.32 (0.44)	
	20cs	0.66 (0.11)			20cs	1.06 (0.21)			20cs	1.22 (0.47)	
	30cs	1.04 (0.41)			30cs	2.49 (1.1)			30cs	1.69 (0.55)	

Table 9 Unsaturated hydraulic conductivity ratios in clay (cc=clay cylinders, cs= clay spheres) and regression with *Rv*

K (h)	Rv	real ratio	Regression	K (h)	Rv	real ratio	Regression	K (h)	Rv	real ratio	Regression
K (-100)	0s	1 (0)	p=0.0847	K (-200)	0s	1 (0)	p=0.0069 $K(-200)=0.80-2.22*R_v$ r= -0.78	K (-330)	0s	1 (0)	p=0.0061 $K(-330)=1.01-1.66*R_v$ r=-0.9
	5sc				5sc	0.53 (0.08)			5sc	0.53 (0.08)	
	10sc	2.17 (0.36)			10sc	0.4 (0.03)			10sc	0.4 (0.03)	
	20sc	6.72 (0)			20sc	0.29 (0.04)			20sc	0.29 (0.04)	
	30sc				30sc	0.23 (0.01)			30sc	0.23 (0.01)	
	0s	1 (0)			0s	1 (0)			0s	1 (0)	
	5ss	6.15 (2.31)			5ss	0.4 (0.03)			5ss	0.83 (0.21)	
	10ss	3.28 (1.67)			10ss	0.43 (0.11)			10ss	0.76 (0.12)	
	20ss	7.5 (1.74)			20ss	0.57 (0.3)			20ss	0.68 (0.13)	
	30ss	4.73 (2.2)			30ss	0.15 (0.03)			30ss	0.43 (0.06)	

Table 10: Unsaturated hydraulic conductivity ratios in sand (sc=sand cylinders, ss= sand spheres) and regression with R_v

Theoretical R_v	θ_r (cm^3 cm^{-3})	θ_s (cm^3 cm^{-3})	α (cm^{-1})	n	K_s (cm d^{-1})
0 c	0.068	0.54	0.008 (0.001)	1.372 (0.044)	13.853 (2.931)
5 cc	0.001	0.537	0.017 (0.002)	1.278 (0.02)	33.661 (9.931)
10 cc	0	0.437 (0.055)	0.004 (0.001)	1.764 (0.292)	6.603 (2.707)
20 cc	0	0.393 (0.024)	0.004 (0)	1.593 (0.095)	2.825 (0.435)
30 cc	0.068	0.54	0.008 (0.001)	1.372 (0.044)	13.853 (2.931)
0 c	0.224 (0.04)	0.53	0.015 (0.011)	1.546 (0.28)	34.3 (72.33)
5 cs	0.068	0.54	0.008 (0.001)	1.372 (0.044)	13.853 (2.931)
10 cs	0.001	0.537	0.017 (0.002)	1.278 (0.02)	33.661 (9.931)
20 cs	0	0.437 (0.055)	0.004 (0.001)	1.764 (0.292)	6.603 (2.707)
30 cs	0	0.393 (0.024)	0.004 (0)	1.593 (0.095)	2.825 (0.435)
0 s	0	0.486 (0.017)	0.0077 (0.0005)	3.493 (0.33)	26.711 (9.36)
5 sc	0	0.45	0.0079 (0.0001)	5.413 (0.194)	24
10 sc	0	0.404 (0.012)	0.0067 (0.0001)	5.869 (0.564)	5.183 (0.426)
20 sc	0	0.404 (0.016)	0.0081 (0.0004)	5.295 (0.338)	59.448 (21.342)
30 sc	0	0.333 (0.013)	0.0084 (0.0003)	3.388 (0.168)	54.156
0 s	0	0.486 (0.017)	0.0077 (0.0005)	3.493 (0.33)	26.711 (9.36)
5 ss	0	0.455 (0.027)	0.0079 (0.0003)	4.154 (0.39)	12.386 (0.778)
10 ss	0	0.442 (0.019)	0.0084 (0.0003)	3.176 (0.166)	11.167 (0.724)
20 ss	0	0.39	0.0082 (0.0002)	4.156 (0.261)	26.638 (3.154)
30 ss	0.001	0.35	0.00823	3.729	13.262 (0.707)

Table 11: Parameters values (S.E. coefficient) fitted by RETC.

Variable	R_v	bd_{fe}	θ_s	α	n	K_s
R_v	1.00					
bd_{fe}	**0.73**	1.00				
θ_s	**-0.96**	**-0.72**	1.00			
α	**-0.68**	**-0.86**	**0.71**	1.00		
n	0.24	0.64	-0.34	-0.66	1.00	
K_s	-0.67	**-0.76**	0.64	**0.89**	-0.52	1.00

Table 12: Correlation matrix in clay (in bold p<0.05).

Variable	R_v	bd_{fe}	θ_s	α	n	K_s
R_v	1.00					
bd_{fe}	-0.61	1.00				
θ_s	**-0.97**	0.55	1.00			
α	0.63	**-0.69**	-0.47	1.00		
n	-0.25	**0.67**	0.15	-0.59	1.00	
K_s	0.56	0.06	-0.45	0.57	0.09	1.00

Table 13: Correlation matrix in sand (in bold p<0.05)

	100-600 $(cm^3 cm^{-3})$	75-100 $(cm^3 cm^{-3})$	30-75 $(cm^3 cm^{-3})$	5-30 $(cm^3 cm^{-3})$	0.1-5 $(cm^3 cm^{-3})$	<0.1 $(cm^3 cm^{-3})$	bd_t $(g cm^{-3})$	bd_{fe} $(g cm^{-3})$	$log K_s$ $(cm d^{-1})$	$K(-330)$ $(cm d^{-1})$	$\theta(-330)$ $(cm^3 cm^{-3})$	θ_s $(cm^3 cm^{-3})$	α (cm^{-1})	n	$log K_s$ (Hyd) $(cm d^{-1})$	l	$\theta(-15,000)$ $(cm^3 cm^{-3})$
mean	3.66 (0.28)	0.82 (0.06)	2.32 (0.15)	3.34 (0.22)	7.7 (1.12)	8.34 (0.36)	1.36 (0.02)	1.24 (0.03)	1.88 (0.19)	0.02 (0.003)	0.41 (0.02)	0.51 (0.02)	0.03 (0.005)	1.3 (0.04)	1.86 (0.14)	1.11 (0.47)	0.24 (0.01)
median	3.47	0.75	2.22	3.2	6	8.61	1.38	1.27	1.71	0.01	0.47	0.51	0.02	1.21	1.93	0.5	0.25
min	1.23	0.22	0.63	1.2	1.27	0	1.08	0.74	-0.16	0.004	0.15	0.17	0	1.11	0.19	0.00001	0.02
max	7.57	1.58	3.85	8.33	40.93	12	1.71	1.5	4.11	0.08	0.59	0.87	0.12	2.07	3.61	16.01	0.39

Table 14: main characteristics of undisturbed samples considering: porosity classes, expressed in volume basis ($cm^3 cm^{-3}$) (600-100 μm, 100-75 μm, 75-30 μm, 30-5 μm, 5-0.1 μm, 0.1-0.001 μm), *log K_s* (cm d^{-1}), total (*bd_t*) (g cm^{-3}) and fine earth bulk density (*bd_{fe}*) (g cm^{-3}), coarse fraction (*Rv*), K(-330) (cm d^{-1}), *θ (-330)* (cm^3 cm^{-3}) from the evaporation experiments, inverted parameters by Hydrus 1D (*θ_s* (cm^3 cm^{-3}); *α* (cm^{-1}); *n*; *K_s* (cm d^{-1}); *l*), θ(-15,000) (cm^3 cm^{-3}).

	100-600	75-100	30-75	5-30	0.1-5	<0.1	bd_t	bd_{fe}	R_v	$\log K_s$	K (-330)	θ (-330)	θ_s	α	n	$\log K_s$ (Hydrus)	l	θ (-15,000)	Sand	Clay
100-600	1.00																			
75-100	**0.79**	1.00																		
30-75	**0.66**	**0.86**	1.00																	
5-30	0.16	0.30	**0.68**	1.00																
0.1-5	-0.18	-0.17	0.04	**0.39**	1.00															
<0.1	-0.04	-0.04	-0.18	-0.31	**-0.75**	1.00														
bd_t	0.06	-0.03	-0.05	-0.15	-0.16	0.21	1.00													
bd_{fe}	-0.28	-0.12	-0.09	-0.06	-0.11	0.29	**0.48**	1.00												
R_v	**0.35**	0.09	0.04	-0.09	-0.02	-0.13	**0.44**	**-0.57**	1.00											
$\log K_s$	**0.33**	0.29	0.28	0.07	-0.10	-0.21	0.01	**-0.41**	**0.47**	1.00										
K (-330)	0.07	0.05	0.20	**0.37**	**0.47**	-0.25	**-0.33**	-0.04	-0.27	-0.22	1.00									
θ (-330)	**-0.38**	-0.14	-0.20	-0.14	-0.04	0.22	-0.32	**0.46**	**-0.78**	**-0.53**	0.13	1.00								
θ_s	**-0.36**	-0.12	-0.09	-0.06	0.06	0.01	0.05	**0.37**	**-0.35**	-0.25	0.02	**0.57**	1.00							
α	0.30	0.23	0.13	-0.07	-0.11	-0.07	0.17	-0.20	**0.36**	0.27	-0.22	**-0.53**	-0.13	1.00						
n	0.14	0.01	0.22	**0.39**	-0.02	0.17	-0.13	-0.20	0.07	0.08	0.19	**-0.34**	**-0.37**	0.06	1.00					
$\log K_s$ (Hydrus)	0.17	0.12	0.09	0.06	0.16	-0.22	-0.22	**-0.35**	0.17	0.25	0.14	**-0.32**	0.01	**0.73**	0.19	1.00				
l	-0.14	-0.04	-0.14	-0.18	-0.24	0.14	-0.25	-0.01	-0.22	-0.18	-0.10	**0.39**	0.08	-0.26	-0.15	-0.19	1.00			
θ (-15,000)	**-0.33**	-0.10	-0.16	-0.10	-0.25	**0.45**	-0.22	**0.58**	**-0.80**	**-0.51**	0.08	**0.83**	**0.36**	**-0.38**	-0.10	-0.28	0.16	1.00		
Sand	0.20	0.16	0.28	**0.38**	0.17	**-0.40**	-0.02	**-0.42**	**0.42**	0.28	0.06	**-0.56**	**-0.46**	0.24	0.31	0.12	-0.18	**-0.53**	1.00	
Clay	-0.03	-0.01	-0.14	-0.32	**-0.39**	**0.45**	-0.07	**0.33**	**-0.42**	-0.18	-0.17	**0.56**	**0.36**	-0.17	-0.25	-0.06	0.29	**0.57**	**-0.85**	1.00

Table 15: correlation matrix for the undisturbed samples, considering, porosity classes (600-100 µm, 100-75 µm, 75-30 µm, 30-5 µm, 5-0.1 µm, 0.1-0.001 µm), log Ks, total (bd_t) and fine earth bulk density (bd_{fe}), coarse fraction (R_v), K(-330) and θ(-330) from evaporation experiments, inverted parameters by Hydrus 1D (θ_s, α, n, K_s, l), θ(-15,000) and texture (in bold p<0.05)

4 Hydraulic properties of stony soils: field application

Abstract

Eighteen tension disc infiltration experiments were conducted in three soils of Regione Lombardia, Northern Italy. Soils were different for texture, stone content and organic matter content. The aim of this work were to describe the numerical inversion parameters results of tension disc infiltrometer experiments conducted in three stony soils and to analyse, by mean of the pedotransfer functions(PTFs), used as "multiple regression tool", the role of the coarse fragment content on soil hydraulic properties near saturation. Unsaturated hydraulic conductivity measured by the infiltrometry experiments were, as expected from the intrinsic nature of this soil hydraulic property at field scale, highly variable. Stone effect on unsaturated hydraulic conductivity showed some weak trends, negative at -12 cm of matric potential, positive closer to saturation. PTFs were, at least for the hydraulic conductivity, a useful tool to better understand the stone effects, indeed using the fine earth bulk density as predictor improved the estimation ability. PTFs failed, on the contrary, the prediction for the volumetric water content.

Keywords: coarse fragments, tension disc infiltrometer, van Genuchten-Mualem parameters, pedotransfer functions (PTFs).

Introduction

Knowledge of the soil hydraulic properties, especially hydraulic conductivity near saturation, is important since the water flux and solute transport are highest in near saturated media (Bagarello et al., 2003) which can finally have important consequences on ground water pollution.

Rock fragments content, size and position on soil surface, may both increase and decrease infiltration. In a study in western Africa, Valentin (1994) found that fine and medium gravel, mainly free at soil surface, favoured higher infiltration rate, while coarse gravel embedded in a seal generate high runoff. Considering the shape feature, the more spherical rock fragments, the lower the saturated hydraulic conductivity (Dunn and Mehuys, 1984). Cousin et al. (2003), in calcareous soils, found that the percolation was underestimated when the rock fragments were neglected and the soil was considered only as fine earth, while percolation was overestimated when the rock fragments were considered as non-porous stones.

Sauer and Logsdon (2002) studied the hydraulic properties of stony soils using the tension infiltrometer. They found trends, even thought weak, between the rock fragments content and the hydraulic conductivity. In particular, at saturation, this property tended to increase with increasing stone content, while the opposite was true at a matric potential of -12 cm. Besides stones influence on determining a reduction of the area for water and an increase of the tortuosity of the water paths (Mehuys et al., 1975; Childs and Flint, 1990), they hypothesized that source of rock fragments and fine earth, which surrounded the stones, can influence water flow by affecting hydraulic conductivity near coarse fragment surfaces.

Nowadays knowledge of the soil hydraulic properties may be inferred by direct, inverse and indirect methods. The first approach consists of several laboratory and field methods (e.g., Dirksen, 1991; Dane and Topp, 2002). Field method are usually considered to be more realistic since analyses are conducted in a larger volume of soil and because of continuity and structure in the soil profile are more conserved. Unfortunately several, both laboratory and field, techniques remain costly and time consuming. Moreover hydraulic properties vary widely over time and space, in particular for hydraulic conductivity (van Genuchten and Nielsen, 1985); thus determining a large number of samples to be collected and experiments to be conducted. The second approach, the inversion, is widely based on the numerical solution of the Richard equation: simulation of individual processes are of particular interest to gain better description of the mechanisms involved in the processes, particularly when data are limited or not available (Saxton and Rawls, 2006). Inversion is based on the minimization of a suitable objective or likelihood function, which expresses

the discrepancy between the observed values and the predicted system response. Initial estimates of the parameters are iteratively improved during the minimization process until a desired precision is obtained (Šimůnek and van Genuchten, 1996). The third approach, the indirect one, which can be defined as pedotransfer function (PTF), aims to estimate more complex soil properties (i.e. water retention and hydraulic conductivity) from readily available soil data (texture, soil organic carbon content, bulk density, etc.). The accuracy obtains in this way is lower than those obtain with the previously described approaches, but PTFs might be successfully applied to a wide variety of situations, like territorial studies. All three approaches are important to achieve a better knowledge about the roles of soil on ecosystem processes.

The aim of this work were to describe the numerical inversion parameters results of tension disc infiltrometer experiments conducted in three stony soils and to analyse, by mean of the PTFs used as "multiple regression tool", the role of the coarse fragment content on soil hydraulic properties near saturation.

Material and methods

<u>Soil classification</u>

Three soils, located in Regione Lombardia, were selected to perform tension disc infiltometer analysis. The first one, Monzambano (South-Eastern of Lombardia), was a Typic Udorthent sandy skeletal, sub-alkaline soil, cultivated with vine grapes. The second soil, Ghisalba (central of Lombardia), was an Inceptic Hapludalf, loamy skeletal, with a neutral reaction, cultivated with maize. The last soil, Boffalora (Western Lombardia), was classified as Aquic Udorthent sandy skeletal and the reaction was sub-acid-neutral, cultivated with maize.

Tension disc infiltrometer

Six tension disc infiltrometer analysis were conducted in each soil, applying transient flow condition. Before starting the analysis, the soil was layered and the contact material (Spheriglass No. 2227) studied by Reynolds e Zabchuk (1996) was used to make a smoother surface where laying the infiltrometer. This contact material was wetted before the analysis started. The infiltrometer (Soil Moisture, 1997) (ø 20.4 cm) was saturated before starting the experiment. The applied pressure were -12, -9, -6, -3, 0 cm, in this order, thus the analysis was conducted in the wetting branch of the water retention curve. The readings of the applied pressure and of the cumulative infiltration were done visually. The change in the pressure was done at least 15 min after the start of the prescribed pressure and when at least three consecutive reading had the same rate. Just before the start of the experiment, a sample to determine the initial water content was taken near the site of analysis. At the end of the experiment, the sand cone apparatus was used to determine the soil bulk density (Grossman and Reinsch, 2002). Escavation was done within a 30 cm diameter, 20 cm depth. Soil moisture content was then calculated for the fine earth fraction and recognized as the final water content at the end of the analysis. Sample derived from the sand cone apparatus were entirely collected to determine the stone fraction and the fine earth bulk density. The latter was determined considering a stone bulk density equal to 2.65 g cm^3. Besides, coarse fragment content was determined by dividing two size classes: smaller than 2 cm and between 2 to 10 cm (Glendon e Dani, 2002). Texture was determined using the hydrometer method (ASTM, 2000) and soil organic matter by Walkley-Black method (Walkley and Black, 1934). Tension disc analyses were conducted between July and September 2007.

Numerical inversion

Infiltration data were analysed using HYDRUS 2D/3D (Šimůnek et al., 2006), in the parameter estimation mode. HYDRUS 2D/3D solved numerically (Šimůnek et al., 1996) the following modified Richards equation (Warrick, 1992):

$$\frac{\partial \theta}{\partial t} = \frac{1}{r}\frac{\partial}{\partial r}\left(rK\frac{\partial h}{\partial r} \right) + \frac{\partial}{\partial z}\left(K\frac{\partial h}{\partial z} \right) + \frac{\partial K}{\partial z} \qquad (1)$$

where θ is the volumetric water content (cm^3 cm^{-3}), r is a radial coordinate (cm), h is the soil-water pressure head (cm), K is the hydraulic conductivity (cm s^{-1}), z is a vertical coordinate (cm) positive upward and t is time (s). Initial and boundary conditions used were:

$$h(r,z,t) = h_i \qquad\qquad t = 0 \qquad\qquad (2)$$

$$h(r,z,t) = h_0 \qquad\qquad 0 < r < r_0, z = 0 \qquad (3)$$

$$-\frac{\partial h(r,z,t)}{\partial z} - 1 = 0 \qquad r > r_0, z = 0 \qquad (4)$$

$$h(r,z,t) = h_i \qquad\qquad r^2 + z^2 \rightarrow \infty \qquad (5)$$

where h_i is the initial pressure head (cm), h_0 is the time-variable supply pressure head imposed by tension disc infiltrometer (cm) and r_0 is the disc radius (cm). Domain was: 15 cm of radius and 20 cm of depth; Z axis was considered the symmetrical axis. The initial condition were on water content basis, considering as initial volumetric water content that sampled at the proximity of the experiment site. Top boundary conditions was defined as variable head up to 10.2 cm (disc radius) and as no flux from that point to 15 cm. Bottom boundary condition was set to free drainage condition.

Cumulative infiltration and volumetric water content at the end of the experiment (related with the last imposed tension) were the observation measurements which were to estimate to minimize the objective function Φ, which was defined as:

$$\Phi(b,p) = \sum_{j=1}^{m} v_j \sum_{i=1}^{nj} w_{i,j}\left[p_j * (t_i) - p(t_i, b) \right]^2 \qquad (6)$$

where m represents the different sets of measurements (cumulatve infiltration and volumetric water content), n_j is the number of measurements in each meaurement set, $p*j(t_i)$ are specific measurements at time t_i for the j_{th} measurement set, $p_j(t_i,b)$ are the corresponding model predictions for the vector of optimized parameters b (e.g., θ_r, θ_s, α, n, and K_s), and v_j and $w_{i,j}$ are weights associated with a particular measurement set or point, respectively.

The van Genuchten equation (1980) related with the Mualem approach (1976) was the hydraulic model used in the numerical solution. The fitted parameters were θ_s, α, n, K_s.

Pedotransfer functions (PTFs)

To better understand the studied soil behaviour, some pedotransfer function (PTFs) were applied.

Fine earth bulk density data were tested to understand whether the empirical equation of Torri et al. (1994) could describe the considered soils.

$$bd_{fe} = bd_{fe0}(1 - 1.67 R_w^{3.39} \tag{7}$$

where bd_{fe} (g cm^{-3}) is fine earth bulk density, bd_{fe0} soil bulk density (g cm^{-3}) in absence of rock fragments, R_w rock fragment content expressed in weight basis. Since bdfe0 was not known, it was estimated using Kaur et al. (2002) equation

$$\ln(bd) = 0.313 - 0.191 * oc + 0.02102 * c - 0.000476 * c^2 - 0.00432 * si \tag{8}$$

where bd (g cm^{-3}) bulk density, oc (%) organic carbon, c (%) and si (%) clay and silt, respectively.

Saturated hydraulic conductivity was estimated using:

a) Saxton et al. (1986)

$$K_s = 2,778^{10^{-6}} \exp(X)$$
$$X = 12,012 - 7,55^{10^{-2}} s + \frac{(-3,895 + 3,671^{10^{-2}} s - 0,1103c + 8,7546^{10^{-4}} c^2)}{1 - (bd/2,65)} \tag{9}$$

where K_s (saturated hydraulic conductivity) (cm s^{-1}), s (%) and c (%) sand and clay, respectively, bd (g cm^{-3}) bulk density. This equation was evaluate using both measured fine earth bulk density and estimated by Kaur et al. (2002);

b) Rosetta, a software released by Schaap et al. (2001), can predict, by mean of neural networks, the VGM parameters in a hierarchical approach. It was used only using the texture data.

c) Saxton and Rawls (2006)

$$K_s = 1930(\theta_s - \theta_{33})^{(3-\lambda)} \tag{10}$$

where θ_s (cm^3 cm^{-3}) and θ_{33} (cm^3 cm^{-3}) are moisture at saturation (at 0 cm) and at -330 cm, respectively, λ slope of logarithmic tension-moisture curve.

d) Saxton and Rawls (2006), with a density reduction factor,

$$\rho_n = (1 - \theta_s) * 2.65$$
$$\rho_{dr} = \rho_n * dr \tag{11}$$

where ρ_n (g cm^{-3}) is normal bulk density, ρ_{dr} is reduced bulk density (g cm^{-3}) and d_r is density reduction factor, suggested by the authors to be set at 0.9 to account for the presence of coarse fragments.

Retention data were estimated in the range of 0÷-12 cm using:

I. Rosetta (Schaap et al. 2001), utilizing both texture data and texture plus measured bulk density;

II. Vereecken et al. (1992) approach, which permitted to calculate the van-Genuchten (1980) parameters by mean of texture, organic matter content and bulk density, which was set to the measured fine earth bulk density:

$$\theta_r = 0,015 + (0,005c) + (0,0081om)$$
$$\theta_s = 0,81 - (0,283bd) + (0,001c)$$
$$\ln(a) = -2,486 + (0,025s) - (0,204om) - (2,617bd) - (0,023c) \tag{12}$$
$$\ln(n) = 0,053 - (0,009s) - (0,013c) + (0,00015s^2)$$

where c (%) clay, s (%) sand, om (%) organic matter, bd (g cm^{-3}) bulk density.

Principal Component Analysis

Principal Component Analysis (PCA) is a statistical descriptive method which allows to extract, from the studied data, their main characteristics. Multivariate treatment of the data is the ground of this kind of analysis: original studied variables are diagonalized and fewer components are extracted. Each component is characterized by factor weights, which relate each original variable with the analysed component. Higher, in absolute value, the factor weight, greater the weight of the original variables. Total variance of the original variables does not change for the PCA. The variables used to conduct the PCA were:

-         R_w, coarse fragments content in weight basis;
-         $R_w<2$, coarse fragments smaller than 2 cm;
-         $R_w>2$, coarse fragments bigger than 2 cm;
-         bd_{fe} (g cm^{-3}) fine earth bulk density;
-         θ_s (cm^3 cm^{-3}) saturated moisture content, α (cm-1), n and K_s (cm $^{-s}$); as estimated by Hydrus;
-         sand (%) and clay (%).

Results and discussion

Volume coarse fraction content (R_v) ranged from 7 to 25 %, which corresponded to 19-65 % by weight (R_w) (tab. 1). In average, Boffalora was the more stony (19 % R_v) and sandy (70% sand and 15% clay) (fig. 1) and with higher organic matter content (6% OM), Monzambano presented intermediate values (18.5% R_v and 57% sand 16% , 27% clay, 5% OM). Ghisalba was the less stony and the more clayey and with less organic matter content with 9.2 % R_v and 41% sand and 40% clay and 5% *OM*, respectively. Moreover, at increasing R_v, there was a decrease of fine earth bulk density (bd_{fe}) and the sand.

Ratio of measured fine earth bulk density to estimated bulk density, using Kaur et al. (2002) equation was quite well described by the Torri et al. equation (fig. 2).

Infiltrometry data are highly variable among and within field experiments (tab. 1 and fig. 3). Samples with higher sand content tended to have higher α, and thus higher air entry potential, and higher n, which could be explained by an higher macroporosity. Some experiments have a very narrow range in volumetric water content (between initial and final value), thus it is not possible to infer the entire retention curve from the fitted parameters, but some considerations are however possible. There was not a clear relationship between the stoniness and the unsaturated hydraulic conductivity at different matric potential: at – 12 cm there was a weak negative trend, while at higher matric potential very weak positive trends were found (fig. 3). These trends are similar to those described by Sauer and Logsdon (2002). They explained it, considering both the tortuosity effect and hydraulic continuity induced by the stones. It was not possible to observe any factors affecting the hydraulic continuity in the studied soils. Nonetheless, since there was a negative

relationship between bd_{fe} and α, and thus a negative relationship with the air entry potential, it could be hypothesized that the observed trends might be explained by the reduction in fine earth bulk density, which could partly mask the tortuosity effect too.

When comparing the K_s value inverted with the numerical solutions with those estimated by the PTFs, it is possible to affirm that K_s was better explained with Saxton et al. (1986) which considered the bulk density as input parameter, both measured and estimated (fig. 4). Approaches of Schaap et al. (2001) Saxton and Rawls (2006), even considering the density reduction of 0.9, underestimated, of about half order the K_s values. It was thus important to know, or at least, estimate the bd_{fe} to improve the prediction. PTFs were further used to estimate the water retention characteristics. The overall fitting was definitely not good, even if the bd_{fe} was considered (fig. 5÷7). Within Bollafora (fig. 5), only Vereecken et al. (1992) could estimate the retention curve only in few samples, while Schaap et al. (2001) approach, using only the texture, was able to estimate few curves of Ghisalba and Monzambano (fig. 6 and 7). This partial fit was, however, achieved until about -9 cm, thus all PTFs failed at -12 cm.

PCA extracted two factors, which explained 70 % of the total variance . The first factor was mostly related with texture, indeed sand and clay had weight of 0.97 and -0.95 respectively, and to coarse fragment content (R_w) and fine earth bulk density (bd_{fe}) with weighting factor of 0.87 and -0.89, respectively. The second factor was explained by coarse fragments smaller ($R_w<2$) and greater ($R_w>2$) than 2 cm with weight of 0.92 and -0.92, respectively, and finally with K_s with a factor of 0.7 (tab. 2). Figure 8 showed how the variables behaved in respect to the extracted factor. It is possible to observe that $R_w<2$ and $R_w>2$ laid along the y-axis, the former in the positive direction, the latter in the negative direction. Sand and R_w laid along the x-axis, in the positive direction, while clay and bd_{fe} in the negative direction. Both $θ_s$ and K_s laid in the second quadrant, thus it seemed that these variables might be explained by different effects determined by sand, R_w, and stones bigger that 2 cm.

Conclusions

Unsaulic hydraulic conductivity measured by the infiltrometry experiments were, as expected from the intrinsic nature of this soil hydraulic property at field scale, highly variable. Stone effect on unsaturated hydraulic conductivity showed some weak trends, negative at -12 cm of matric potential, positive closer to saturation. Stone content was negatively related with the fine earth bulk density, which also was negatively related with α, and thus, positively to the air entry potential. The used of PTFs was, at least for the hydraulic conductivity, a useful tool to better understand the reality: indeed it underlined the importance of using the fine earth bulk density as predictor to improve the estimation ability. PTFs failed, on the contrary, the prediction for the volumetric water content.

To explain all the processes that are taking place it might be important not only to consider the tortuosity effect induced by the presence of stones, but even to account for the reduction of fine earth bulk density.

References

ASTM, 2000. Standard test method for particle-size analysis of soils. D 422-63 (1998). 2000 Annual book of ASTM Standards 04.08:10-17. ASTM, Philadelphia, PA, USA;

Bagarello V. and Iovino M., 2003. Field testing parameter sensitivity of the two-term infiltration equation using differentiated linearization. Vadose Zone Journal 2:358–367;

Childs S.W., and Flint A.L., 1990. Physical properties of forest soils containing rock fragments. In: Sustained Productivity of Forest Soils (eds Gessel S.P., Lacate D.S., Weetman G.F. and Powers R.F.), pp. 95-121. University of British Columbia, Faculty of Forestry, Vancouver, BC

Cousin I., Nicoullaud B. and Coutadeur C., 2003. Influence of rock fragments on the water retention and water percolation in a calcareous soil. Catena 53:97-114;

Dirksen C., 1991. Unsaturated hydraulic conductivity. In: Soil Analysis: Physical Methods. Marcel Dekker, Inc., New York, NY. 1991. p 209-269;

Dane J.H. and Topp C.G, 2002. Methods of soil analysis. Part 4. Physical methods. Madison, WI, SSSA,

Dani O. and Glendon W.,2002. S.S.S.A. book series 5: Particle-Size Analysis cap 2.4. Ed: S.S.S.A;

Dunn A.J. and Mehuys G.R., 1984. Relationship between gravel content of soils and saturated hydraulic conductivity in laboratory tests. In Erosion and Productivity of Soils Containing Rock Fragments, pp. 55-63. Spec. Publ. No. 13, Soil Sci. Soc. Am., Madison, Wisconsin;

Grossman R.B. and Reinsch T.G., 2002. In: SSSA Book Series: 5 - Methods of Soil Analysis Part 4 Physical Methods: cap. 2.1. Eds: Dane J.H. e Topp G.C., Soil Science Society of America, Inc.;

Kaur R., Kumar S. and Gurung H.P., 2002. A pedotransfer function (PTF) for estimating soil bulk density from basic soil data and its comparison with existing PTFs. Austr. J. Soil Res. 40: 847–857;

Mehuys G.R., Stolzy L.H., Letey J. and Weeks L.V., 1975. Effect of stones on the hydraulic conductivity of relatively dry desert soils. Soil Sci. Soc. Amer. Proc, 39: 37-42;

Mualem Y., 1976. A new model for predicting the hydraulic conductivity of unsaturated porous media. Water Resour. Res.: 12, 513-522

Reynolds W. D. and Zabchuk W. D., 1996. Use of contact material in tension infiltrometer measurements. Soil Technology 9:141-159;

Sauer T.J. and Logsdon S.D., 2002. Hydraulic and physical properties of stony soils in a small watershed. Soil Science Society of America Journal 66:1947-1956;

Saxton K.E., Rawls W. J., Romberger J. S. and Papendick R. I., 1986. Estimating Generalized Soil-water Characteristics from Texture. Soil Sci Soc Am J. 50:1031-1036;

Saxton K.E. and Rawls W.J., 2006. Soil water characteristic estimates by texture and organic matter for hydrologic solutions. Soil Science Society of America Journal 70:1569-1578;

Schaap M.G., Leij F.J., and van Genuchten M.T., 2001. ROSETTA: a computer program for estimating soil hydraulic parameters with hierarchical pedotransfer functions. Journal of Hydrology 251:163-176;

Šimůnek J. and van Genuchten M. Th., 1996. Estimating unsaturated soil hydraulic properties from tension disc infiltrometer data by numerical inversion. Water Resources Research 32: 2683-2696;

Šimůnek J., van Genuchten M. and Th., Šejna M. The HYDRUS software package for simulating the two- and three-dimensional movement of water, heat, and multiple solutes in variably-saturated media. Technical manual. PC Progress, Prague, Czech Republic;

Soil Moisture, 1997. Guelph Tension Infiltrometer: Operating instruction. Santa Barbara, CA, USA;

Torri D. and Styczen M. E., 1998. The European Soil Erosion Model (EUROSEM): a dynamic approach for predicting sediment transport from fields and small catchments. Earth Surface Processes and Landforms 23: 527–544;

Valentin C., 1994. Surface sealing as affected by various rock fragment covers in West-Africa. Catena 23:87-97;

van Genuchten M. Th., 1980. A closed form equation for predicting the hydraulic conductivity of unsaturated soils. Soil Science Society of American Journal.:44, 892-898

van Genuchten M. Th. and Nielsen D. R., 1985. On describing and predicting the hydraulic properties of unsaturated soils. Annales geophysicae 3: 615-627;

Vereecken H., Diels J., Vanorshoven J., Feyen J. and Bouma J., 1992. Functional-evaluation of pedotransfer functions for the estimation of soil hydraulic-properties Soil Science Society Of America Journal 56 1371-1378

Walkley A. and Black I.A., 1934. An examination of the Degtjareff method for determining organic carbon in soils: Effect of variations in digestion conditions and of inorganic soil constituents. Soil Sci. 63:251-263;

Warrick A.W., 1982. Model for disc infiltrometers, Water Resources. Research 28: 1319-1327

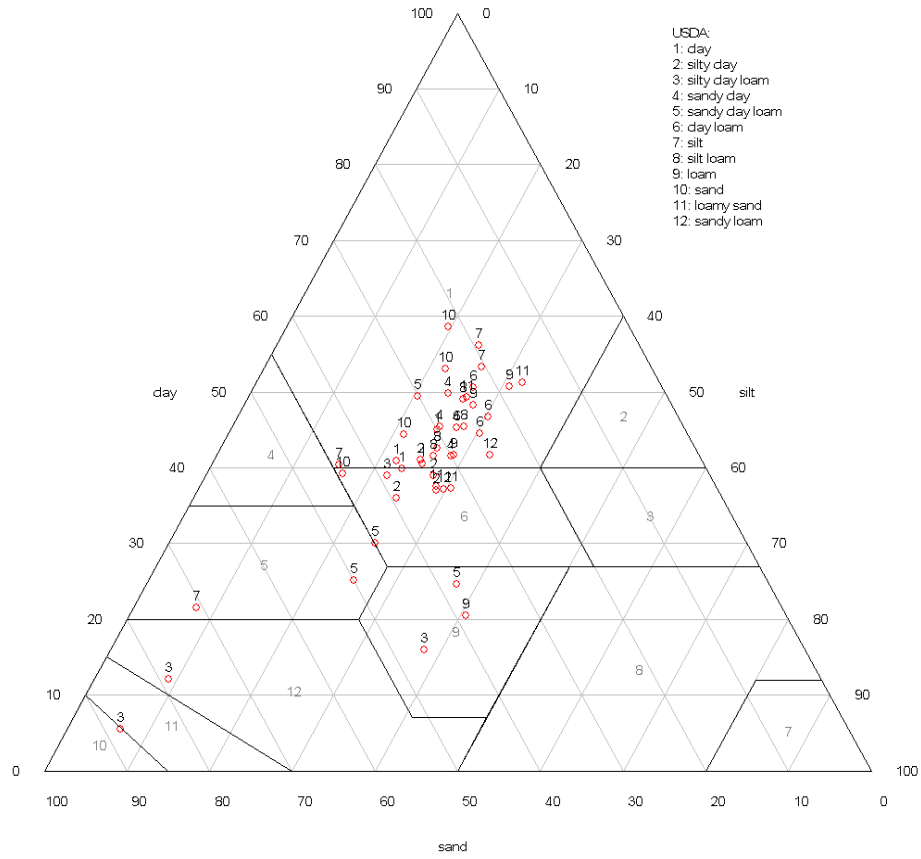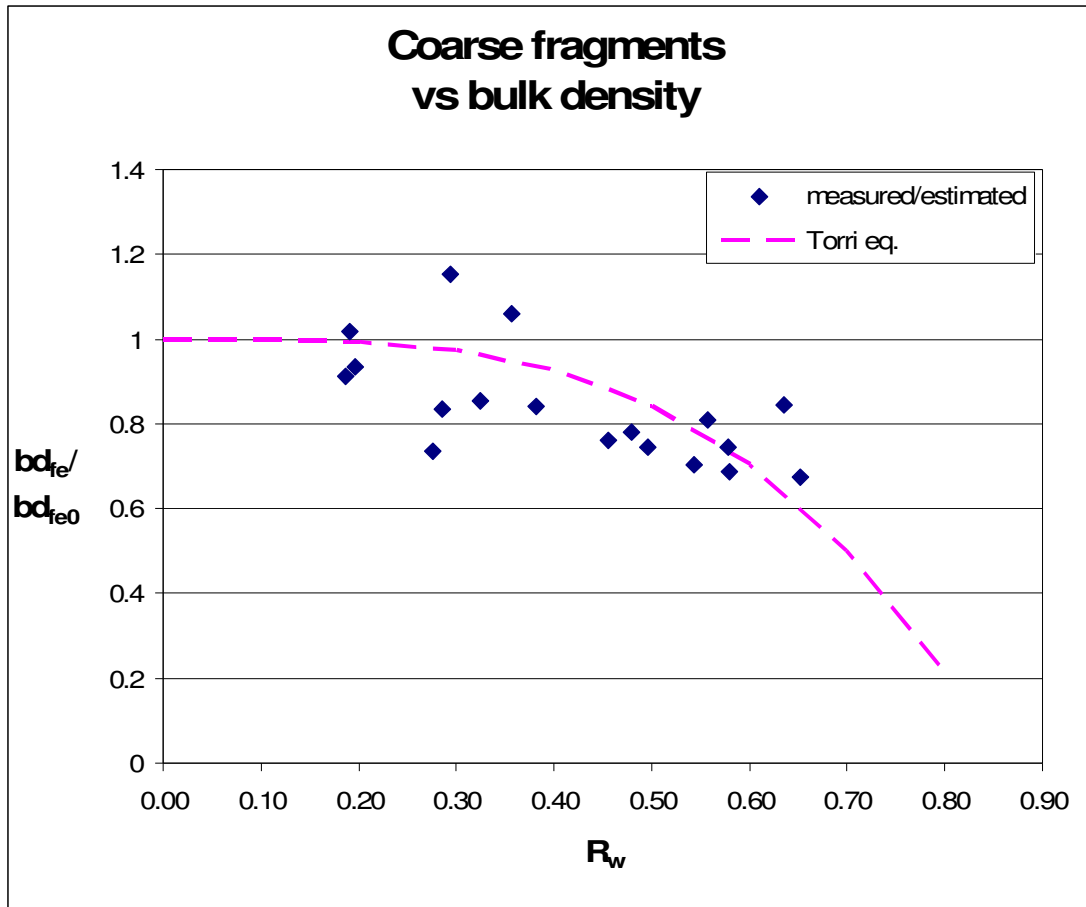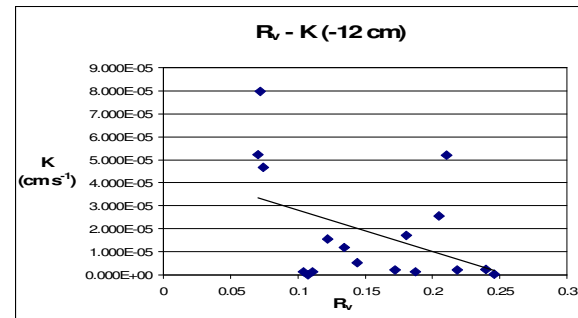**Figure 1:Texture of the undisturbed samples, according to USDA classification.**
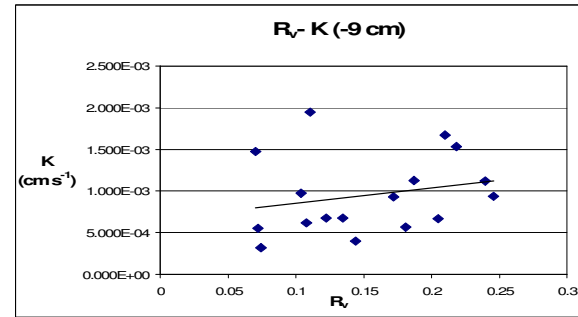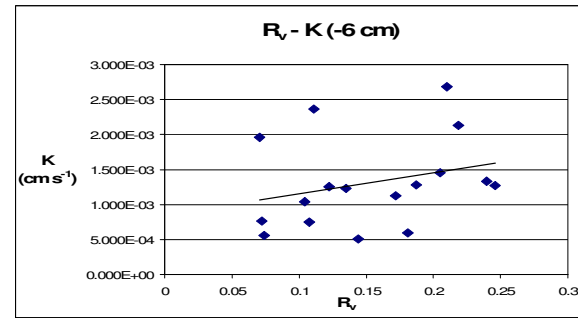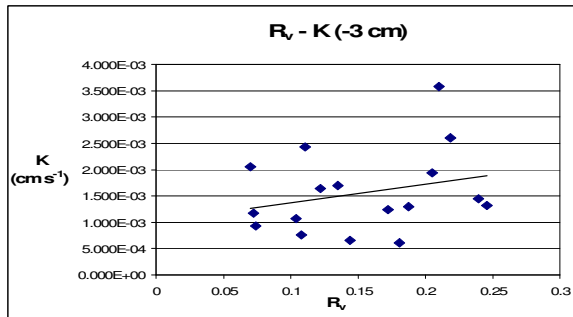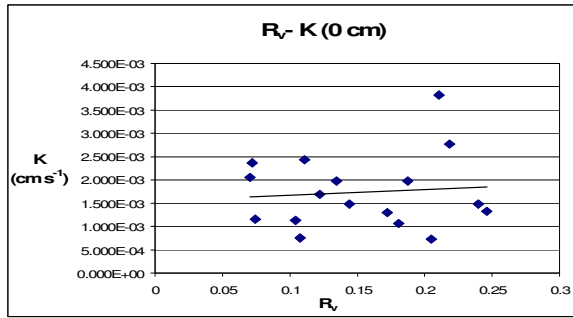
Figure 2: Ratio (rhomb, blu) between fine earth bulk density (bdfe) in presence of stone and with no stone content (bdfe0), the latter estimated using Kaur equation (2002), and Torri equation (purple dash line)

Figure 3: R_v vs $K(h)$ relationship

R_v- K (0 cm)

R_v - K (-3 cm)

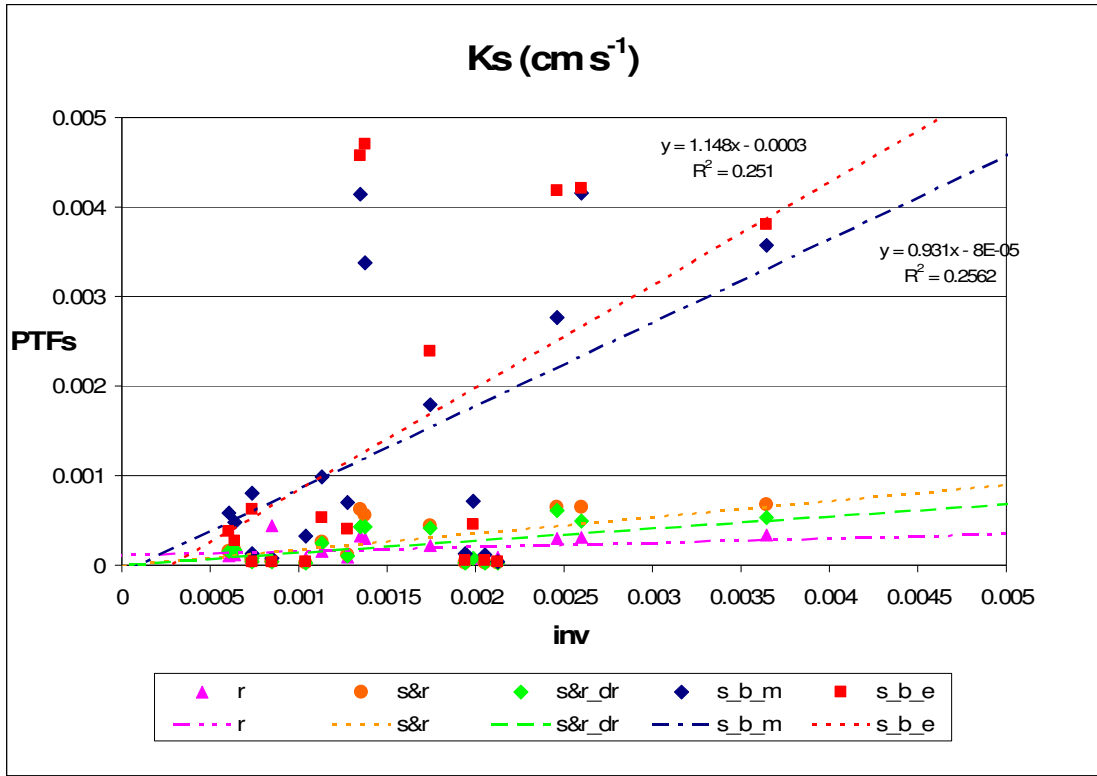R_v - K (-6 cm)

R_v- K (-9 cm)

R_v - K (-12 cm)

Figure 4: Comparison of inverted and predicted K_s using different predictor as input data: *r* (triangle, purle) Rosetta, using only texture; *s&r* (circle, orange) following Saxton and Rawls (2006), *s&r_dr* (rhomb, green) as the previous, but applying density reduction of 0.9; *s_b_m* (rhomb, blu) following Saxton et al. (1986), using measured bd_{fe}; *s_b_e* (square, red) as previous, but using estimated bd_{fe} using Kaur (2002)-Torri(1994) coupling. All K_s estimation were reduced by the volume based (1-R_v) coarse fragments content.
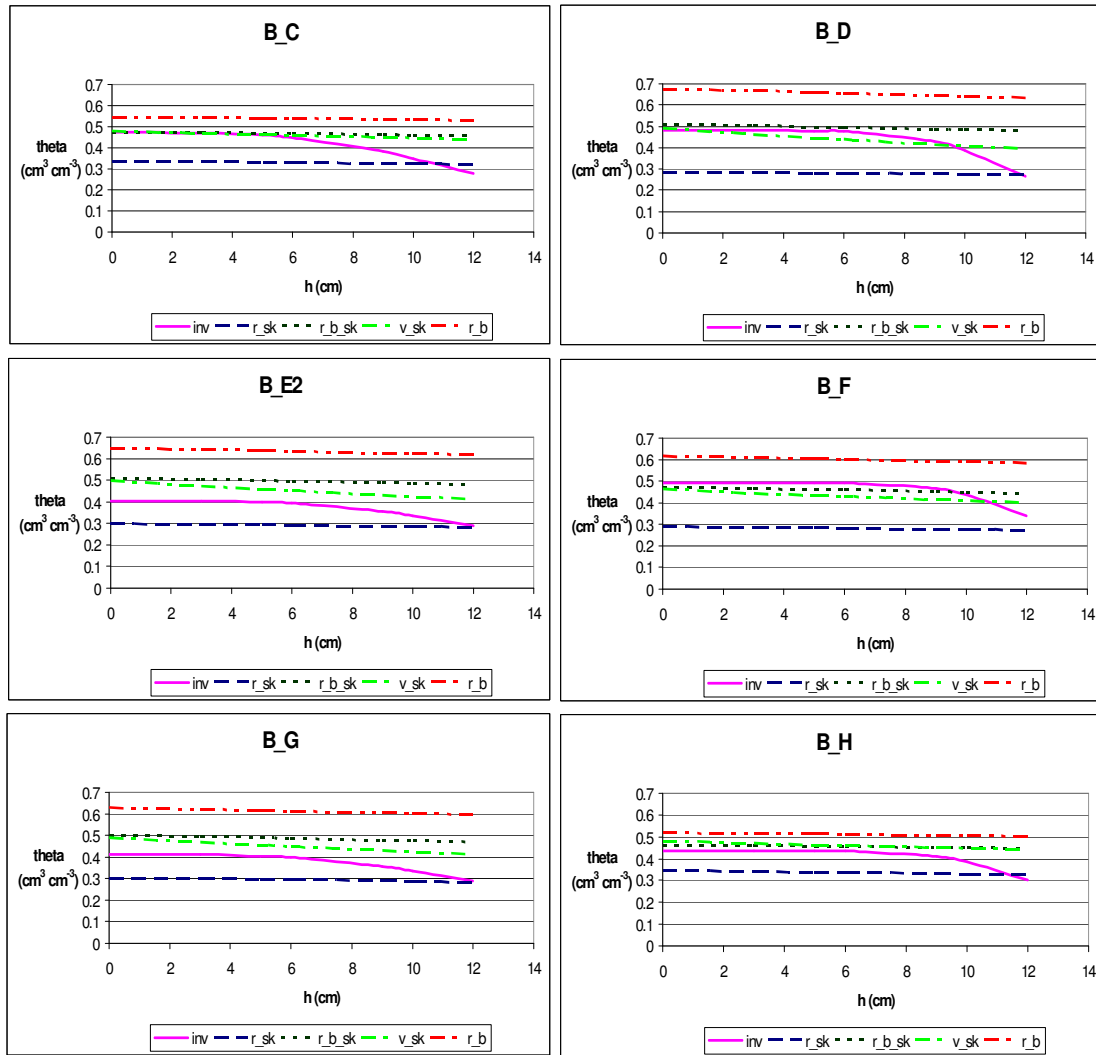
Figure 5: retention curve of Boffalora in the 0÷-12 cm range, derived from inversion (*inv*, purple) and estimated using: a) Rosetta (2001) (*r_sk*, blu) using only texture data; b) as a), but adding measured bdfe (*r_b_sk*, dark green); c) Veerecken et al. (1992) using bdfe (*v_sk*, light green); All previous approaches (a-c) were applied using a coarse fragment reduction (1-R_v), while d) Rosetta was applied as in a), but without coarse fragments reduction.
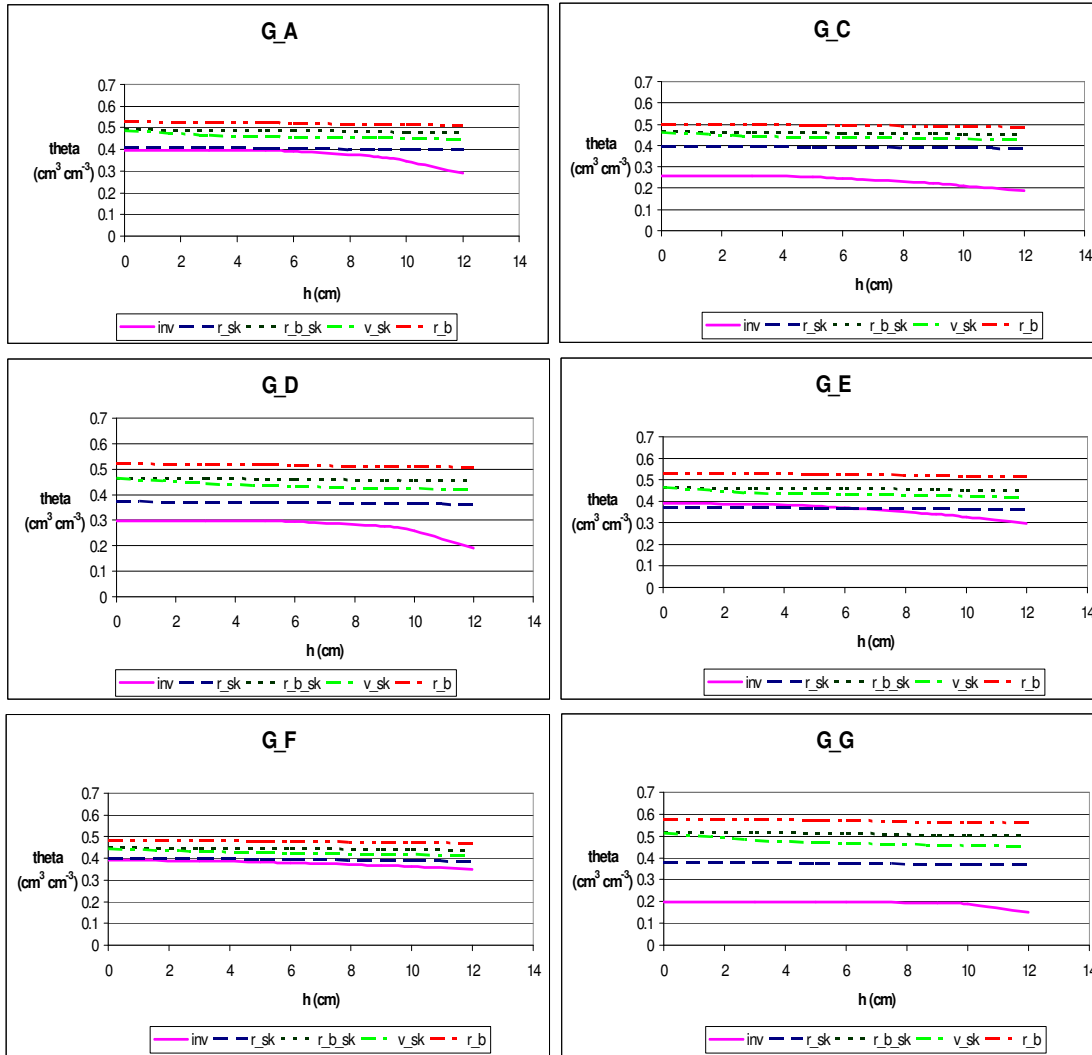
Figure 6: retention curve of Ghisalba in the 0÷-12 cm range, derived from inversion (*inv*, purple) and estimated using: a) Rosetta (2001) (*r_sk*, blu) using only texture data; b) as a), but adding measured bdfe (*r_b_sk*, dark green); c) Veerecken et al. (1992) using *bd_{fe}* (*v_sk*, light green); All previous approaches (a-c) were applied using a coarse fragment reduction (1-*R_v*), while d) Rosetta was applied as in a), but without coarse fragments reduction.
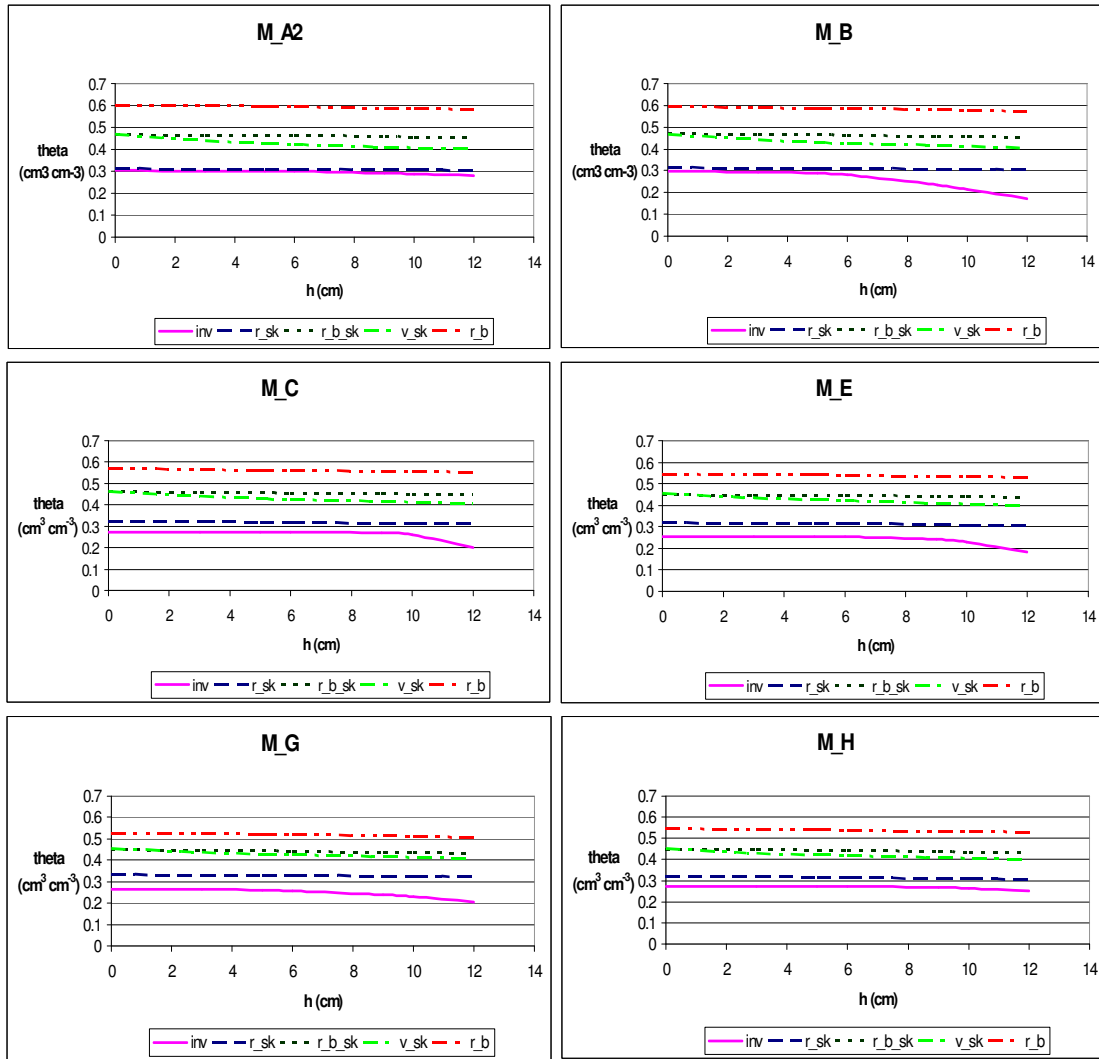
96

Figure 7: retention curve of Monzambano in the 0÷-12 cm range, derived from inversion (*inv*, purple) and estimated using: a) Rosetta (2001) (*r_sk*, blu) using only texture data; b) as a), but adding measured bdfe (*r_b_sk*, dark green); c) Veerecken et al. (1992) using bd_{fe} (*v_sk*, light green); All previous approaches (a-c) were applied using a coarse fragment reduction (1-R_v), while d) Rosetta was applied as in a), but without coarse fragments reduction.
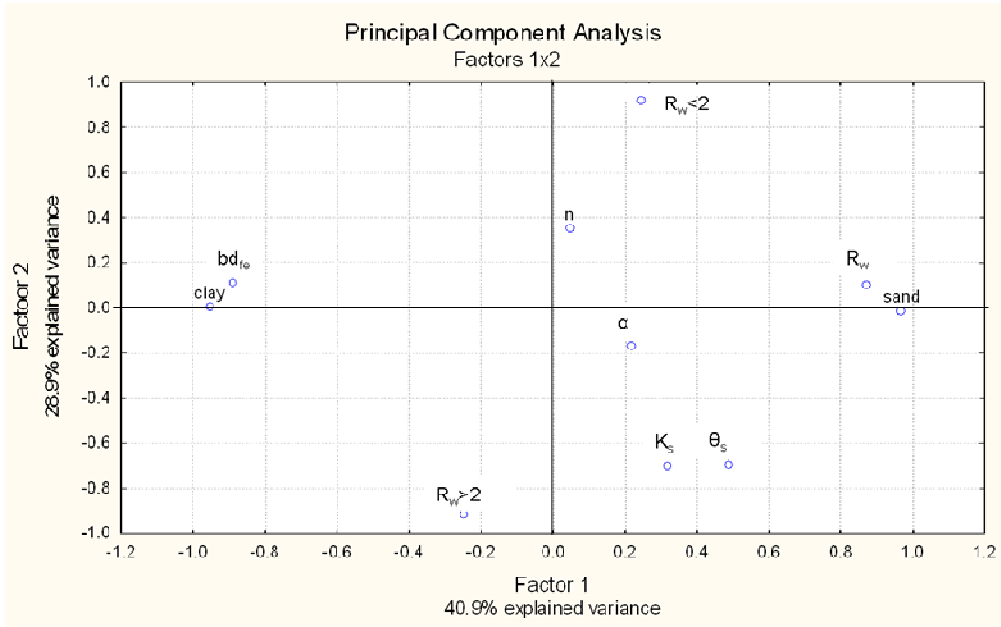
Figure 8: PCA result, 1X2 factors

Tables

exp	Sand	Clay	Silt	OM (%)	R_w	Fr. R_w (<2 cm)	Fr. R_w (2÷10 cm)	R_v	bd_t (g cm^{-3})	bd_{fe} (g cm^{-3})	Init. θ (cm^3 cm^{-3})	Fin. θ (cm^3 cm^{-3})	θ_s (cm^3 cm^{-3})	α (cm^{-1})	n (-)	K_s (cm s^{-1})
B_C	64	18	18	5.87	0.357	0.71	0.29	0.135	1.298	0.964	0.151	0.472	0.472	0.084	3.921	0.002
B_D	74	14	12	6.67	0.652	0.59	0.41	0.246	1.333	0.616	0.247	0.479	0.479	0.083	7	0.001
B_E2	72	14	14	4.99	0.636	0.54	0.46	0.24	1.596	0.765	0.291	0.494	0.494	0.077	7.159	0.001
B_F	72	14	14	6.09	0.579	0.60	0.40	0.218	1.251	0.674	0.214	0.405	0.405	0.073	3.963	0.003
B_G	74	14	12	5.70	0.557	0.52	0.48	0.21	1.316	0.738	0.219	0.413	0.413	0.073	3.516	0.004
B_H	64	14	22	5.86	0.294	0.89	0.11	0.111	1.269	1.008	0.125	0.437	0.437	0.076	6.983	0.003
G_A	36	42	22	3.65	0.186	0.34	0.66	0.07	1.563	1.159	0.352	0.398	0.398	0.072	5.12	0.002
G_C	40	40	20	2.65	0.197	0.74	0.26	0.074	1.68	1.239	0.222	0.259	0.259	0.071	3.07	0.001
G_D	44	38	18	3.16	0.285	0.62	0.38	0.108	1.72	1.157	0.117	0.297	0.297	0.079	7.266	0.001
G_E	42	40	18	3.38	0.324	0.47	0.53	0.122	1.676	1.146	0.348	0.39	0.39	0.066	2.479	0.002
G_F	40	42	18	3.09	0.191	0.48	0.52	0.072	1.771	1.314	0.37	0.393	0.393	0.043	1.665	0.002
G_G	42	40	18	3.35	0.276	0.60	0.40	0.104	1.551	0.985	0.165	0.196	0.196	0.075	10	0.001
M_A2	52	30	18	6.23	0.58	0.79	0.21	0.219	1.602	0.861	0.298	0.302	0.303	0.038	2.508	0.001
M_B	54	30	16	4.77	0.543	0.70	0.30	0.205	1.546	0.889	0.202	0.296	0.296	0.085	3.669	0.002
M_C	54	28	18	4.98	0.497	0.96	0.04	0.187	1.526	0.946	0.146	0.275	0.275	0.077	10	0.001
M_E	62	22	16	5.97	0.456	0.88	0.12	0.172	1.513	0.994	0.189	0.255	0.254	0.075	7	0.001
M_G	58	26	16	3.94	0.382	0.80	0.20	0.144	1.505	1.087	0.199	0.263	0.263	0.065	3.788	0.001
M_H	60	26	14	3.86	0.479	0.91	0.09	0.181	1.605	1.021	0.258	0.272	0.271	0.057	6.044	0.001

Table 1: tension disc experiment: field and inversion data

	Factor 1	Factor 2
$R_w<2$	0.25	**0.92**
$R_w>2$	-0.25	**-0.92**
R_w	**0.87**	0.10
bd_{fe}	**-0.89**	0.11
θ_s	0.49	-0.70
α	0.22	-0.17
n	0.05	0.35
K_s	0.32	**-0.70**
sand	**0.97**	-0.02
clay	**-0.95**	0.00

Table 2: Factors extracted by PCA (in bold weight > 0.7)

5 Hydraulic properties of stony soils: fine earth characteristics and tortuosity effect

Abstract

To study the steric effect of coarse fragments on hydraulic conductivity, PEST-Hydrus 3D interface was used to determine van Genuchten-Mualem (VGM) parameters of the fine earth fraction (sieved clay) of reconstructed samples, characterized by cylinder or sphere glass as coarse fragments. Comparison was done among no fragment and 10% and 30% coarse fragment content samples. Unsaturated hydraulic conductivity, as influenced by tortuosity, was determined by simulated infiltration events using Hydrus 3D. Different domains, which contained different "empty spaces", comparable to the coarse fragment content, were used to run the simulations. PEST-Hydrus 3D interface showed a good ability to estimate the VGM parameters, i.e. the overall mean *RMSE* value was of 0.009 and a maximum value of 0.01538. It has, however, to be tested with other textural classes to observe whether it could be a useful approach for all soil conditions.

K_{soil}/K_{fe} ratio is normally used to determine hydraulic conductivity reduction in increasing coarse fragment content. K_{soil}/K_{fe} was used to observe the stone positive effect on fine earth characteristics: it showed a tendency of increase of the hydraulic conductivity as stone content increased. K_{soil}/K_{fe} ratio was also used to determine tortuosity effect: for the studied soils, there were not differences between cylinder and sphere effect on hydraulic conductivity. Moreover, it was observed that tortuosity effect decreased as matric potential, in absolute value, increased. This is in contrast with the normally used approaches which uses a constant reduction factor for the overall matric potential range. More studies are necessary to understand whether the two contrasting behavior (fine earth characteristics and tortuosity effect) characterized other textural classes than the studied clayey soil.

Keywords: PEST, Hydrus 3D, coarse fragments, fine earth characteristic, tortuosity effect

Introduction

Stones play a role in soil by modifying the pore space (Fiès et al., 2002). In natural soils, increasing rock fragments content is correlated with increasing total bulk density of the soil (bd_t - stones plus fine earth) and decreasing bulk density of the fine earth (bd_{fe}) (Torri et al., 1994). There are a number of possible reasons for the occurrence of the latter negative relationship (Poesen and Levee, 1994):

- at high stone contents there may happen a situation where fine earth is insufficient to fill the voids in between the rock fragments determining lower bd_{fe} values;

- in a mixture of different particle size grades, the smaller particles cannot pack as closely to the larger particles as they can within each other;

- fine earth and stones react in a different way when expanding and contracting (e.g. during the process of wetting and drying or of freezing and thawing), thus causing void formation;

- nature of the fine earth fraction is changed by the presence of stones, indeed in a decreasing mass of fine earth several biogeochemical processes are concentrated, i.e. decay of organic matter, fertilizer inputs, etc., thus affecting other soil properties such as soil structure.

Ingelmo et al. (1994) reported that the formation of macroporosity might be a consequence of physical processes (swelling-shrinking; freezing-thawing), chemical processes (aerobic-anaerobic conditions), and ecological changes (soil fauna may dig deeper to find favorable conditions in the contact areas between soil and rock fragments).

Using reconstructed samples Mehuys et al. (1975) studied the unsaturated hydraulic conductivity (K_u) of stony and non-stony dry soils and they found that the relationship between K_u and matric potential of stony soils can be described by that one of the non-stony soil. On the contrary, the relationship K_u -water content of the non-stony soil may not be used in the same way because they found an higher K_u in the stony soil compared with the non-stony soil. Moreover, they underlined that, if the bulk density of the reconstructed column is the same of the bulk density of the field, it is possible to use the hydraulic properties of the fine earth particle without any correction.

Bouwer and Rice (1984) studied the behaviour of saturated (K_s) and unsaturated hydraulic conductivity (K_u) in reconstructed stony columns and they concluded that:

1. K_s of the stony soil (stones plus fine particles - K_{soil}) can be calculated multiplying the K_s of the fine earth particle (K_{fe}) with the void ratio of stony – non-stony soils;

2. K_u of the stony soil can be determined from K_u of the fine earth fraction, using as matching factor the K_s calculates as previously mentioned, thus the air entry value remains the same for the stony and non-stony soils;

3. the volumetric water content of the stony soil can be reduced multiplying the volumetric water content of the fine particle with the stone volume fraction.

On the other hand, Ravina and Magier (1984) studied the behaviour of compacted clayey stony soil and they affirmed that "the effect of rock fragments on hydraulic conductivity and moisture retention of aggregated clay soils cannot be adequately accounted for by simple corrections for the reduced area available for flow and reduced total pore volume, at least not in the high moisture (low suction) range".

By mean of a dual porosity (dual permeability) model (Ross and Smettem, 2000; Šimůnek et al. 2001), Ma and Shao (2008) simulated 1D infiltration processes in soil containing coarse fragment and evaluated the effects of stone properties in this process. Their main conclusions were:

a) stoniness, reducing the cross-sectional area for water flow, is one of the most important factors to hamper infiltration into stony soils. This effect is exacerbated at higher coarse fraction content. Moreover spherical stones accelerated infiltration compared to cylindrical stones and big stones hampered infiltration more than small stones.

b) stone water content cannot be neglected in all cases;

c) coarse fragments can exchange water with the fine earth fraction, thus they serve as source or sink to exert influences on infiltration;

d) rock fragments may make the pore structure of the fine earth changes due to stones, making water infiltration more favourable than in non stony soils.

From the previous consideration could be useful to be able to describe the behaviour of the fine earth fraction in soil containing coarse fragments, and understand their steric effect on tortuosity. Bulk hydraulic conductivity (fine earth plus stones) is effected by the fine

earth characteristic and the tortuosity. The former could be achieved by mean of 3D nonlinear parameter estimation technique, the latter by the use of 3D domain, where it would possible to define the coarse fragment and the fine earth fraction spaces. The aims of this work were: a) to estimate, using PEST (Doherty, 2004), a model-indipendent parameter optimiser, coupled with Hydrus 3D (Šimůnek et al., 2006), the van Genuchten (1980) – Mualem (1976) (VGM) parameters, by the inversion of evaporation experiments conducted on samples having different "coarse fragment" (glass fragment) contents, and thus to describe the fine earth behaviour; b) to use the former VGM parameters to simulate infiltration events using Hydrus 3D, and thus to describe the tortuosity effect.

Material and methods

<u>Sample preparation</u>

The steric influence of the "coarse" fragments was studied by mean of reconstructed samples. They were manually constructed using 2 mm sieved clay (25% sand, 23 % silt and 52% clay –USDA, pH 6.5 , SOC 1.2%) as fine earth fraction and glass spheres (average diameter 1.59 cm) or glass cylinders (2 cm x 1 cm) as coarse fraction. Arrangements of spheres and cylinders were as symmetrical as possible within the samples. The choice to use the glass was to have a material which did not have any porosity, so it could be possible to evaluate the steric role of coarse fragment on soil hydraulic properties. Volume coarse fractions used were: no fragments, 10%, 30%, with two replicates (tab. 1) As the samples were prepared, they were saturated by freely bottom infiltration at atmospheric pressure, laying the sample in a water bath for at least a couple of days. Samples were then set in the sandbox apparatus and subjected to -50 cm of matric suction, which was applied for at least a couple of days to consolidate the samples (Dane and Hopmans, 2002).

<u>Evaporation experiments</u>

Evaporation experiments were conducted using the ku-pF Apparatus DT 04-01 (UGT, 2005). Two electronic tensionmeters, after calibration, were inserted inside the sample, at

1.5 cm and 4.5 cm height. Matric potential and water loss values were stored every 10 minutes using a datalogger. Samples were let to freely evaporate at the surface, while no flux was allowed at the bottom, since it was sealed. Experiments were stopped when the top tensionmeter reached a value of about -800÷-900 cm (UGT, 2005), or when the tensionmeters value were not reliable anymore (i.e., bottom value smaller than top one). At the end of the analysis, the samples were destroy, and after removal of the coarse fragments, the gravimetric water content of the fine earth fraction was determined after 12 h in oven at 105° C. Stored data were used to directly calculated the retention curve and the hydraulic conductivity. Assuming quasi-stationary flow, the Darcy- Buckingham equation was used to calculate the hydraulic conductivity of the soil samples. Constant hydraulic gradient was always considered throughout the sample height. The matric (tensiometer measurement) and gravitation potential formed the (total) gradient. Due to the experiment set up (freely evaporation at the top and sealed bottom), it was possible to consider a mean flow rate between tensionmeters, allowing to calculate a sample-halfway hydraulic conductivity, at least since the difference of the matric potential between the tensionmeters was less than about -50 cm. The retention curve was calculated as the relationship between the actual water content of the sample and the taken mean of the two tensiometer measurements.

HYDRUS 3D-PEST interface – Numerical Simulation

To characterise the fine earth fraction of the reconstructed samples, evaporation data were analysed using HYDRUS 3D (Šimůnek et al, 2006) coupled with PEST (ver. 11.3 for UNIX) (Doherty, 2004), the latter in the parameter estimation mode.

HYDRUS 3D

For a three-dimensional isothermal uniform Darcian flow of water in a variably saturated rigid porous medium, considering that the air phase plays an insignificant role in the liquid flow process, Hydrus 3D solved numerically the following modified form of the Richards' equation:

$$\frac{\partial \theta}{\partial t} = \frac{\partial}{\partial x_i} \left[K \left(K_{ij}^A \frac{\partial h}{\partial x_j} + K_{iz}^A \right) \right] \tag{1}$$

where θ is the volumetric water content (cm^3 cm^{-3}) h is the pressure head (cm), x_i (i=1,2,3) are the spatial coordinates (cm), t is time (d), K^A_{ij} are components of a dimensionless anisotropy tensor K^A, and K is the unsaturated hydraulic conductivity function (cm d^{-1}) given by

$$K(h, x, y, z) = K_s(x, y, z) K_r(h, x, y, z) \tag{2}$$

where K_r is the relative hydraulic conductivity and K_s the saturated hydraulic conductivity (cm d^{-1}), where z is the vertical coordinate, positive upward. Top and bottom boundary condition were the evaporation rate (cm d^{-1}) during the experiment and no flux, respectively. Initial condition, expressed as pressure head, was the linear distribution of the matric potential of the tensionmeters at the beginning of the experiment.

The van Genuchten (VG) equation (1980), related with the Mualem approach (1976) was the hydraulic model used in the numerical solution. VG equation is defined as:

$$S_e = \frac{1}{\left[1 + (\alpha h)^n \right]^m} \tag{3}$$

where

$$S_e = \frac{\theta - \theta_r}{\theta_s - \theta_r} \tag{4}$$

with Se ($0 \leq S_e \leq 1$) effective saturation degree, θ_s and θ_r respectively saturated and residual water content, α, n e m (m set equal to 1-1/n) are empirical parameters which influence the shape of the curve. $1/\alpha$ is normally considered as the air entry pressure.

Mualem (1976) model can be described as:

$$K(S_e) = K_s S_e^l \left[\frac{f(S_e)}{f(1)} \right]^2 \tag{5}$$

where

$$f(S_e) = \int_0^{S_e} \frac{1}{h(x)} dx \tag{6}$$

S_e is the effective saturation degree (4), K_s is the saturated hydraulic conductivity, l is the pore connectivity and tortuosity parameter.

The fitted parameters were θ_r, θ_s, α, n, K_s, l.

Domain was 3.61 cm of radius and 6.1 cm of depth, besides that, five different domains which differed by the inner characteristics (tab. 2) were defined in according to coarse fraction content experiments which were to be parameterized. Coarse fragments, both cylinders (cyl) and spheres (sphe) were considered as empty elements (thus from a computational point of view they were subtracted from the entire domain) within the entire domain. Due to Hydrus 3D feature, it was not possible to define smooth cylinder and sphere shapes, indeed parallelogram and cube shape were instead defined. The rational used to defined the "cylinders" and the spheres" was firstly to maintain the closest possible comparison with the real volume: for that reason the "cylinders", laying horizontally, were defined as 2 cm length and 0.9 cm, both height and depth, while the "spheres" had a 1.3 cm side. Moreover the number of elements (i.e. cylinders and spheres) were the same as the real evaporation experiments. Their position within the samples was the closest possible reconstruction of the real coarse fragment distribution (fig. 1).

The parameter estimation was done using PEST (Doherty, 2004), which is a model-indipendent non linear parameter estimation software, which uses non-linear Levenberg-Marquardt algorithm (1963). The objective function Φ, which has to be minimised during the parameter estimation process, is defined as:

$$\Phi = (c - c_0 - J(b - b_0))^t Q(c - c_0 - J(b - b_0)) \tag{7}$$

where $(b - b_0)$ is the upgrade vector on the basis of the vector $(c - c_0)$ which defines the discrepancy between the model-calculated observations c_0 and their experimental counterparts c, J is the Jacobian matrix of M, i.e. the matrix comprised of m rows (one for each observation and the n elements of each row being the derivatives of one particular observation with respect to each of the n parameters), Q is the observation weight matrix, it is a diagonal matrix, with m rows and m columns (i.e. the diagonal elements of Q contain the relative weight of each observation in the total model error) and the "t" superscript indicates the matrix transpose operation. b_0 is the initial parameter set and b is the parameter vector estimated during the estimation process and it is then used as a starting point in determining a subsequently parameter upgrade vector.

Volumetric water content, corrected for the coarse fragment content, at the end of the evaporation experiment, and matric potential values were the observation measurements to be estimated.

One of PEST characteristic is the possibility given to the user to change the way in which the least squares method is implemented, i.e. users may define the number of parameters group, which defines how the derivatives are calculated, either using forward difference or central difference method or both. Most of the variables given by PEST in its PEST control file (fig. 2) were maintained as default, with the exception of a) only one parameter group was defined; b) the real variable DERINCMUL (which defines how the parameter increment is added/subtracted to the current parameter) was set to 1.5; c) the initial parameters estimates (θ_r=0.095 cm^3 cm^{-3}, θ_s=0.47 cm^3 cm^{-3}, α=0.019 cm^{-1}, n=1.31, K_s=12.29 cm d^{-1} and l=0.5) and their range were always the same for all the parameter estimation processes; d) two observation groups were defined: "obsgroup"=matric potential value and "gr_2"=volumetric water content value; e) weight of "obsgroup" group was

calculated as the mean ratio between the volumetric water content and the matric potential values, while "gr_2" weight varied, from 5 to 100, according to the goodness of estimation process.

Goodness of fit was evaluated using the *RMSE* value, as described by Goegebeur and Pauwels (2007), which is defined as:

$$RMSE = \sqrt{\frac{1}{n_t} \sum_{i=1}^{n_t} \left(v_{o_i} - v_{s_i}\right)^2} \qquad (8)$$

where n_t is the number of data points, v_o and v_s are the observed and simulated variables (i.e. matric potential and/or volumetric water content values). The *RSME* calculated in that way is not equal to the minimisation of the objective function, even though, as obviously, a decrease of Φ leads to a decrease of *RMSE* (Goegebeur and Pauwels, 2007).

Hydraulic conductivity (*K(h)*) simulations

Once obtained the two set of van Genuchten-Mualem (VGM) parameters of the fine earth characteristics at 0% of coarse fragments, they were used in Hydrus 3D, with direct mode, to simulate the effect of the tortuosity on the hydraulic conductivity at six different pressure head (0, -10, -20, -50, -100 and -330 cm). The previously described domains were used to conduct the simulations. Top boundary conditions (BC) used was constant pressure head at prescribed pressure, while bottom BC was, for all the studied pressure head, with the exception of 0 cm, the free drainage condition. At 0 cm pressure head, the seepage face BC was used: this was done because of instability problems that were faced when the free drainage BC was tested. The initial condition was, in the entire domain, the same head as prescribed by the top BC. Simulation time was 10 days, with time discretisation defined as 0.1, 0.001 and 1 for the initial, minimum and maximum allowed time step, respectively. It was possible to achieve quasi-unit gradient condition within the sample at the end of each the simulation. The flux leaving the domain at the end of the simulation was divided by the area, thus the hydraulic conductivity of the bulk soil at prescribed pressure head was calculated.

To understand the behaviour of fine earth in presence of coarse fragments compared with the fine earth behaviour in absence of coarse fragment, the ratio K_{soil}/K_{fe} was the tool used to investigate it. In general K_{soil}/K_{fe} ratio is considered by several authors (Peck and Watson, 1979 and Morgan, 1985; among others) as the ratio between K_{soil}, the hydraulic conductivity in presence of coarse fragment, and K_{fe}, hydraulic conductivity in absence of coarse fragment. Moreover, simulated hydraulic conductivity derived from the simulations were used to calculate K_{soil}/K_{fe} ratios, which were furthermore compared with the theoretical approaches, which predict a decrease of K_{soil}/K_{fe} in respect to the volumetric coarse fraction content (R_v). The analysed equations were:

1) $K_{soil}/K_{fe} = (2*(1-R_v))/(2+R_v)$, as described by Peck and Watson (*P&W*) (1979)

2) $K_{soil}/K_{fe} = 1 - R_v$, as described by Morgan (*M*) (1985).

Results and discussion

Hydrus 3D- PEST parameter estimation processes showed a mean *RMSE*, of both matric potential plus volumetric water content values and only matric potential values, of 0.009 with a minimum value of about 0.006 in the first replicate of 10% spheres, and the maximum values of 0.01538 in the second replicate of 0% coarse fragment content (tab. 3). The mean *RMSE* for the volumetric water content by itself was about 0.006, and a minimum and maximum value of 0.00004 and 0.016, respectively in the second replicate of 10% cylinders and 0%. Analysing the relationship between R_v and the VGM parameters only θ_r was negative related with the reduction of effective domain for the flux. Among the relationships between the VGM parameters, the only one, that might be warily seen, was the logarithm relationship between K_s and l. It has to be mentioned that 3D simulation are, for their intrinsic nature, very complex and required a very high computational demand. Before obtaining the presented results, several trial-and-error attempts were conducted, as suggested by Doherty (2004), to understand which was the more reliable way to run the simulation. Attempts were done without estimation of l, thus maintaining it fixed at 0.5, as suggested by Mualem (1976): the main arisen problem was that the PEST gave K_s estimation which was at the upper threshold value (i.e. if the upper range value was 100 cm

110

d^{-1}, with l=0.5, K_s estimate was 100 cm d^{-1}). Even though it is known that, increasing the number of parameters to be estimated, might increase the computational demand and the correlation between parameters, this choice seemed obliged to obtain a K_s value that was not constrained by the imposed range. All the l values, with the exception of one (that with the highest K_s value – second replicate of 30% cylinders) were negative, thus it is not possible to consider, for the shown data, this parameter as physically related to the hydraulic conductivity, but only as empirical parameter (Schaap et Leij, 2000).

To understand fine earth behaviour, the K_{soil}/K_{fe} was calculated between the unsaturated hydraulic conductivity ($K(h)$) of fine earth fraction as estimated by PEST in different domains, with increasing coarse fragments content, to the $K(h)$ of fine earth fraction estimated in the 0% coarse fraction domain . In figure 4, that ratio was related with the matric potential values. The ratio K_{soil}/K_{fe} was, with the exception of the fine earth behaviour at 10 % cylinders at saturation, always higher that the unit ratio (which represented the behaviour of fine earth at 0% coarse fragments) and tended to decrease, as the matric potential, in absolute value, increased. The described behaviours leaded to the following considerations: a) the coarse fragments influenced the fine earth behaviour, with an increase of K_{soil} in increasing coarse fragment content. Ravina and Magier (1984), although with completely different experiments and approach found the same relationship; b) the coarse fragments expressed their effects with lesser extent at higher (absolute value) matric potential value.

To understand the influence of the tortuosity, K_{soil}/K_{fe} ratios were calculated between the $K(h)$, which was simulated in presence of coarse fragment (i.e. same VGM parameters simulated in different domains), and the $K(h)$, which was simulated in absence of coarse fragment, i.e. 0% domain (fig.7). In figure 7 showed that, for the studied reconstructed clay-coarse fragments soils: a) K_{soil}/K_{fe} decreased in increasing coarse fragments, although no difference is evident between cylinders and spheres. This is in contrast with Bouwer and Rice (1984) and Ma and Shao (2008) results, which showed that spheres accelerated infiltration compared to the cylinders; b) K_{soil}/K_{fe} increased, with a non linear-relationship, with the increase (in absolute value) of the matric potential, i.e. the tortuosity effect induced by the coarse fragments decreased as the soil was drying. This behaviour is completely different from what is expected by the *P&W* and *M* approaches, which apply a constant

reduction of hydraulic conductivity in respect to the coarse fragment content increase, in the entire matric potential range. *P&W* and *M* approaches seemed slightly to be able to describe the K_{soil}/K_{fe} behaviour only at saturation (figure 8).

Conclusions

PEST-Hydrus 3D interface showed a good ability to estimate the VGM parameters, i.e. the overall mean *RMSE* value was of 0.009 and a maximum value of 0.01538. Due to the fact that all, except one, the estimated l values did show negative value, this parameter has not to be considered with a physical meaning, but just as empirical factor (Schaap and Leij, 2000). Even though K_s and l were found to be correlated to each other, this did not invalidate the parameter estimation process. Nevertheless, PEST-Hydrus 3D interface seemed a good tool to estimate hydraulic properties in 3D domains, for clay textured soils. It has, however, to be tested with other textural classes to observe whether it could be a useful approach for all soil conditions.

By mean of the results given by PEST-Hydrus 3D interface and by subsequently simulated infiltration events conducted by Hydrus 3D, it was possible to study the steric influence of coarse fragments on hydraulic conductivity in the 0÷-330 cm of matric potential. It was possible to separately analyze the fine earth characteristics and the tortuosity effect, as both influenced by different coarse fragment content. With respect to the fine earth characteristics, in increasing coarse fragment content, hydraulic conductivity increased, but with lesser extent at more negative pressure head. This support Ravina and Magier (1984) results. Coarse fragment content determined a reduction of the hydraulic conductivity when the tortuosity effect was analyzed. Cylinders and spheres influenced the *K(h)* in the same way, which was in contrast with previous works (i.e. Bouwer and Rice, 1984 and Ma and Shao, 2008). Moreover, according to the presented dataset, *K(h)* was less influenced by the coarse fragment in increasing (in absolute value) matric potential value. This is in contrast with the normally used approaches which uses a constant reduction factor for the overall matric potential range. More studies are necessary to understand whether the two contrasting behavior (fine earth characteristics and tortuosity effect) characterized other textural classes than the studied clayey soil.

Acknowledgements

References

Bouwer H. and Rice R.C., 1984. Hydraulic properties of stony vadose zones. Ground Water 6: 696-705;

Dane J.H. and Hopmans J.W., 2002. In: SSSA Book Series: 5 - Methods of Soil Analysis Part 4 Physical Methods: cap. 3.3. Eds: Dane J.H. e Topp G.C., Soil Science Society of America, Inc;

Doherty J., 2004. Model-Indipendent Parameter Estimation. User manual: 5th Edition. Watermark Numerical Computing. Fiès J.C., De Louvigny N., and Chanzy A., 2002. The role of stones in soil water retention. European Journal of Soil Science 53:95-104;

Goegebeur M. and Pauwels V.R.N., 2007. Improvement of the PEST parameter estimation algorithm through Extended Kalman Filtering. Journal of Hydrology, 337:436-451;

Ingelmo F., Cuadrado S., Ibanez A. and Hernandez J., 1994. Hydric properties of some spanish soils in relation to their rock fragment content - implications for runoff and vegetation. Catena 23:73-85;

Ma D.H. and Shao M.G., 2008. Simulating infiltration into stony soils with a dual-porosity model. European Journal of Soil Science 59:950-959;

Marquardt D.W., 1963. An algorithm for least-squares estimation of non linear parameters. J. Soc. Ind. Appl. Math.: 11, 431-441;

Mehuys G.R., Stolzy L.H., Letey J. and Weeks L.V., 1975. Effect of stones on the hydraulic conductivity of relatively dry desert soils. Soil Sci. Soc. Amer. Proc, 39: 37-42;

Morgan R.P.C., Quinton J.N., Smith R.E., Govers G., Poesen J.W.A., Auerswald K., Chisci G., Torri D. and Styczen M. E., 1998. The European Soil Erosion Model (EUROSEM): a dynamic approach for predicting sediment transport from fields and small catchments. Earth Surface Processes and Landforms 23: 527–544;

Mualem Y., 1976. A new model for predicting the hydraulic conductivity of unsaturated porous media. Water Resour. Res.: 12, 513-522

Peck A.J. and Watson J.D., 1979. Hydraulic conductivity of flow in non-uniform soil. Workshop on Soil Physics and Field heterogeneity;Camberra, Australia. Unpublished.

Poesen J. and Lavee H., 1994. Rock fragments in top soils - significance and processes. catena 23:1-28;

Ravina I. and Magier J., 1984. Hydraulic conductivity and water retention of clay soils containing coarse fragments Soil Sci. Soc. Am. J., Vol. 48:736-740;

Ross P.J. and Smettem K.R., 2000. A simple treatment of physical nonequilibrium water flow in soils. Soil Sci. Soc. Am. J. 64:1926–1930;

Schaap M.G. and Leij F.J., 2000. Improved prediction of unsaturated hydraulic conductivity with the Mualem-van Genuchten model. Soil Science Society of America Journal 64:843-851;

Šimůnek J., Wendroth O., Wypler N. and van Genuchten M.T., 2001. Non-equilibrium water flow characterized by means of upward infiltration experiments. European Journal of Soil Science 52:13-24;

Šimůnek J., van Genuchten M.Th. and Šejna M., 2006. The HYDRUS software package for simulating the two- and three-dimensional movement of water, heat, and multiple solutes in variably-saturated media. Technical manual. PC Progress, Prague, Czech Republic

Torri D., Poesen J., Monaci F. and Busoni E., 1994. Rock fragment content and fine soil bulk-density. Catena 23:65-71;

UGT, 2005. Operating instruction for ku-pF Apparatus DT 04-01. Müncheberg, Germany;

van Genuchten M. Th., 1980. A closed form equation for predicting the hydraulic conductivity of unsaturated soils. Soil Science Society of American Journal.:44, 892-898

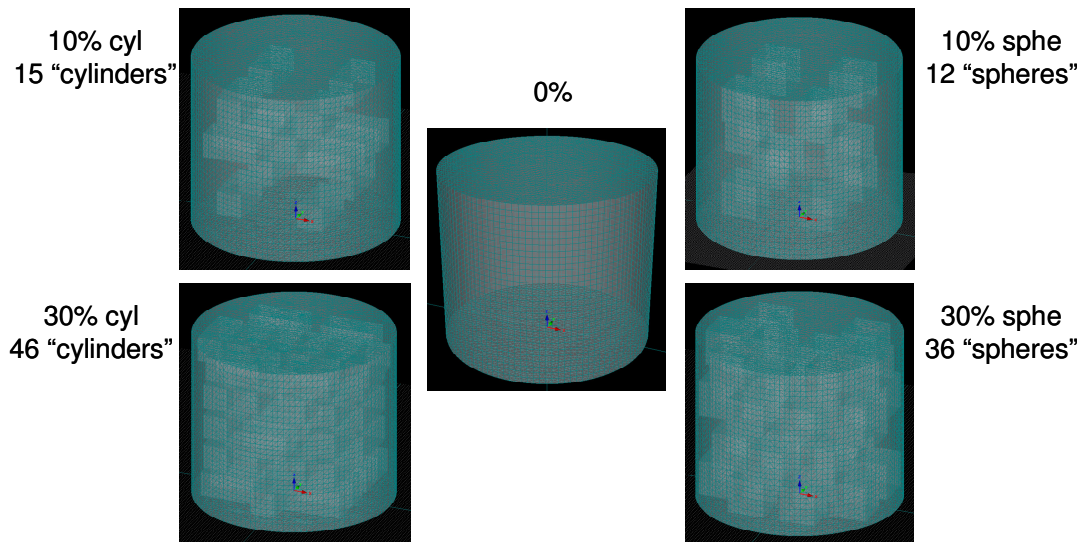**Figure 1: 3D visualisation of the Hydrus 3D domains used.**

```
pcf
* control data
restart   estimation
     6     131      1      0      2
     1      2 double point    1    0    0
   5.0    2.0    0.3   0.03     10   999
   3.0    3.0  0.001   0
   0.1
    30   0.01      3      3   0.01      3
     1      1      1
* parameter groups
vg            relative 0.01   0.0   switch   1.5 parabolic
* parameter data
th_r          none relative    0.095          0.05         0.3  vg     1.0000           0.0000      1
th_s          none relative    0.47           0.35         0.65 vg     1.0000           0.0000      1
alf           none relative    0.019          0.0001       0.1  vg     1.0000           0.0000      1
enne          none relative    1.31           1.0001       3.0  vg     1.0000           0.0000      1
k_s           none relative    12.29          2.0       10000.0  vg     1.0000           0.0000      1
elle          none relative    0.5           -10.0        10.0  vg     1.0000           0.0000      1
* observation groups
obsgroup
gr_2
* observation data
hn_1_1                -3.05910      0.001715   obsgroup
hn_2_1                -6.11820      0.001715   obsgroup
hn_1_2                -5.20050      0.001715   obsgroup
hn_2_2                -8.36150      0.001715   obsgroup
hn_1_3                -8.25960      0.001715   obsgroup
```

Figure 2:fragment of PEST control file used in the parameter estimation process, where are shown the main variables which determine how the derivatives are calculated. In particular the parameter data section defined the Van-Genuchten Mualem parameters (θ_r=th_r, θ_s=th_s α=alf, n=enne, K_s= k_s, l=elle)
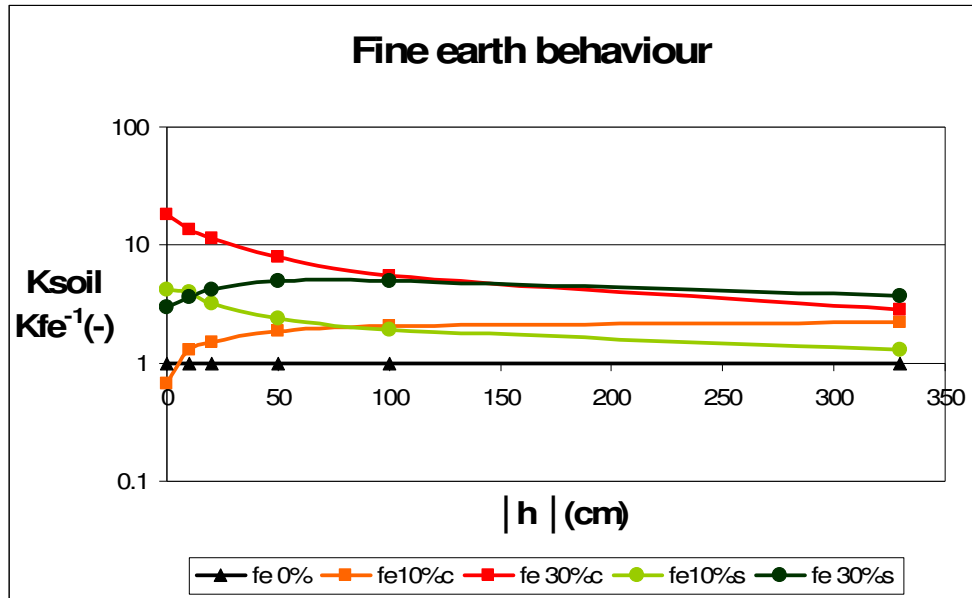
Figure 3: the fine earth behaviour at different coarse fragment content: ratio between the K_{soil}, calculated using the parameter which characterized the fine earth fraction in presence of coarse fragment to K_{fe}, calculated using the parameters which characterized the fine earth fraction in absence of coarse fraction. Their behaviour in respect to the matric potential values.
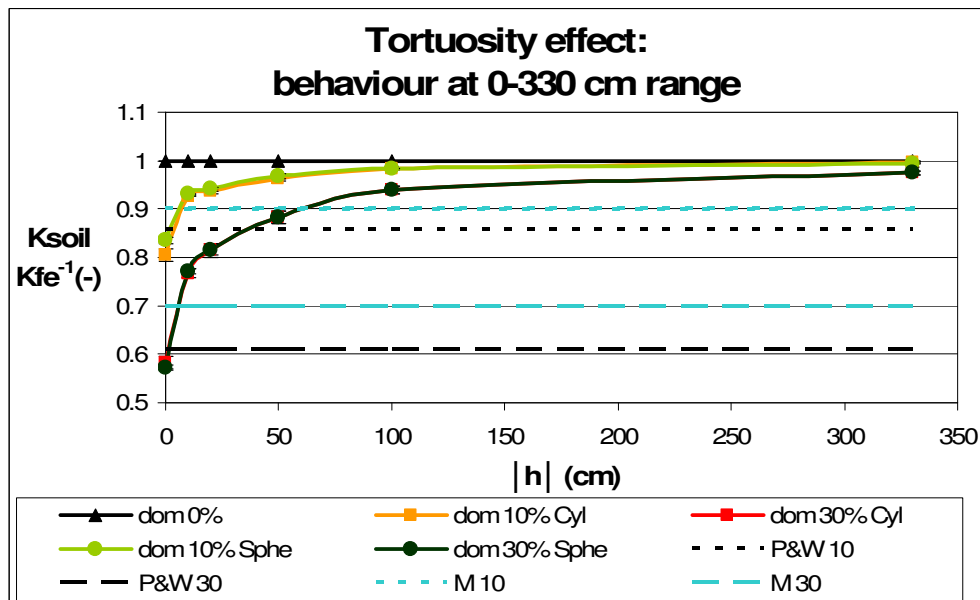

Figure 4: domains influence on hydraulic conductivity: ratio between the $K(h)$, which was simulated in presence of coarse fragment (i.e. same VGM parameters simulated in different domains), and the $K(h)$, which was simulated in absence of coarse fragment, i.e. 0% domain. $K_{soil}/K_{fe}=1$ represents the behaviour of fine earth at 0% coarse fragments. Their behaviour in respect to the matric potential values and to the theoretical approaches, at 10% (*P&W* 10 and *M* 10) and 30% (*P&W* 30 and *M* 30) of coarse fragments, respectively.
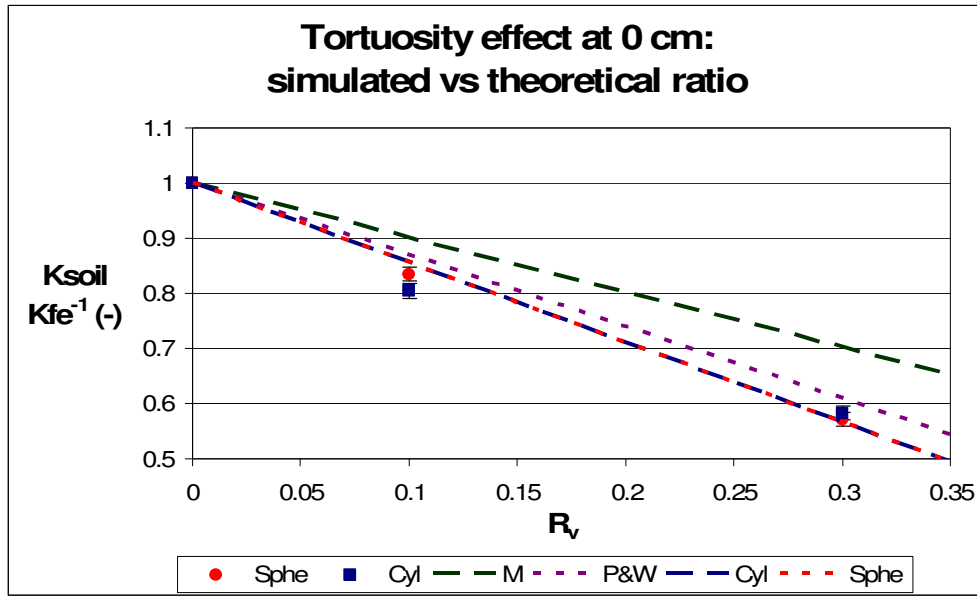
Figure 5: K_{soil}/K_{fe} **behaviour at 0 cm pressure head with respect to volumetric coarse fragment content** (R_v). **Comparison between cylinders (Cyl) and spheres (Sphe) and Peck and Watson (P&W) and Morgan (M) approaches.**

118

Tables

thesis	R_v	S.E.	bd_{fe} (g cm^{-3})	S.E.
0	0	0	1.04	0.008
10c	0.103	0.001	1.042	0.002
30c	0.304	0.005	1.023	0.03
10s	0.102	0.0005	1.01	0.037
30s	0.309	0.005	1.096	0.037

Table 1: coarse fragment content (R_v) and fine earth bulk density (bd_{fe}) of the reconstructed samples

domain	No. of Empty Elements	R_v	No of Nodes	No. of 1D-Elements	No. of 2D-Elements	No. of 3D-Elements
0%	0	0	50220	113	3233	93757
10%cyl	15	0.097	51293	444	3505	276159
30%cyl	46	0.298	53379	1098	4230	251214
10%sphe	12	0.106	53725	411	3698	290082
30%sphe	36	0.317	44915	750	3582	219258

Table 2: Domains characteristics. (R_v = fraction of the empty element with respect to the total volume)

thesis	no. of h	no. of θ	weight for each h	weight for θ	θ_r (cm^3 cm^{-3})	θ_s (cm^3 cm^{-3})	α (cm^{-1})	n (-)	K_s (cm d^{-1})	l (-)	RMSE (h+θ)	RMSE (only h)	RMSE (only θ)
0%	130	1	0.00172	100	0.190	0.584	0.046	1.304	13.508	-3.417	0.006841	0.006867	0.000736
0%	116	1	0.00140	5	0.201	0.609	0.047	1.344	38.629	-1.670	0.015380	0.015372	0.016287
10% cyl	86	1	0.00109	5	0.184	0.575	0.033	1.353	13.202	-2.973	0.012305	0.012374	0.002033
10% cyl	80	1	0.00082	5	0.206	0.577	0.029	1.397	22.088	-2.192	0.007579	0.007626	0.000043
30% cyl	134	1	0.00107	5	0.128	0.591	0.031	1.260	40.094	-2.674	0.010690	0.010727	0.003142
30% cyl	94	1	0.00136	3	0.167	0.609	0.043	1.288	908.462	0.777	0.008291	0.008237	0.012330
10% sphe	96	1	0.00140	5	0.185	0.562	0.035	1.343	54.560	-1.659	0.005918	0.005949	0.000602
10% sphe	90	1	0.00285	100	0.240	0.580	0.082	1.524	162.232	-0.823	0.006386	0.006262	0.013500
30% sphe	80	1	0.00107	7	0.119	0.599	0.050	1.247	65.310	-2.720	0.012396	0.012463	0.004471
30% sphe	70	1	0.00104	10	0.131	0.557	0.019	1.281	89.858	-0.676	0.005893	0.005923	0.003161

Table 3: van Genuchten –Mualem parameters estimated by PEST and *RMSE* of each process

6   Concluding remarks

This thesis faced two different, but related, aspects which regard stony soils: sampling and hydraulic properties.

Defining a sampling survey design, which tries to account for the within field spatial variability, might be useful to achieve greater knowledge of stones influences on several soil properties. The proposed method showed that EM38DD could be advantageously used to infer soil spatial variability in gravelly soils, even if it should not be forgotten that apparent soil EC is a quite complex measurement that requires knowledge and experience to be interpreted, thus ground-truth soil samples are obligatory to understand and interpret EMI mapping.

Soil hydraulic properties are intrinsically highly variable. Variability is furthermore greater in presence of stones compared with stone-free soil. Nevertheless the high variability characterizing the results of this thesis, it is possible to evidence, within different approaches, some general trends to describe stone influence on hydraulic properties:

I.   reduction of water content in stony soils, with increasing volume based coarse fragment content, as described by the theoretical approach, resulted in a good estimation of this property. This was true in decreasing matric potential too;

II. stone effects on hydraulic conductivity is evident in a more complex way. It is physically undoubted that stones increase the tortuosity, thus the water flow is decreased compared with stone-free soil. Presented results underline, however, that besides the tortuosity effect, it is important to consider the influence of stone on fine earth bulk density, and thus indirectly on soil porosity, especially at high matric potentials. Moreover, interaction between fine earth characteristics induced by stones and tortuosity effect is more difficult to be studied due to the great numbers of variables that are taking place (i.e. kind of texture, organic matter content, and, generally speaking, all the soil structured related problems). None of the theoretical approaches does explicitly consider this dual contrasting influence of rock fragments on hydraulic conductivity. Furthermore, 3D modelisation results

showed, for the studied soils, that tortuosity effect was not constant as the matric potential decreased, thus casting doubt on the reliability of the theoretical approaches to account for the tortuosity itself along the matric potential decrease.